

# Assistive Device for Lower Extremity Gait Training and Assistance

**LI JINFU**

(B. Eng., Harbin Institute of Technology)

**A THESIS SUBMITTED**

**FOR THE DEGREE OF DOCTOR OF PHILOSOPHY**

**DEPARTMENT OF MECHANICAL ENGINEERING**


**NATIONAL UNIVERSITY OF SINGAPORE**

**2015**

# Declaration

I hereby declare that the thesis is my original work and it has been written by me in its entirety. I have duly acknowledged all the sources of information which have been used in the thesis.

This thesis has also not been submitted for any degree in any university previously.



---

Li Jinfu

30 July 2015

# Acknowledgements

First of all, I would like to acknowledge the National University of Singapore (NUS) for awarding me the Research Scholarship and giving me the opportunity to pursue my PhD degree at this prestigious university. Then thanks to my thesis advisor and main supervisor A/Prof. Chew Chee Meng and co-supervisor A/Prof. Teo Chee Leong for their constant guidance, support and freedom during the course of my PhD study. I am very grateful to have the opportunity to work on this robotic project under the supervision of them.

Secondly, I would like to express my sincere gratitude to my senior, Dr. Shen Bingquan, for the very pleasant collaboration during the entire course of this project. Without his constant dedication and assistance, this work would not have been possible. Also, special thanks to Sven Knuefer for his assistance to implement the proposed friction compensation algorithm for harmonic drive actuator.

Next, I would like to thank all the staff and students from Control and Mechatronics Laboratory for their support and friendship over the past few years. In particular, my gratitude goes to Mrs. Ooi-Toh Chew Hoey, Miss Hamidah Bte Jasman, Ms. Tshin Oi Meng and Mr. Sakthiyavan s/o Kuppusamy for their very kindly support and assistance in the laboratory.

Finally, I would like to thank my parents and sisters, who have fully supported me in my entire study life and have always encouraged me to work hard for everything. Also, thank my girlfriend Yaoyao for her care and understand.

This work was supported by the Singapore Ministry of Education (MOE) Academic Research Fund (Grant No.: R-265-000-419-112).

I would like to dedicate this thesis to my loving family ...



# Table of Contents

<b>Declaration</b>	<b>i</b>
<b>Acknowledgement</b>	<b>ii</b>
<b>Table of Contents</b>	<b>iv</b>
<b>Summary</b>	<b>viii</b>
<b>List of Tables</b>	<b>x</b>
<b>List of Figures</b>	<b>xi</b>
<b>Nomenclature</b>	<b>xviii</b>
<b>1 Introduction</b>	<b>1</b>
1.1 Background and Motivation . . . . .	1
1.2 Objective and Scope . . . . .	4
1.3 Thesis Contributions . . . . .	5
1.4 Thesis Outline . . . . .	7
1.5 Note on Data in this Thesis . . . . .	8
<b>2 Literature Review</b>	<b>9</b>
2.1 Lower Extremity Assistive Devices . . . . .	9
2.1.1 Treadmill Gait Trainers . . . . .	10

## TABLE OF CONTENTS

---

2.1.1.1	Lokomat . . . . .	11
2.1.1.2	ReoAmbulator . . . . .	12
2.1.1.3	LokoHelp . . . . .	13
2.1.1.4	LOPES . . . . .	13
2.1.1.5	ALEX . . . . .	14
2.1.1.6	Others . . . . .	15
2.1.1.7	Summary . . . . .	16
2.1.2	Overground Wearable Gait Trainers . . . . .	17
2.1.2.1	HAL . . . . .	17
2.1.2.2	ReWalk . . . . .	18
2.1.2.3	Ekso . . . . .	19
2.1.2.4	Indego . . . . .	20
2.1.2.5	Summary . . . . .	20
2.2	Gait Training Strategies . . . . .	21
2.2.1	Gait Trajectory Tracking Control . . . . .	21
2.2.2	Impedance Control . . . . .	23
2.2.3	Performance-based Adaptive Control . . . . .	26
2.2.4	Virtual Reality Techniques . . . . .	28
2.3	Gait Assistance Strategies . . . . .	30
2.3.1	EMG-based Control . . . . .	30
2.3.2	Gait Phase Detection-based Control . . . . .	32
2.4	Chapter Summary . . . . .	33
<b>3</b>	<b>Hardware Architecture</b>	<b>35</b>
3.1	Lower Extremity Assistive Device . . . . .	35
3.1.1	Design Considerations . . . . .	36
3.1.1.1	Degree of Freedom . . . . .	36

## TABLE OF CONTENTS

---

3.1.1.2	Range of Motion . . . . .	36
3.1.1.3	Power and Torque Requirements . . . . .	37
3.1.1.4	Adjustability . . . . .	40
3.1.1.5	Attachment . . . . .	41
3.1.2	Joint Actuator Design . . . . .	42
3.1.3	Electrical Architecture . . . . .	44
3.1.4	Final Experimental Prototypes . . . . .	46
3.2	Friction Compensation for Harmonic Drive Actuator . . . . .	48
3.3	Chapter Summary . . . . .	51
<b>4</b>	<b>FAT-based Adaptive Gait Trajectory Tracking Control</b>	<b>53</b>
4.1	Introduction . . . . .	54
4.2	Dynamics Modelling . . . . .	55
4.3	Gait Trajectory Generation . . . . .	57
4.4	FAT-based Adaptive Controller . . . . .	58
4.5	Simulation Results . . . . .	63
4.6	Implementation Results . . . . .	65
4.7	Chapter Summary . . . . .	68
<b>5</b>	<b>Functional Task-based Impedance Control</b>	<b>69</b>
5.1	Introduction . . . . .	70
5.2	Functional Task-based Impedance Controller . . . . .	71
5.3	Experimental Study with Healthy Subjects . . . . .	76
5.4	Results and Discussions . . . . .	79
5.5	Chapter Summary . . . . .	84
<b>6</b>	<b>Functional Task-based Gait Assistance Control</b>	<b>87</b>
6.1	Introduction . . . . .	88

## TABLE OF CONTENTS

---

6.2	Functional Task-based Gait Assistance Control Architecture . . . . .	91
6.2.1	FSM-based Gait Period Detector . . . . .	92
6.2.2	Impedance-based Assistance . . . . .	95
6.3	Experimental Protocols and Data Analysis . . . . .	97
6.3.1	Experimental Protocols . . . . .	97
6.3.2	Data Analysis . . . . .	100
6.4	Results and Discussions . . . . .	100
6.4.1	Experimental Results . . . . .	100
6.4.2	Limitations of the Study . . . . .	107
6.5	Chapter Summary . . . . .	108
<b>7</b>	<b>Conclusion and Future Work</b>	<b>111</b>
	<b>Publications by the Author</b>	<b>115</b>
	<b>Bibliography</b>	<b>117</b>
	<b>Appendix</b>	<b>135</b>

# Summary

Physical therapy is an effective treatment for post-stroke patients to recover their walking functions. In recent years, significant efforts have been made by researchers to develop robotic devices for gait rehabilitation and assistance of stroke patients. However, current commercial systems are typically bulky, costly and limited in functions. They are available only in large hospitals for acute patients. To encourage the patients to continue their rehabilitation process and also enable them to perform independent walking on a daily basis, it is desirable to have home-based assistive device for each of them. Hence, this research work aims to introduce a low-cost, lightweight and wearable assistive device for lower extremity rehabilitation and assistance. Three robust and intuitive control algorithms have also been developed for home-based gait rehabilitation and assistance.

For the hardware development, a compact harmonic drive actuator was customized based on torque and power requirements of the hip and knee joints. To improve back-drivability of this actuator, a friction compensation algorithm was developed and it could compensate most of the internal frictions. Based on this actuator, a wearable lower extremity assistive device controlled by a real-time controller was designed. Then, three robust and intuitive control algorithms for gait rehabilitation and assistance were explored. They are called “Function Approximation Technique (FAT) based adaptive gait trajectory tracking control”, “functional task-based impedance control based on virtual gait period sequence” and “functional task-based gait assistance control based on Finite State Machine (FSM) gait detection”.

The FAT adaptive gait trajectory tracking control algorithm was proposed for passive gait training of the stroke patients in the early rehabilitation phase. This algorithm is able to cater to the variability of the wearer’s dynamic models. This

algorithm was verified being able to provide good tracking performance of the hip and knee joint trajectories, both in simulation and physical implementation. With the trajectory tracking approach, the subjects cannot actively modify their leg's movements. For those patients with some voluntary motor control capabilities, it would limit the possibility of motor learning and may also result in discomfort during usage. To address this shortcoming, the "functional task-based impedance control based on virtual gait period sequence" algorithm was developed. It could provide more compliant assistance with various assistance levels. It also enables active participation of the subjects to promote motor learning.

Besides the gait training, in order to enable the device to be used for daily gait assistance as well, the "functional task-based gait assistance control based on Finite State Machine (FSM) gait detection" algorithm was developed. This algorithm utilizes a FSM-based gait period detector to estimate current gait period of the user among six major periods. Furthermore, an impedance-based controller is used to produce functional gait assistance at hip and the knee joint in each detected gait period. In this approach, the user can actively trigger the walking assistance only using the 'affected' limb. Preliminary experimental results with healthy participants show that it can effectively provide smooth gait assistance and help to achieve normal gait patterns. Moreover, heart rate results show evidence that the device could help to reduce human physical efforts if the weight of the device can be reduced further. The above results show its potential for use in daily gait assistance outside hospital environment.

In summary, the main contribution of this thesis is the development of a low-cost, lightweight and wearable lower extremity assistive device. The three control algorithms for the device have been realized intended for different stages of the recovery for a stroke patient. The algorithms were fully tested on healthy subjects to verify their performance.

# List of Tables

2.1	Some robotic treadmill gait trainers in the literatures . . . . .	11
2.2	Some overground wearable gait trainers . . . . .	17
3.1	Range of motion [92–94] . . . . .	38
3.2	Anthropometrical data of Singapore’s males . . . . .	40
3.3	Harmonic drive actuator specifications . . . . .	43
3.4	Fitting coefficients of exponential friction model for each joint ac- tuator . . . . .	50
4.1	Fourier series fitting results . . . . .	57
5.1	Gait periods and functions . . . . .	72
5.2	Impedance parameters under 100% assistance . . . . .	74
5.3	Direction of assistive torque of joints for each virtual gait period . .	75
6.1	Finite state transitions for level walking . . . . .	95
6.2	Direction of assistive torque of joints for each gait period . . . . .	96
6.3	Calibrated impedance parameters . . . . .	98

# List of Figures

2.1	Treadmill gait trainers (Lokomat, ReoAmbulator, LokoHelp, LOPES and ALEX) . . . . .	12
2.2	Treadmill gait trainers (ARTHuR, POGO&PAM and RGR) . . . . .	16
2.3	Overground wearable gait trainers (HAL, ReWalk, Ekso, Indego) . . . . .	18
2.4	Impedance control architecture used on the Lokomat [19] . . . . .	24
2.5	Force field controller with a “virtual wall” implemented on the ALEX [39] . . . . .	25
2.6	Two types of performance-based adaptive control algorithms: 1.gait pattern adaptation; 2.impedance magnitude adaptation [19] . . . . .	27
2.7	Virtual reality integrated with the Lokomat . . . . .	29
2.8	Two examples of EMG-based control . . . . .	31
3.1	Degrees of freedom . . . . .	37
3.2	Sagittal plane joint angles, moments and powers for the hip and knee during level walking [92] . . . . .	39
3.3	Sliding frame mechanisms for user customization adjustments . . . . .	40
3.4	Off-the-shelf orthotic cuffs [98] . . . . .	41
3.5	Customized electric joint actuator (key components include: 1. incremental encoder; 2. DC frameless motor; 3. Harmonic Drive gear) . . . . .	42



## LIST OF FIGURES

---

3.6	Placement of resistive force sensors . . . . .	44
3.7	The electrical hardware . . . . .	45
3.8	The electrical architecture . . . . .	45
3.9	The first prototype of lower extremity assistive device: single-leg version and double leg-version . . . . .	46
3.10	The second prototype of lower extremity assistive device . . . . .	47
3.11	A model-based feedback friction compensation scheme for harmonic drive actuator . . . . .	48
3.12	Frictional torque in a harmonic drive actuator (left knee joint) as function of its rotational velocity . . . . .	49
4.1	A simplified two link model . . . . .	56
4.2	Normal gait trajectory fitting results: normal hip and knee tra- jectories are plotted in red dashed lines, and fitting hip and knee trajectories are plotted in blue solid lines . . . . .	58
4.3	FAT-based adaptive control scheme . . . . .	62
4.4	<span style="border: 1px solid black; padding: 2px;">SIM</span> Tracking performance for hip and knee joint (reference trajec- tories are plotted in solid lines, and tracking trajectories are plotted in dashed lines) . . . . .	64
4.5	<span style="border: 1px solid black; padding: 2px;">SIM</span> Output torques of hip and knee actuator . . . . .	64
4.6	<span style="border: 1px solid black; padding: 2px;">SIM</span> FAT adaptive gains for D, C and G matrices . . . . .	65
4.7	<span style="border: 1px solid black; padding: 2px;">REAL</span> Tracking performance for hip and knee joint (reference tra- jectories are plotted in solid lines, and tracking trajectories are plot- ted in dashed lines) . . . . .	66
4.8	<span style="border: 1px solid black; padding: 2px;">REAL</span> Output torques of hip and knee actuator . . . . .	66
4.9	<span style="border: 1px solid black; padding: 2px;">REAL</span> FAT adaptive gains for D, C and G matrices . . . . .	67

## LIST OF FIGURES

---

5.1	Normal walking cycle for a single limb illustrating major gait phases, subdivided gait periods and their starting and ending percentage [92]. The red arrows indicate the intended motion in the coming gait period for hip and knee joint . . . . .	72
5.2	Functional task-based impedance control architecture . . . . .	73
5.3	Sigmoid function used to smooth the torque profile . . . . .	76
5.4	The experimental setup: the subject was wearing the assistive device and performing treadmill gait training with body weight support	77
5.5	<span style="border: 1px solid black; padding: 2px;">REAL</span> Results under different assistance levels for the whole gait cycle . . . . .	79
5.6	<span style="border: 1px solid black; padding: 2px;">REAL</span> Results under different assistance levels for the flexion motion	80
5.7	<span style="border: 1px solid black; padding: 2px;">REAL</span> Results under different assistance levels for the extension motion . . . . .	81
5.8	<span style="border: 1px solid black; padding: 2px;">REAL</span> Average joint trajectories and assistive joint torques from all gait cycles for three subjects (assistance level labeled as: green-20%, red-40%, blue-60%, black-80%). All plots show $\pm 1$ standard deviations in lighter colored bands. . . . .	82
6.1	Functional task-based gait assistance control architecture . . . . .	92
6.2	Normal walking cycle for a single limb . . . . .	93
6.3	Diagram of FSM-based gait detector for level walking . . . . .	94
6.4	<span style="border: 1px solid black; padding: 2px;">REAL</span> Three samples of 20 seconds gait assistance results from one subject under different treadmill speeds of 1 <i>km/h</i> , 1.5 <i>km/h</i> and 2 <i>km/h</i> . . . . .	103
6.5	Experimental results from HAL 5 for comparison [91] . . . . .	104

## LIST OF FIGURES

---

- 6.6 REAL Average joint trajectories and assistive torques among all gait cycles for five healthy subjects. The top plots show the hip (blue) and knee (red) angles, and the bottom plots show the hip (blue) and knee (red) assistive torques. All plots show  $\pm 1$  standard deviations in lighter colored bands . . . . . 106
- 6.7 REAL Boxplots of heart rate values from five healthy subjects. The healthy subject's heart rate was measured under four conditions: resting (R), free walking (F), unassisted (U) and assisted (A) . . . . . 107

# Nomenclature

## Important Symbols

$\alpha_0$	coefficient of Coulomb friction
$\alpha_1$	coefficient describing the difference between stiction and Coulomb friction
$\alpha_2$	coefficient of viscous friction
$\Delta\dot{q}$	deviation of the measured joint velocity from the reference joint velocity
$\Delta q$	deviation of the measured joint angle from the reference joint angle
$\dot{\theta}$	rotational velocity of the actuator
$\hat{W}_D, \hat{W}_C, \hat{W}_G$	estimated weighting matrices
$\lambda_k$	kth gait period
$\omega_i^k$	mixture weight
$\vec{\mu}_i^k$	mean vector
$\vec{x}$	sensor measurement vector
$\tau$	actuator torques
$\tau_h$	human active joint torques
$\tau_{curr}$	assistive torque in the current gait period

---

$\tau_d$	desired joint torque
$\tau_f$	frictional torque
$\tau_{Imp}$	impedance torque
$\tau_{prev}$	assistive torque from the previous gait period
$\theta$	rotational angle of the actuator
$\theta_0$	equilibrium angle
$\theta_d$	desired gait trajectories
$\theta_{hip/knee}$	gait angle in degrees
$A$	amplitude scaling
$a_0, a_j, b_j, w$	Fourier series curve fitting parameters
<i>Assist</i>	assistance level
$B$	amplitude offset
$b$	viscosity term
$C(\theta, \dot{\theta})$	Centripetal and Coriolis matrix
$C_i^k$	covariance matrix
$D(\theta)$	inertia matrix
$e$	error
$f$	forgetting factor
$g$	gain factor

---

$G(\theta)$	gravitational components
$g_i^k$	multivariate Gaussian probability density function
$k$	stiffness term
$K_d$	diagonal positive definite matrix
$k_s$	slope adjustment factor
$M$	impedance magnitude
$N$	number of components of the mixture model
$p$	probability
$Q_D, Q_C, Q_G$	positive definite weighting gain matrices
$T$	gait cycle time
$t$	time
$V$	Lyapunov function
$v_s$	Stribeck velocity
$Z_D, Z_C, Z_G$	matrices of basis functions

### **Abbreviations**

*ES<sub>t</sub>* Early Stance

*ES<sub>w</sub>* Early Swing

*FSM* Finite State Machine

*GMM* Gaussian Mixture Model

---

*LSt* Late Stance

*LSw* Late Swing

*MSt* Mid Stance

*M<sub>Sw</sub>* Mid Swing

*PD* Proportional-Derivative

*PID* Proportional-Integral-Derivative

*CGA* Clinical Gait Analysis

*EMG* Electromyography

*FAT* Function Approximation Technique

*GRF* Ground Reaction Force

# Chapter 1

## Introduction

### 1.1 Background and Motivation

In Europe and the USA, strokes are the third most frequent cause of death and the leading cause of permanent disability [1]. Post-stroke neurological impairments frequently result in hemiparesis or partial paralysis of one side of the human body. This can affect a patient's capability to carry out certain daily living activities like eating, standing, sitting and walking. As a result, it is vital and essential to embrace a specific rehabilitation therapy and training to help the post-stroke patient develop functional mobility and regain their living independence.

Gait restoration through gait rehabilitation training therapies is one of the major concerns of neurological rehabilitation to enable the stroke patient to improve their motor functions and regain their ability to walk. The conventional manually assisted treadmill gait training with a body weight support system, as a regular gait training therapy for many years, has proved successful among stroke patients in improving lower limb motor functions and gait [2-4], especially for the patients who have moderate walking deficits. This form of therapy, however, has several



major limitations as well. The training is a highly repetitive, labor-intensive task that often necessitates up to three therapists to manually stabilize the torso and assist the legs of a patient to perform gait training. This imposes significant muscle fatigue and back pain to the therapists. As a result, each training session is typically limited to 20-30 minutes, which limits the training intensity, duration and frequency of these therapies to the patients. Additionally, the repeatability of the therapy is poor, as the quality of training differs significantly among therapists. Additionally, the process of training cannot be recorded for supplementary qualitative assessment.

Over the years, researchers have carried out considerable research into the development of robotic-assisted gait training devices [5–11] to overcome the shortcomings of conventional manually assisted treadmill gait training. These novel devices are principally designed to actuate on the hip, knee and ankle joints or all of these joints using an exoskeleton-based structure. Nonetheless, the current commercialized robotic systems are bulky, stationary, expensive, and limited in functions. They can only be found in large capacity hospitals for acute patients. Once the patients are discharged, equipment access becomes significantly limited for them. To encourage the patients to continue with the rehabilitation process after they are discharged from hospitals, it is desirable to have a home-based rehabilitation system for each of them. Hence, a low-cost, lightweight and wearable assistive device for home-based lower extremity rehabilitative gait training can be developed such that more stroke patients can afford and benefit from it.

Additionally, stroke patients often suffer from muscle weakness [12, 13] and impaired gait disorders [14] in their daily walking tasks even after the gait rehabilitation training. The majority of the stroke patients still need to rely on motorized wheelchairs for their daily motion guidance or mobility. However, the lack of limb exercise might cause further damage to their rehabilitation progress

and lower limbs as it might reduce their muscle capacity and can even result in paralysis. Therefore, it is critical that patients can walk on their own as healthy persons do on a daily basis, and this is important for maintaining their physical and mental health. The lightweight and wearable nature of the lower extremity assistive device gives it the ability to be used as a standalone device, thus helping stroke patients in walking and other tasks.

In addition to the lightweight, low-cost and wearable nature of the assistive device, elaboration of proper control strategies for this device is critical for effective gait rehabilitation and assistance. The way to improve motor adaptation and learning using proper control strategies is an additional open setback in this field. This is mainly because different control strategies are required in different rehabilitation stages of stroke as well as for the different severity levels of stroke patients.

The initial robotic assistive devices were predominantly passively position controlled to achieve passive gait training. The devices simply moved the patient through a predetermined and fixed gait pattern. As a result, the patients could not actively adjust the movement of their legs during the training process. Such a control strategy was only applicable in the early rehabilitation stage for acute stroke patients because their muscles were too weak to exert any force. If the patients have already regained some motor functions, the robotic assistive device and its inadequacy in cycle-to-cycle variation in sensorimotor and kinematic feedback would limit the possibility of motor learning for them [15]. It has been clinically proven that increasing a stroke patient's active involvement and participation in the voluntary movement of their affected limbs is highly crucial for successful gait training [16–18].

When increasing a patient's active involvement, the most common technique used is controlling the interaction forces through the incorporation of impedance-

based control algorithms. For instance, the Lokomat, applies impedance control, adaptive control and visual feedback algorithms to realize patient-cooperative strategies to enhance active participation of patient [19]. The exoskeleton device referred to as the LOPES implements the impedance control using cable-based elastic actuators [11]. The ALEX device applies the “assist-as-needed” (ANN) paradigm to achieve the same [10]. These devices depend on the classical impedance control of using reference gait trajectories to produce assistive torques, which might still result in discomfort for the patients. For example, patients can feel their assistive or resistive torques if they lag behind or lead the predefined trajectory of equilibrium points. This is, in particular, troublesome for the patients who are capable of accomplishing some functional tasks, but face difficulties to synchronize with the robot in realtime. Autonomous controllers can be used to mitigate this shortcoming, such include EMG-based controllers and gait phase detection-based controllers, which can be applied to perform overground gait rehabilitation training and also provide daily gait assistance during walking. The existing lower extremity assistive devices, as well as their control strategies, will be adequately elaborated in Chapter 2.

Based on the current research as covered in Chapter 2, it can be concluded that the main focus of this thesis is the development of a low-cost, lightweight and wearable lower extremity assistive device. This device should be able to integrate appropriate control strategies for home-based gait rehabilitation training and gait assistance.

## 1.2 Objective and Scope

This thesis was developed based on an academic research project meant to develop a lower extremity assistive device with the purpose of rehabilitating and

assisting stroke patients. Additionally, the primary objectives of this study are:

- Developing a low-cost, lightweight and wearable lower extremity assistive device to aid in hip and knee joint movements with the aim of gait rehabilitation training and gait assistance for home-based stroke patients.
- Investigating and implementing different intuitive and robust control algorithms for the assistive device. Using the developed control algorithms, operation of the device can be tailored towards gait rehabilitation training. In this mode, subjects would repetitively and passively be assisted by the device with body weight support. Additionally, the device can also be applied for gait assistance. In this mode the subjects can actively control the device while being assisted during daily walking tasks.
- Evaluating the device initially on healthy subjects to test and verify the design and control performance in the lab.

This thesis will focus on investigating the control algorithms for level walking task aimed at gait rehabilitation and assistance. Assistance for sit-to-stand and stand-to-sit tasks are beyond the scope of this work, and it has been covered by the earlier work of Shen [20].

### 1.3 Thesis Contributions

The results presented in this study can serve as a framework for the development of a home-based lower extremity assistive device that can be applied to gait rehabilitation training and gait assistance. The major contributions of this thesis are expressly abridged as follows:

- Design and construction of a low-cost, lightweight and wearable assistive device for lower extremities. This device can be used for gait rehabilitation

training on treadmills with a low-cost body weight support system. It could also be used as a standalone gait assistive device for daily walking.

- Development of a friction compensation algorithm for the customized harmonic drive joint actuator to increase transparency of the assistive device.
- Development of a Function Approximation Technique (FAT) based adaptive gait trajectory tracking controller aimed at passive gait training of stroke patients in the early rehabilitation stage. Both simulation and physical implementation results confirm its feasibility for passive gait training.
- Development of a functional task-based impedance controller based on virtual gait period sequence. This algorithm can provide functional task-specific gait assistance, and the assistance levels can be easily adjusted both in the whole gait cycle and in each virtual gait period. It is anticipated that this can help improve the active participation of stroke patients with some voluntary motor control abilities. To the best of our knowledge, no published research has tried this approach for active gait training.
- Development of a functional task-based gait assistance control architecture. This novel approach utilizes a Finite State Machine (FSM) to implement a gait period detector to estimate current gait period of the user among six major periods. Furthermore, an impedance-based controller is applied to produce functional gait assistance at the hip and knee joint in each detected gait period. Compared to existing control, this is the first experimental trial to offer smooth gait assistance based on gait period functionality. Preliminary experimental results on healthy participants show its potential for the application of daily gait assistance of home-based lower extremity assistive device.

## 1.4 Thesis Outline

The outline of the thesis is structured as follows:

**Chapter 2** gives a detailed literature review of the existing lower extremity assistive devices and their control strategies for gait rehabilitation training and gait assistance.

**Chapter 3** presents the hardware architecture of the developed lower extremity assistive device. A friction compensation algorithm for the customized harmonic drive joint actuator to increase the device transparency is also described in this chapter.

**Chapter 4** presents a Function Approximation Techniques (FAT) based adaptive gait trajectory tracking control algorithm for passive gait rehabilitation training purpose. Simulation and physical implementation results will be presented.

**Chapter 5** presents a functional task-based impedance control algorithm based on virtual gait period sequence for active gait rehabilitation training purpose. Compared with the gait trajectory tracking based algorithms, this approach can provide more compliant assistance with various assistance levels. It enables active participation of the subjects to promote motor learning. Preliminary evaluations are performed on healthy participants.

**Chapter 6** presents a functional task-based gait assistance controller using a finite state machine gait period detector for level walking. The controller enables the device to be actively controlled by the user's 'affected' single limb. The effectiveness of this controller is verified by healthy subject experiments as well.

**Chapter 7** summarizes the research and discusses possible improvements and directions for future work.

## 1.5 Note on Data in this Thesis

This thesis present data both from simulations and from the real implementations. The figure captions indicate the source of the data. Figures with simulated data are marked with SIM while figures with data from the real implementations are marked with REAL. This approach is borrowed from [\[21\]](#).

# Chapter 2

## Literature Review

The work presented in this thesis is largely based on the state of the art existing robotic devices for lower extremity gait rehabilitation and assistance. This chapter will present a detailed review of the existing lower extremity robotic assistive devices. It will also summarize the control strategies used for gait rehabilitation training and gait assistance. The wearable exoskeletons explicitly developed for the military purpose instead of therapeutic use do not fall within the scope of this work and hence will not be reviewed here. The remainder of this chapter is organized as follows: Section 2.1 shows various robotic lower extremity assistive devices including treadmill gait trainers and overground wearable gait trainers. Section 2.2 presents the existing control strategies for gait rehabilitation training, and Section 2.3 presents the two specific control strategies for gait assistance. Finally, Section 2.4 summarizes the reviews done in the chapter.

### 2.1 Lower Extremity Assistive Devices

Over the last ten years, robotic assistive devices have been developed in large quantities to aid lower extremities. They have also been evaluated for gait rehabil-



itation training and gait assistance [22–26]. Depending on the systems employed, treadmill and body weight support system, these assistive devices can be generally categorized into two major groups: treadmill gait trainers and overground wearable gait trainers. Similar to conventional manually assisted treadmill gait training systems, treadmill gait trainers still employ a treadmill and body weight support system. However, they replace the physical therapists involved in the training process with robotic exoskeletons to guide the patient’s leg movements, reducing the intensity and work done by the physical therapists. In hospitals, their main aim is to offer gait rehabilitation training to neurological patients. Comparatively, overground wearable gait trainers are wearable and portable robotic lower extremity exoskeletons that can be carried home to aid the disabled in their daily walking tasks. The following subsections will review several representative robotic lower extremity assistive devices from each group.

### 2.1.1 Treadmill Gait Trainers

Treadmill gait trainers automate the conventional manually assisted body weight support treadmill gait training system. They normally employ the body weight support system and the treadmill, but the lower extremity exoskeletons substitute the physical therapists in supporting and controlling a patient’s leg movements. Development of the robotic treadmill gait trainers up to present times has been steady, and some of the devices are commercially available. The commercially available systems include the Lokomat (Hocoma, Switzerland), the ReoAmbulator (Motorika Ltd., USA) and the LokoHelp (LokoHelp Group, Germany). Other similar systems are either still at a research stage of development or under clinical evaluations. Some of the representative treadmill gait trainers are summarized in Table 2.1 below. These robotic treadmill gait trainers will be further elaborated in the coming subsections.

Table 2.1: Some robotic treadmill gait trainers in the literatures

Treadmill gait trainer	Company/University	References
Lokomat	Hocoma	[5, 19, 27–31]
ReoAmbulator	Motorika	[6, 32, 33]
LokoHelp	LokoHelp Group	[7, 34]
LOPES	University of Twente	[11, 35, 36]
ALEX	University of Delaware	[10, 37–40]
ARTHuR	University of California, Irvine	[41, 42]
POGO & PAM	University of California, Irvine	[43–45]
RGR	Northeastern University	[46–49]

### 2.1.1.1 Lokomat

Developed in Hocoma AG, Switzerland, Lokomat, as shown in Fig. 2.1(a) is among the first devices built, it is also the most successful commercialized automated treadmill gait training system. The device is made up of a bilateral, wearable robotic gait orthosis, a treadmill, and an advanced body weight support system. The Lokomat can carry out gait rehabilitation training in the sagittal plane. Customized linear drives (DC motors with ball and screw mechanisms) are used to actuate the hip and knee joints. They are further integrated into an exoskeleton structure. The rubber foot lifter passively governs the ankle joints during the swing phase. The drives can synchronize precisely in real-time with the speed of the treadmill. During its development, the first Lokomat prototype, also referred to as driven gait orthosis (DGO) is detailed further in [5]. While using the early version of the Lokomat, a patient’s legs are enforced to follow fixed and predefined hip and knee trajectories repeatedly and consistently in a pure position control strategy. Improved generations and versions of the Lokomat have integrated interaction force sensors, making possible for implementing



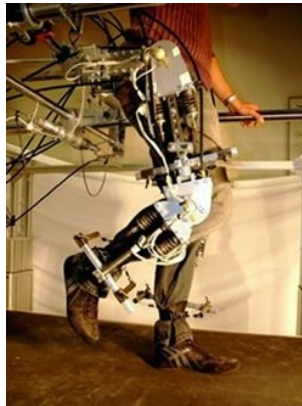
(a) Lokomat



(b) ReoAmbulator



(c) LokoHelp



(d) LOPES



(e) ALEX

Figure 2.1: Treadmill gait trainers (Lokomat, ReoAmbulator, LokoHelp, LOPES and ALEX)

the patient-cooperative control strategies [19]. Up to now, the Lokomat is still the most clinically appraised robotic training system for stroke and spinal cord injury patients [27–30].

### 2.1.1.2 ReoAmbulator

The ReoAmbulator, developed by Motorika Ltd in the USA, also referred to as “AutoAmbulator” as shown in Fig. 2.1(b), is an alternative commercialized treadmill robotic system for lower-limb rehabilitation therapy [6, 32]. Powered leg orthosis, referred to as “robotic arms”, are strapped to a patient’s leg on the

thighs and ankles, driving the robotic arms through a stepping pattern. The ReoAmbulator is still under evaluation for its effectiveness among stroke patients in conjunction with the Health South Network of Rehabilitation Hospitals. The evaluation is based on a pilot study conducted on stroke patients on the ReoAmbulator [33]. The study concluded that the robot-assisted gait training could produce similar clinical outcomes in comparison to the conventional physical rehabilitation therapies.

### 2.1.1.3 LokoHelp

The other device is the LokoHelp from the LokoHelp Group in Germany. As shown in Fig. 2.1(c), it is an electromechanical gait device with a treadmill developed to improve a patient's gait after brain injury. The device is placed in the middle of the treadmill, on a surface that is parallel to a patient's walking direction. It is fixed to the front of the treadmill with a simple clamp, and it also offers body weight support for a patient. The LokoHelp can aid in moving a patient's foot trajectory with a fixed length of 400 *mm*, which allows for a variation of the gait cycle speed from 0 *km/h* up to 5 *km/h*. Analyses on its effectiveness and practicability have been carried out through clinical trials [7, 34]. Results from these clinical trials reveal that the system improves the gait recovery ability among patients. These results are similar to the manual treadmill gait training. However, using the LokoHelp, the required therapeutic assistance is reduced, thus greatly reducing the therapists discomfort. The conclusion derived from the LokoHelp applies to nearly all robotic treadmill gait training systems.

### 2.1.1.4 LOPES

The Lower Extremity Powered Exoskeleton (LOPES) as shown in Fig. 2.1(d) uses a unique Bowden-cable motorized series elastic actuator (SEA) [35] in its

joint actuation design. The LOPES actuation system comprises an adaptable Bowden-cable transmission, servomotor, and series elastic elements that can be applied to force measurements. The servomotors are placed on the remote station, and actuation is transmitted through the cable, therefore making the exoskeleton inherently lightweight and compliant to the user. The device has three actuated degrees of freedom in every leg: two located at the hip joint (hip flexion/extension and hip abduction/adduction) and one at the knee joint (knee flexion/extension). There is no actuation considered for the ankle joint. This assistive device mainly implements impedance control, which allows for both the “robot-in-charge” mode and “patient-in-charge” mode. Under the “robot-in-charge” mode, the robot’s impedance is set to high and it guides the patient’s limbs through a predefined and fixed path, which is very similar to the position control. In the “patient-in-charge” mode, the robot’s impedance is set to low, making the robot highly compliant in a manner that the patient and the robot can actively interact. This helps increase the voluntary active participation for the patient. Evaluations of the LOPES were conducted on healthy and stroke subjects in several studies [11, 36]. However, there are some reported restrictions presented by the current LOPES device [11]. The joint angular position measurements were not sufficiently accurate for inverse dynamic modeling, thus making the estimated joint torques estimated based on the inverse dynamic model inaccurate at best. Additionally, the actuator forces could not be accurately measured by the displacement of springs due the high inner joint friction.

### 2.1.1.5 ALEX

The Active Leg Exoskeleton (ALEX) is another recent robotic gait orthosis that was developed at the University of Delaware to train stroke survivors [10]. Its structure resembles that of the Lokomat, and it employs electrical linear actu-

ators to drive the hip and knee joints in the sagittal plane, however, it does not offer any actuation to the ankle joints. Springs are passively used to assist hip abduction/adduction and four trunk rotations. The robotic gait orthosis used in the system is heavy, but it is offset by a gravity balancing system, which can compensate for nearly all the orthosis weight. Force-torque sensors are installed at every joint, which allows the ALEX to achieve direct force control at the joint level. The ALEX propositions an original "assisted-as-needed" (ANN) control strategy that employs an impedance-based force-field controller. Within the control strategy, the ALEX has been assessed on healthy subjects as well as stroke patients [10, 37–40]. Using the ALEX, it has been revealed that intensive gait re-training can drastically change and improve a stroke patient's gait pattern. The changed gait pattern closely resembles that of a healthy subject.

### 2.1.1.6 Others

Still under research are other robotic gait training devices. For instance, the Biomechatronic Lab at the University of California, Irvine, has developed some assistive gait devices for locomotor training for the patients with spinal cord injuries. Namely, these devices are ARTHuR, POGO and PAM. ARTHuR, which is an acronym for the Ambulation-assisting Robotic Tool for Human Rehabilitation as shown in Fig. 2.2(a) is a directly-driven parallel device manipulating human stepping movement on a treadmill [41]. The POGO, which stands for Pneumatically Operated Gait Orthosis, employs two pneumatic cylinders to improve the leg-robot design, and it can help in flexing and extending both the hip and the knee joints. The PAM, which stands for the Pelvic Assist Manipulator, a pneumatically actuated device that can accommodate and control naturalistic pelvic motion during gait training. The POGO and PAM systems were integrated into one pneumatic gait training robot [43] as shown in Fig. 2.2(b). The device was

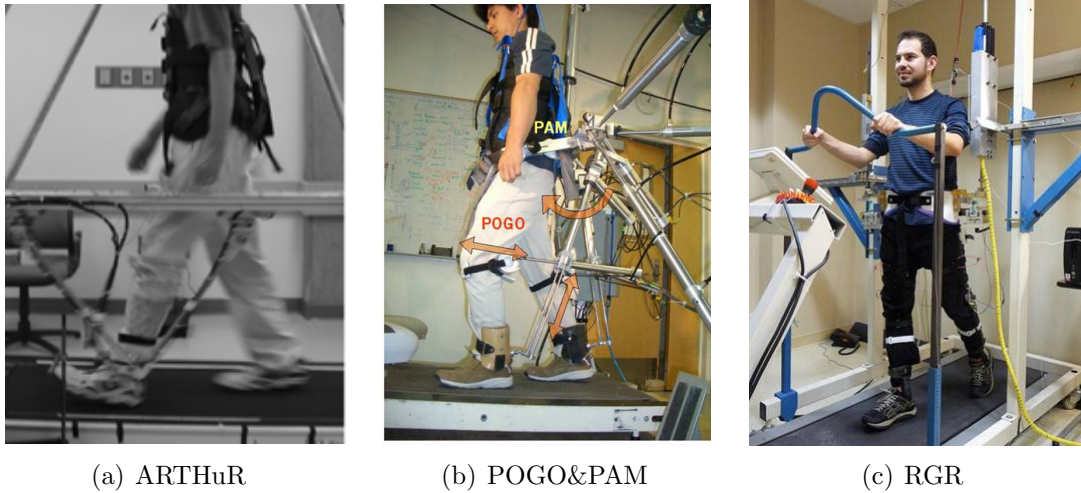


Figure 2.2: Treadmill gait trainers (ARTHuR, POGO&PAM and RGR)

tested and evaluated in clinical trials applied to spinal cord injured (SCI) patients [44]. The Robotic Gait Rehabilitation trainer, RGR, is another new gait training robot as shown in Fig. 2.2(c) [48]. The Northwestern University developed it and it can generate force-fields to facilitate treadmill gait retraining among stroke patients associated with exaggerated or unconditional movements of the pelvis. This device is still under development, and tests are being carried out on its effectiveness and efficacy.

### 2.1.1.7 Summary

The development of these devices is at an advanced level since they have readily replaced the conventional manually assisted body weight support gait training systems used by neurological patients. Despite the improvements that were done to devices, they still fall short in some areas. The devices are normally very bulky, stationary and expensive. They are also mainly reserved for acute patients in large hospitals. In a bid to boost patients to continue gait rehabilitation at home and also practice independent walking everyday, the assistive devices should



Table 2.2: Some overground wearable gait trainers

Overground gait trainer	Company/University	References
HAL	Cyberdyne Inc	[50–52]
ReWalk	Argo Medical Technologies	[53–56]
Ekso	Berkeley Bionics	[57, 58]
Indego	Parker Hannifin Corp	[59–63]

be made to fit their life-styles both at the hospitals and at home. Therefore, to address the shortcomings of the treadmill-based assistive devices, several portable and wearable gait-training devices for overground mobility were developed over the years, and shall be comprehensively covered in the coming section.

### 2.1.2 Overground Wearable Gait Trainers

These gait trainers are anthropomorphic lower extremity exoskeletons designed to either assist individuals with paralysis to recover their walking abilities or assist neurological patients with gait disorders to achieve overground gait rehabilitative training. There are several successful examples and they include HAL (Cyberdyne, Japan), ReWalk (Argo Medical Technologies, Israel), Ekso (Ekso Bionics, USA), Indego (Parker Hannifin Corp, USA), as summarized in Table 2.2. Through research, there is clear evidence that each one of these devices has been properly developed and commercialized.

#### 2.1.2.1 HAL

The Hybrid Assistive Leg, HAL, was developed by Cyberdyne Inc. in Japan as shown in Fig. 2.3(a). It is a wearable robot suit meant for non-military functions, ranging from the rehabilitation of neurological patients, everyday assistive walking





Figure 2.3: Overground wearable gait trainers (HAL, ReWalk, Ekso, Indego)

among the elderly and the disabled, to human ability reinforcement during heavy-duty work. In the latest version, HAL 5, several models were made to increase the scope of functionality of the device: the full-body, double-leg and single-leg models were built [50]. The single-leg model can be used to help the persons with hemiplegia to walk. The HAL is powered by DC servomotors with harmonic drive gears. The control computer and battery are strapped around the user's waist. Ground reaction force sensors (GRF) and Surface electromyography (sEMG) sensors are incorporated to estimate the motion intention and help control the device. The double-leg HAL 5 model is approximately 10 *kg* in weight and has been employed in carrying out clinical trials among stroke patients in hospitals [51, 52]. The HAL system, in 2013, became the pioneer powered exoskeleton to receive a global safety certification.

### 2.1.2.2 ReWalk

The ReWalk, a product of the Argo Medical Technologies in Israel as shown in Fig. 2.3(b) is another wearable, motorized quasi-robotic suit that approximately weighs 23.3 *kg*, and ranges between US\$69,500 and US\$85,000 cost per unit. It

is made up of a light wearable brace support suit that integrates the DC motor-based actuators at the hip and knee joints. It also has rechargeable batteries, an arrangement of sensors and a computer-based control system. The ReWalk enables paraplegics to sit, stand upright, walk and climb stairs. During operation, through a wrist-mounted keypad placement, users can manually change between various types of movements. Coupled with a torso tilt sensor, users can trigger and maintain walking steps while walking. The crutches in the device are used to maintain the user's overall balance while walking. Not much detail can be found on how the ReWalk was designed and controlled since it is largely a commercial product. The ReWalk is undergoing clinical trials [55, 56] at the Moss Rehabilitation Hospital in Philadelphia. In 2011, the Food and Drug Administration Agency (FDA) approved its use in hospitals and in 2014 it was approved for home and public use in the USA.

### 2.1.2.3 Ekso

Another exoskeleton is the Ekso developed by Berkeley Bionics, in the US formerly known as the Berkeley eLEGS, as shown in Fig. 2.3(c). The Ekso assists paraplegics in sitting, standing, walking with a walker or crutches and this is quite similar to the ReWalk. Its computer interface implements both motion and force sensors to monitor a user's motion and gestures. It then translates the information intelligently to interpret the intent of the user, which is then translated into actions that are fed to the exoskeleton. The Ekso exoskeleton weighs approximately 20 *kg*, can attain a maximum speed of 3.2 *kph*, has a battery life of 6 hours and costs approximately US\$100,000. The Ekso also received FDA approval like the ReWalk, and it is undergoing additional development and clinical trials in rehabilitation hospitals and centers [58].

### 2.1.2.4 Indego

As shown in Fig. 2.3(d), the Indego, formerly known as the Vanderbilt exoskeleton developed at the Vanderbilt University, was recently commercialized by the Parker Hannifin Corporation. This powered lower-limb exoskeleton is rather lightweight, approximately 12 *kg*, and has novel modular design and is compact in size. It provides for a wide range of mobility that includes sitting, standing, walking and stair climbing for paraplegic users [61, 62]. Preliminary clinical trials have been carried out on one complete paraplegic patient to validate its efficacy [60, 63]. Additionally, it is the first overground wearable gait trainer that has successfully integrated functional electrical stimulation (FES), in which small electrical pulses are applied to paralyzed muscles [64, 65]. Moreover, this exoskeleton also allows for spinal cord injured patients to contribute to overground gait rehabilitation training. Pilot clinical trials are currently being carried out at the Shepherd Center in Atlanta.

### 2.1.2.5 Summary

In summary, the development of overground wearable trainers is at an advanced stage similar to the treadmill gait trainers. Compared to treadmill gait trainers, overground wearable trainers are nimbler and more compact, meaning that their applications can be done at home in activities of daily living. Presently, overground wearable trainers are chiefly used to empower paraplegic individuals to recover their ability to walk. Also, they have also shown that they are adequately capable of overground rehabilitative gait training of neurological patients. The main drawback of the current devices is that they are still out of the price range of most patients.

## 2.2 Gait Training Strategies

In addition to the design of different robotic assistive devices, researchers additionally concentrate on developing various gait rehabilitation training strategies to enhance training performance. The aim of rehabilitative gait training is to restore patients' neurocapacity to allow the patients to increase their motor functions and recover their walking independence. While successful rehabilitative gait training determinants are still unknown, repetitive, intensive and task-oriented training strategies have revealed their ability in meaningfully improving gait functionality. The training strategies are categorized into two general types: passive gait training strategies and active gait training strategies. The passive gait training strategies mainly utilize position-based control algorithms. They force the patient's lower limbs to track normal gait trajectories. For the active gait training strategies, impedance control, performance-based adaptive control and virtual reality techniques are employed to encourage a patient's active participation in the training process. The mentioned control strategies are primarily developed for treadmill gait trainers and will be discussed in the coming section.

### 2.2.1 Gait Trajectory Tracking Control

Gait trajectory tracking control was initially implemented by early robotic gait training devices [5]. It has then been widely applied to nearly every commercially available robotic treadmill gait trainer. The control mainly applies a position-based controller with reference gait trajectories as its inputs, and the robotics device would force the patient's lower limbs to track a specific path and follow a preset gait movement pattern. An important concern with the gait trajectory tracking control is how to determine the reference gait trajectories. There are a few approaches available in literatures. The most commonly used approaches

are based on mathematical models of normative gait trajectories and prerecorded trajectories derived from healthy subjects [5, 19, 45]. Another common approach is the "teach and replay" approach that was initially introduced and tested in ARTHuR [42], and it was later implemented in POGO & PAM [45] as well. Lastly, reference gait trajectories from the impaired limb can also be generated in real-time from the movement of the unimpaired contralateral limb for those hemiparetic patients. This algorithm has been implemented and evaluated on the LOPES [66, 67]. After achieving the reference gait trajectories, certain customizations can be done to tailor them to each patient.

The gait trajectory tracking control is mainly applied for the passive gait training in the early rehabilitation stage of acute stroke patients when they still lack the muscular strength to move their lower limbs. The potential drawback of this control strategy is that the preemptive robotic guidance and lack of cycle-to cycle variation in kinematics and sensorimotor feedback may decrease human motor learning [15]. This applies especially to those moderately impaired stroke survivors who have already recovered some of their voluntary motor control functions. Trajectory tracking controlled robotic gait devices, are often very rigid and stiff, which would discomfort the patients, reduce their physical efforts, and may also decrease the efficacy of the rehabilitative gait training. On the extreme side, it could result in abnormal gait pattern generations and make the patients unable to acclimate to physiological gaits.

Away from the mentioned gait trajectory tracking based passive gait training, an increased number of researchers have shifted their focus to investigating control strategies that enable active gait training. Several studies have been conducted on both animals and human in an effort compare active training with passive training [16–18]. These studies found that increasing a subject's participation and involving them in the training process results in more meaningful and ef-

fective training. Therefore, so as to encourage a patient's active participation both psychologically and physiologically while undergoing robotic gait training, impedance control, performance-based adaptive control and virtual reality techniques have been introduced so as to promote active gait training.

### 2.2.2 Impedance Control

Impedance control is usually applied to introduce compliance in the robot's behavior. Mechanical impedance is treated as the relationship between the exerted actuator force and its resultant motion. The concept of impedance control was firstly introduced by Hogan [68], and since then a variety of impedance controllers have been applied in the field of robotics and human-robot interaction. The basic idea of the impedance control strategy applied for robotic gait training is to allow a variable deviation from the reference gait trajectories rather than imposing a rigid gait movement pattern generated by the gait trajectory tracking control. The impedance controller implemented on the Lokomat follow the same idea [31], as illustrated in Fig. 2.4. When the reference trajectories are given, then the restorative torque will be related to the deviation of the reference trajectories and its velocities. In the Lokomat, the impedance-based assistance controller achieved in the joint space has the following form

$$\tau_{Imp} = k\Delta q + b\Delta\dot{q} \quad (2.1)$$

where  $\tau_{Imp}$  refers to the impedance torque at each joint,  $\Delta q$  refers to the deviation of the measured joint angle from the reference joint angle,  $\Delta\dot{q}$  is the deviation of the measured joint velocity from the reference joint velocity,  $k$  denotes the stiffness term and  $b$  denotes the viscosity term. The values of impedance could be selected by the physical therapists centered on their experience and the patient's severity

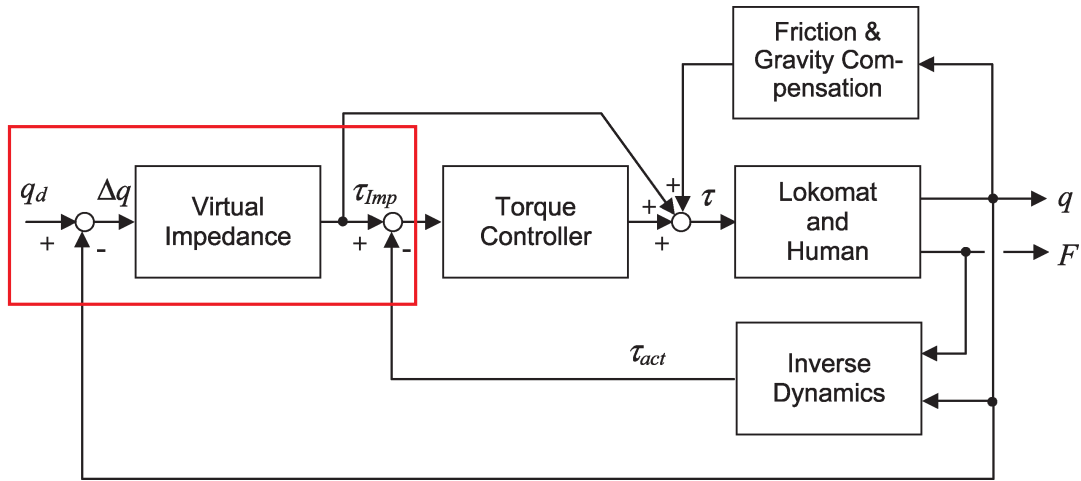


Figure 2.4: Impedance control architecture used on the Lokomat [19]

levels.

Another form of impedance control is the force-field controller that was proposed in controlling the ALEX [10]. In this controller, a “virtual wall” is created along the reference trajectory of the patient’s foot in the sagittal plane, as illustrated in Fig. 2.5. The field forces are a combination of tangential force, normal force, and damping force. The tangential force moves the foot along the predefined trajectory in the forward direction, and the normal force keeps the foot within the tunnel confined by the “virtual wall”. The damping force restricts the velocities. The “path control” approach, which is similar to the force-field control was employed in the Lokomat’s joint space of the hip and knee in the sagittal plane [31]. This approach employs the compliant “virtual wall” to maintain the patients leg within the tunnel around the desired spatial path.

The LOPES also employs the impedance control strategy for its “robot-in-charge” and “patient-in-charge” modes [11]. The LOPES impedance control architecture is based on a Virtual Model Control (VMC) framework [69] used to stimulate its virtual dynamic components like virtual springs and virtual dampers. Under the “robot-in-charge” mode, the controller impedance is set at high. The

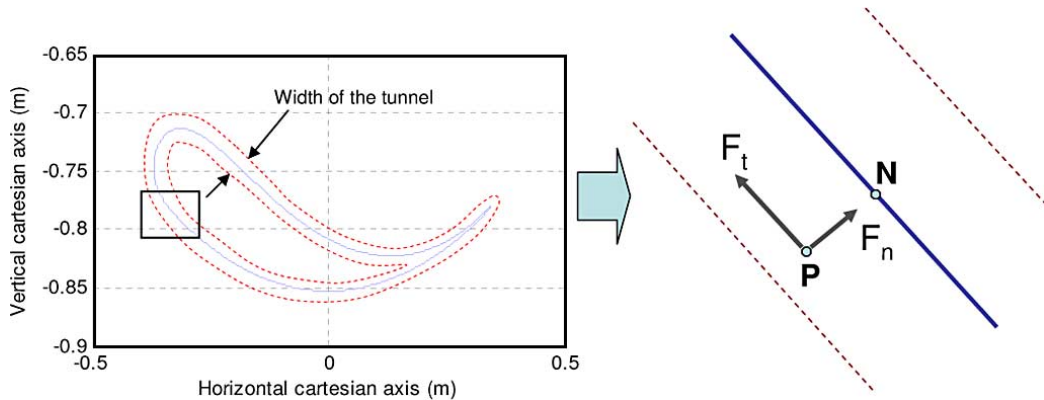


Figure 2.5: Force field controller with a “virtual wall” implemented on the ALEX [39]

robot guides the patient in following a fixed and predetermined gait path much like the gait trajectory tracking control approach. In the “patient-in-charge” mode, the controller impedance is set at low. This setting makes the robot behave more compliant and flexible, and the patient can actively interact with the robot. This helps improve the patient’s active voluntary participation.

The impedance-based triggered assistance is a variation of the impedance control. For this control, the patient starts gait movement without any assistance from the robot, and if the patient cannot achieve a threshold value, then the robotic assistance would be triggered. The threshold value can be the trajectory tracking error or the patient’s minimum force produced. This variant of impedance control inspires the patient’s self-initiated movements. It has been implemented on the robotic gait training system of the POGO & PAM [44].

Even though the impedance control strategy has been implemented in several assistive devices, it still presents several challenges. First, the restorative force determined by reference gait trajectories is still relied upon by these classical impedance controllers. This presents risks that patient and robot might walk out of phase. As a result, the patient can feel their assistive or resistive torques if



they lag behind or lead the predefined trajectory of equilibrium points. This is, in particular, troublesome for those patients who are capable of accomplishing some functional tasks, but encounter difficulties to synchronize with the robot in realtime. Secondly, impedance parameters need to match with the patient's level of disability and recovery progress. This is usually preset manually before the training session by an experienced physical therapist on a trial-and-error basis. Impedance parameters founded on online evaluations of the patient's performance are preferred to enable automatic adjustment. This aspect can be achieved through performance-based adaptive control, which will be covered in the next section.

### 2.2.3 Performance-based Adaptive Control

Performance-based adaptive control aims to adapt automatically the training parameters based on the online measurements of the patient's varying performance. It can be utilized to enhance the patient's active participation while undergoing training. Up to present times, two types of performance-based adaptation algorithms have been developed for rehabilitative gait training, namely gait pattern adaptation and impedance magnitude adaptation, both of which have been employed on the Lokomat, as illustrated in Fig. 2.6.

The purpose of gait pattern adaptation is to generate adaptively appropriate variations in the reference gait trajectories so that the robot can move in a manner that is desired by the patient. To achieve this goal, the reference gait trajectories are firstly parameterized with several adaptable parameters, and the adaptation can be performed by optimizing these parameters to yield the new desired gait trajectories. Over the years, three adaptation algorithms have been developed [70]. The first adaptation algorithm is the inverse-dynamics-based joint-angle adaptation algorithm through minimization of the human-robot interaction torque.

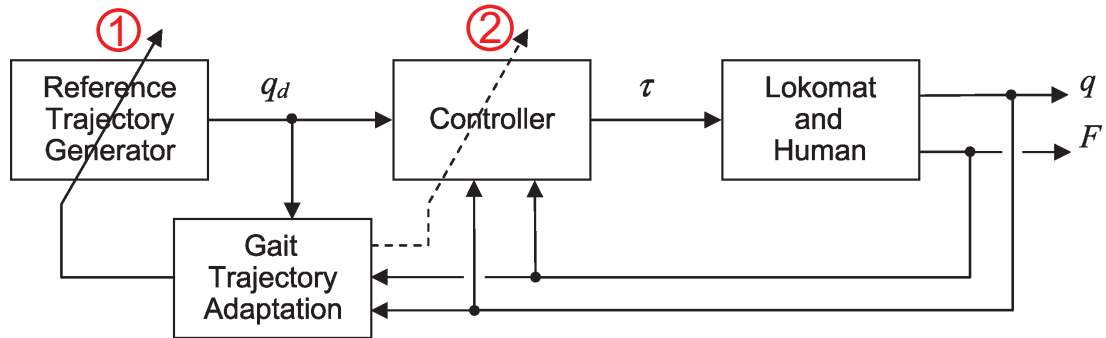


Figure 2.6: Two types of performance-based adaptive control algorithms: 1.gait pattern adaptation; 2.impedance magnitude adaptation [19]

This algorithm's performance is heavily reliant on the accuracy of the inverse dynamic models. The second adaptation algorithm is the direct-dynamics-based joint-angle adaptation algorithm. This algorithm utilizes the measured interaction torques to approximate the variation of the trajectory accelerations desired by the patient, following which adaptation occurs on the trajectory produced to attain the preferred acceleration trajectory deviations. The third adaptation algorithm is an impedance-control-based joint-angle adaptation algorithm. The impedance could directly link the interaction torques and the allowed trajectory deviations. From the preset impedance relationship, interaction torques could reveal how much a patient would like to change the reference gait trajectories. Hence, adaptation to the preferred trajectories can be carried out. The performance of these algorithms was evaluated in computer simulations and through experiments with healthy subjects and spinal cord injured patients [71–73]. The only problem with the gait pattern adaptation is that the adapted gait trajectories desired by the patient may be an unphysiological gait pattern.

Impedance magnitude adaptation is the other form of adaptation. This adaptation mechanism functions through a fixed reference gait trajectory, however, it adjusts the magnitude of the impedance based on a patient's active effort. This

effort is approximated online by the interaction force sensors. If the effort detected from the patient is low, then the magnitude of the impedance is increased to accommodate the patient and enforce the patient to follow the reference gait trajectory. Alternatively, if the sensors detect an increased amount of effort, the magnitude of the impedance is reduced to accommodate greater deviations from the reference gait pattern such that the patient will have an increased motion of freedom. The magnitude of the impedance can be altered through the following error-based adaptive law that has the following form

$$M_{i+1} = fM_i + ge_i \quad (2.2)$$

where  $M$  represents the robot impedance magnitude required to be adapted,  $i$  denotes the  $i^{th}$  movement,  $e$  refers to the error based on performance index that normally specifies the active effort of a patient,  $f$  and  $g$  denote the forgetting factor and gain factor, respectively. The forgetting factor is usually selected as  $0 < f < 1$  to prevent the patient from relying too much on the assistance provided by the device. Using this adaptive law, the impedance magnitude can be altered from trial to trial based on the measured performance indexes. The impedance magnitude adaptation algorithm was tested in computer simulations and assessed through a healthy subject experiment on the Lokomat [19]. Similar impedance adaptive control algorithms were also developed for the ARTHuR [42] and another gait rehabilitation robot developed by Hussain et al. at the University of Auckland [74].

### 2.2.4 Virtual Reality Techniques

Virtual reality can replicate virtual environments of the real world through computer software. In this world, users can interrelate with the generated virtual

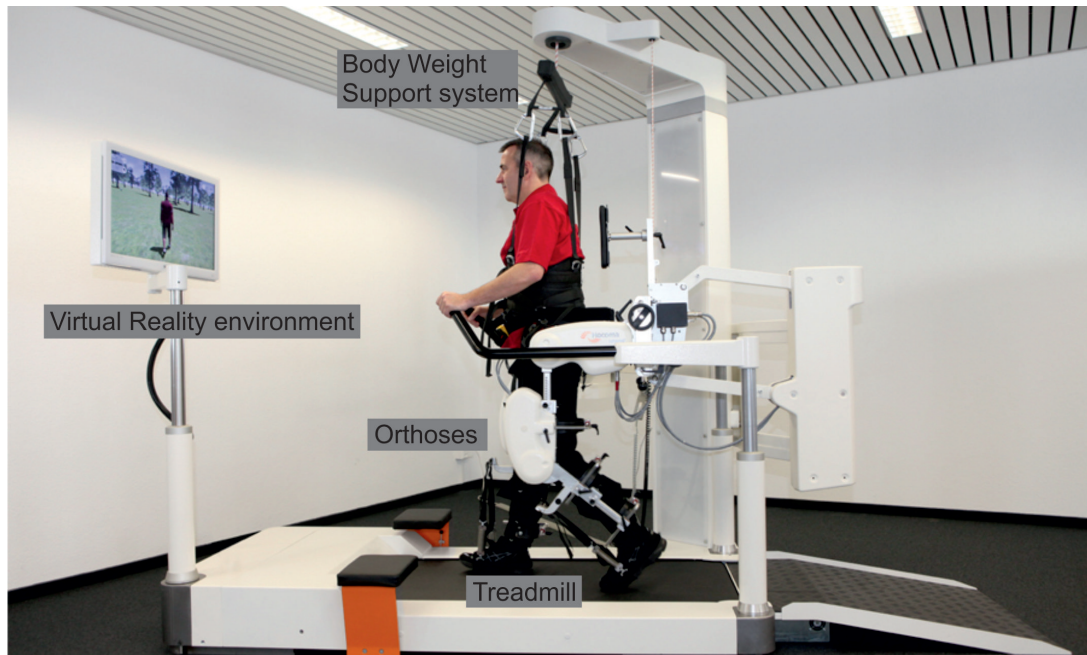


Figure 2.7: Virtual reality integrated with the Lokomat

environments through human-machine interfaces. Over the years, virtual reality techniques have been incorporated into robotic gait training devices to encourage active gait rehabilitation training [36, 75, 76]. Fig. 2.7 shows an example of the virtual reality integrated with the Lokomat gait trainer. The device can map a subject's gait motion into the virtual environment in real-time and provide the subject with visual and haptic feedback. Through virtual reality, the subject can engage in the virtual world and achieve more gait repetitions that are linked to a specific task or goal in the virtual world. This ultimately creates an inspiring motor learning experience.

Gait training using a robot device coupled with virtual environments is more advantageous compared to gait training using a robot alone [77]. Firstly, virtual reality programs have the ability to generate a plethora of enjoyable, interesting and interactive activities, which may not be attained in the typical clinical environment. Switching between different activities is also simple and fast. Additionally, activities can be classified into different difficulty levels. Physical therapists

can also customize stimulating exercises for every patient. Secondly, novel forms of real-time visual and haptic feedback can be created in virtual environments in regards to the subject's training performance. This information is intuitive and useful to the therapists, allowing them to chart a patient's progress. Virtual reality techniques can make gait training more motivational and stimulating.

### 2.3 Gait Assistance Strategies

Overground wearable gait trainers can be employed to aid in daily walking motions in the impaired patients who can stand and walk slowly although they endure gait disorders and muscle weakness. To provide effective and smooth gait assistance, the control of the assistive devices heavily relies on a precise prediction of the user's intention of the motion. Skin surface EMG signals or gait phase detection methods are used to approximate human motion intention for assistive devices. Based on these two techniques, two corresponding autonomous walking gait controllers have been developed and implemented, which are EMG-based control and gait phase detection-based control.

#### 2.3.1 EMG-based Control

Skin surface electromyography (sEMG) signals are produced just before muscle contractions, and these signals can be used to predict the human motion intention and estimate the human muscle forces. Hence, they can be modeled to control the assistive devices. This has been achieved by a “cybernic voluntary control” [78] algorithm as shown in Fig. 2.8(a) on the HAL system. The HAL predicts the intended human motions and approximates the assistive torques of the joints for healthy subjects [79–81]. Another similar algorithm called “proportional myoelectric control” is adopted in a powered ankle-foot orthosis as shown in Fig. 2.8(b),

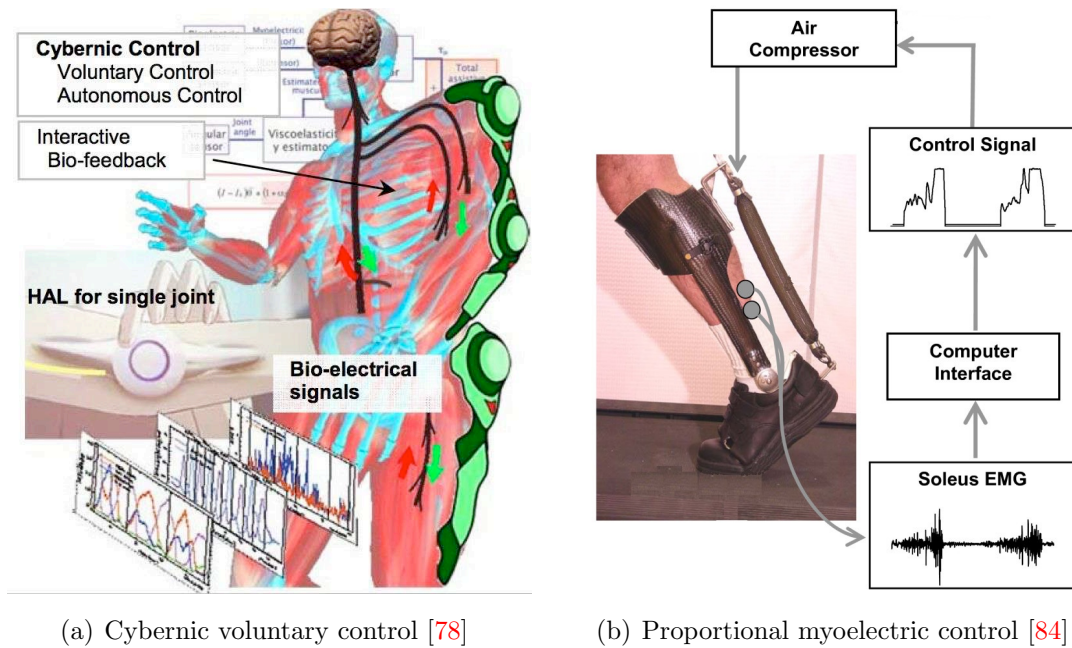


Figure 2.8: Two examples of EMG-based control

in which the assisting forces are produced as proportional to the amplitude of the processed sEMG signals [82–85]. Using this approach, the robotic assistive device can be fully controlled by the user as long as the model relating to the assistive joint torques with the sEMG signals from the muscles can be accurately established.

Even though this control algorithm is highly beneficial, there are some intrinsic limitations associated with sEMG signal practical applications. For instance, the sEMG signals are highly sensitive to the placement of electrodes on the skin, skin properties (e.g. sweat, body hair, blood circulation, etc.), electrical noises from other devices, and interference from neighboring muscle signals. The sEMG signals are also dependent on the overall neurologic condition of each individual. Hence, the sEMG parameters should be calibrated for each individual and recalibrated for every training session, which makes it a tedious and time-consuming process [86]. Additionally, for patients with severe strokes, their sEMG signals

could either be too weak or abnormal. The abnormal and uncoordinated muscle activity patterns can result in undesired responses by the robotic assistive device. This introduces a safety challenge for rehabilitative gait training and assistance for lower extremities. Therefore, the EMG-based control is mainly applied in the rehabilitation of upper extremities and not lower extremities in their current stage of the application.

### 2.3.2 Gait Phase Detection-based Control

Gait phase detection techniques employ different types of sensor information to detect walking phases [87–90] and the transitions between two adjacent gait phases can be used to estimate the human intended motion in the coming gait phase. Then, an appropriate amount of assistance can be provided to the user in the proper direction to fulfill the envisioned motion during the specific phase. This is the fundamental concept behind the gait phase detection-based control for assistive devices.

Some assistive devices have already exploited this control algorithm to offer timely assistance to users. The HAL, for example, implements a “cybernic autonomous control” algorithm that employs ground reaction forces and joint angles as motion information to detect a user’s gait phases. This control approach has been proved to provide effective physical support for healthy individuals and also for stroke patients. Specifically, the HAL 3 broadly classifies the walking cycle to support phase and swing phase based on some thresholds of the ground reaction forces and joint angles. In each phase, constant torques are applied to provide assistance to hip and knee joint [81]. Recently, the HAL 5 applies the similar threshold method to apportion further the walking motion into three phases: swing phase, landing phase and support phase [91]. The reference hip and knee joint patterns are derived from healthy subjects and the employed in generating



the assistive torque required for every phase. The Vanderbilt exoskeleton employs a similar control mechanism that utilizes the estimated pressure center to implement a finite state machine to transition from one motion state to the other motion state [60]. During walking, the gait is categorized in two phases: the stance and swing phase. In each of these phases, a high-gain trajectory-based control is employed. In general, the gait phase detection-based control is capable of offering the user more autonomy over the assistive devices.

The above gait phase detection-based control still has room for improvement. During gait detection, the threshold based method could be inaccurate and result in robustness issues in the presence of sensor noise. Also the classification of the gait to two or three phases is still an oversimplification considering that stance and swing can also be further divided into several sub-gait periods based on the walking gait functionalities [92]. From the perspective of assistance, the assistive controller based on either constant torques or reference gait patterns additionally causes some issues. Constant assistance does not take into consideration the gait dynamics, which discomforts the user. The reference gait tracking pattern-based assistance still has synchronicity problems particularly in the swing phase.

## 2.4 Chapter Summary

In this chapter, we give an overview of two major groups of assistive devices for lower extremity, namely treadmill gait trainers and wearable overground gait trainers. Their major control strategies used in rehabilitative gait training and gait assistance have also been discussed. Although several assistive devices are commercially available, they are still expensive making out of reach for the patients and they still have limited functionality. Therefore, they are still mainly being used in hospital settings.



To achieve the objectives of home-based gait training, low-cost, lightweight and wearable lower extremity assistive devices should be developed. Most importantly, the device should incorporate different control strategies so as to fit into the different rehabilitation stage in stroke patients. These goals will be preliminarily achieved in the following stages of this study. The next chapter will succinctly introduce a lower extremity assistive device developed in the lab, and the follow up chapters will concentrate on three intuitive and robust control algorithms used in rehabilitative gait training and gait assistance, respectively.

# Chapter 3

## Hardware Architecture

This chapter is focused on the hardware architecture of an anthropomorphic under actuated lower extremity assistive device developed in the lab. Section 3.1 will firstly describe the design of the lower extremity assistive device, specifically including some important design considerations, the harmonic drive joint actuator design and the overall electrical architecture. The final experimental prototypes based on these design specifications will also be presented in this section. Next, Section 3.2 will present a friction compensation algorithm for the customized harmonic drive joint actuator to increase the transparency of the device. Lastly, a brief chapter summary will be provided in Section 3.3.

### 3.1 Lower Extremity Assistive Device

The primary function of the developed lower extremity assistive device is to support the post-stroke patients to carry on gait rehabilitation training and also assist them in their daily walking tasks. Desired features of the assistive device include anthropomorphic structure, light weight and portability. Moreover, it would be desirable that the device could be adjusted to fit for a range of users.

Since the existing devices are still too expensive to those who need them, building a low-cost device is of utmost importance. The following section will cover some specific design considerations required to build the assistive device. For brevity as well as confidentiality, only the main ideas will be presented.

### 3.1.1 Design Considerations

Some important design considerations must be taken into account, including the degree of freedom, range of motion, power and torque requirements, adjustability and attachment. These factors will be discussed as follows.

#### 3.1.1.1 Degree of Freedom

The lower extremity assistive device under development should be highly anthropomorphic. The hip and knee joints will be designed as actuated joints, and the ankle joints will not be designed in order to keep overall swing weight of the leg low. If the ankle support is necessary in the future, a passive ankle joint can be designed and attached to the device. For the hip joint, the flexion/extension degree of freedom will be actuated, while the abduction/adduction degree of freedom will be left as passive. For the knee joint, the only degree of freedom is flexion/extension, which will be actuated. This is illustrated in Fig. 3.1.

#### 3.1.1.2 Range of Motion

The joint ranges of motion for the assistive device must be within the normal human ranges of motion during activities of daily living (ADL). The data for human normal range of motions can be found by examining the Clinical Gait Analysis (CGA) data during normal walking [92] and normal stair ascent and descent [93]. To ensure safety, the device range of motion should not exceed the user's range of motion [94]. Therefore, each actuated joint has to be designed

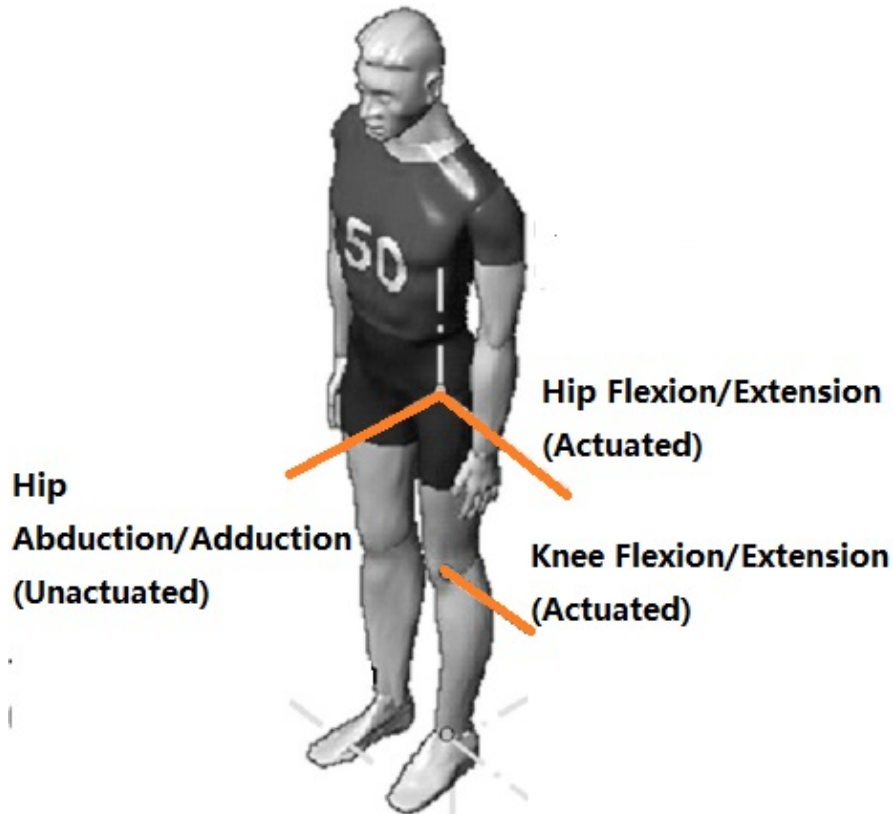


Figure 3.1: Degrees of freedom

with mechanical limits, which make its range of motion slightly less than human's maximum range of motion to prevent hyperextension or hyper-flexion of the joint. Table 3.1 lists the range of motion for the actuated degrees of freedom of the device as compared to that for a human under various locomotion modes.

### 3.1.1.3 Power and Torque Requirements

The joints involved in the sagittal motion consumes the most power during level walking [92] and normal stair ascent and descent [93] based on the clinical gait analysis data. Fig. 3.2 shows the typical profile of the kinematics, moments and powers of the hip and knee joints in a gait cycle during level walking. For the

Table 3.1: Range of motion [92–94]

	Level Walking	Stair Ascent	Stair Descent	Device Max.	Human Max.
Hip Flexion	28.4°	57.2°	35.1°	130°	140°
Hip Extension	14.1°	8.72°	8.40°	15°	45°
Knee Flexion	58.1°	100°	106°	130°	160°
Knee Extension	1.80°	0.86°	0.7°	0°	2°

following analysis, the data will be scaled for a 57.7-kg user, which is the average weight of a human of Asian origin [95].

For the hip joints during level walking, an extensor moment is observed during late swing and early stance for deceleration of the leg and body load support respectively. And an flexor moment is observed during late stance and early swing to propel the body forward. The maximum values of the hip torque are quite symmetrical, 38.0 *Nm* for the flexion and 39.2 *Nm* for the extension. The average power is slightly positive with most effort being spent on body or limb forward propulsion.

For the knee joint during level walking, an extensor moment is observed during early stance since the knee absorbs the impact during heel contact. This corresponds to the negative power region because the knee flexes while the knee moment is extending. During the rest of stance, the knee torque is very small owing to its ability to lock itself during load bearing. Additionally, the torque generating significant knee flexion during early swing is not noteworthy from the observation of knee moment. Overall, the average power is negative, which prompts the use

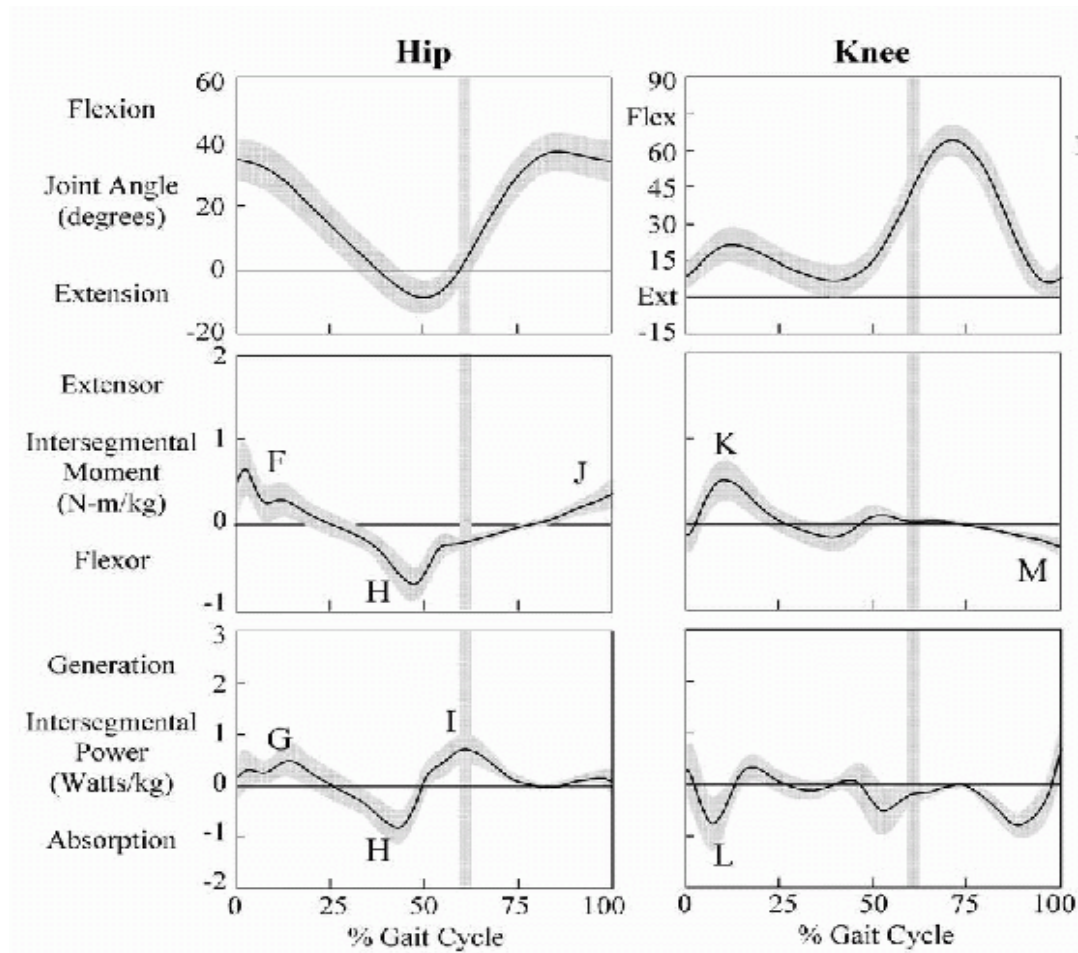


Figure 3.2: Sagittal plane joint angles, moments and powers for the hip and knee during level walking [92]

of a passive damper in many knee prosthetic devices. However, if the stair ascent is concerned, the power required by the knee is largely positive since there is a need for antigravity activity. The maximum of the knee torque derived from stair ascent is  $19.4 \text{ Nm}$  for the flexion and  $83.0 \text{ Nm}$  for the extension.

Considering the size and weight, the joint actuator will be designed to be able to support the whole level walking task and a fraction of the maximum torque required for other tasks like stair ascent and descent. Supporting an amount of the torque requirement is not an issue because the device is meant to help users

instead of taking over the task. Additionally, to ensure safety the gear ratio will be kept small to ensure fundamental joint back-drivability. The joint actuator design and its specifications will be presented in Section 3.2.

### 3.1.1.4 Adjustability

As the assistive device will be worn by users with different physical sizes, thigh and shank sections of the assistive device have to be adjustable. The variation of the length required for each section is derived from the study [96]. To capture most of the population, the anthropometrical data of 5<sup>th</sup> and 95<sup>th</sup> percentiles are used, as shown in Table 3.2.

Table 3.2: Anthropometrical data of Singapore’s males

	Value at 5th Percentile (cm)	Value at 95th Percentile (cm)
Hip to Foot Height	86	106
Knee to Foot Height	49	58
Hip to Knee Height	37	48
Hip Breath	32	39

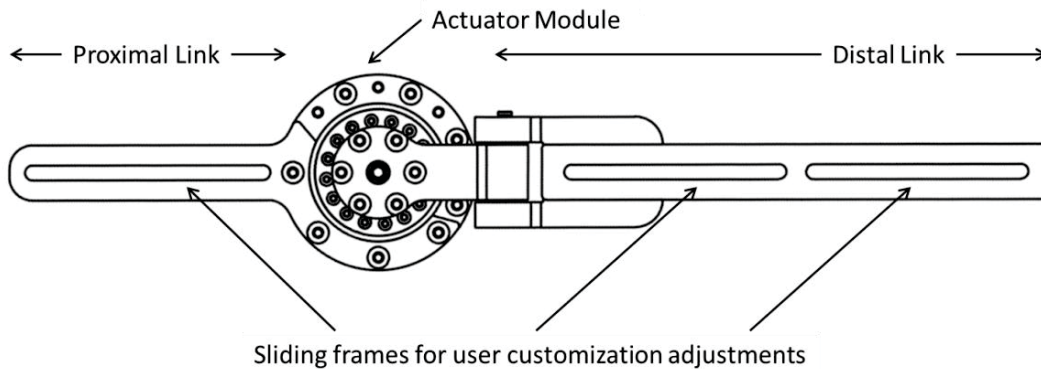


Figure 3.3: Sliding frame mechanisms for user customization adjustments

The assistive device incorporates a sliding frame mechanism that is capable of adjusting link length to fit a range of users, as depicted in Fig. 3.3.

### 3.1.1.5 Attachment

Attachment of the assistive device is quite important because close coupling between the assistive device and the user is required in order to deliver effective assistance to the user. However, the user's soft tissues are very sensitive and susceptible to bruising and damage even with low pressures over a few hours. There is considerable knowledge and experience embedded in the fields of orthotics and prosthetics, which have been addressing the problems of applying significant forces to the skeleton while keeping skin loading to acceptable levels. Fig. 3.4 shows an example of off-the-shelf orthotic cuffs (Newport 3 Hip Orthosis, Orthomerica [97]), which can be used as the attachment interface for the developed assistive device.



Figure 3.4: Off-the-shelf orthotic cuffs [98]



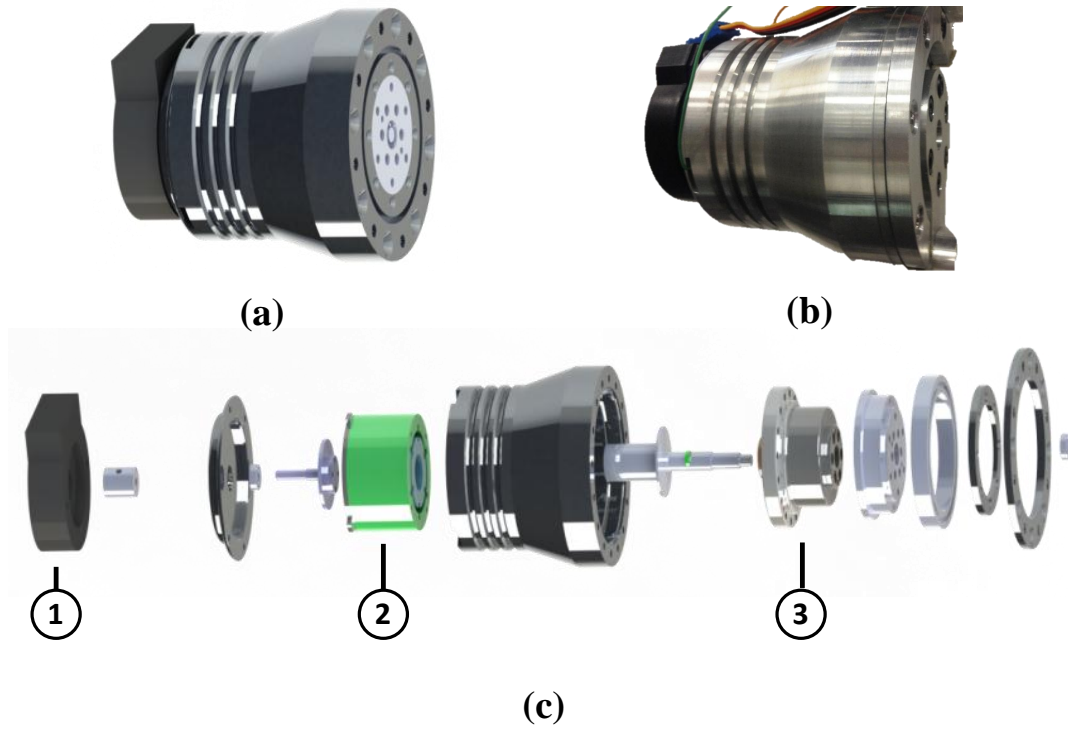


Figure 3.5: Customized electric joint actuator (key components include: 1. incremental encoder; 2. DC frameless motor; 3. Harmonic Drive gear)

### 3.1.2 Joint Actuator Design

Conventional actuators are those that are common for robotic manipulators. There are three major types: electromagnetic (electric motors), pneumatic, and hydraulic. All these actuators have been applied for the assistive devices [99–101]. Pneumatic and hydraulic actuators have high power densities, but they necessitate the use of external pulp systems. They are also bulky and cannot be easily controlled. Electrical motors meet the device power and torque criteria in addition to offering a portable and compact solution for the wearable device. Therefore, electric motors will be used to customize the joint actuators.

Minimizing the size and weight of the joint actuator heavily guided the electric motor and gearing selection. The selected motors are DC frameless high-torque motors (Kollmorgen QT-1406) with relatively large diameter and small width.

They have separate rotor and stator, which can be tightly integrated into a customized mechanical housing structure. This design structure can introduce high portability. However, it must meet the required mounting tolerances and provide necessary bearings. For gearing, harmonic drives are selected due to their large torque capacities, high gear ratios and highly compact size. The CSG series harmonic drives (Harmonic Drive Systems) with gear ratio 50 are specifically selected since they have relatively small width and they are also available as bare components, like the motor, which can be closely integrated into the mechanical housing structure. Lastly, the rotary optical incremental encoders (US Digital) are incorporated to measure the motor shaft angle, from which the joint angle can be calculated. The rotary optical encoder is installed at the back of the actuator. Additionally, several bearings are introduced into the structure to offer support to the rotating components of the electric joint. Fig. 3.5 illustrates the final customized harmonic drive joint actuator design, and Table 3.3 provides the specifications of the actuator.

Table 3.3: Harmonic drive actuator specifications

Joint weight	0.98 Kg
Joint size	95 mm(D), 90 mm(L)
Maximum momentary torque	55 Nm
Maximum continuous torque	35 Nm
Maximum Power	347 W
Maximum output speed	60 RPM

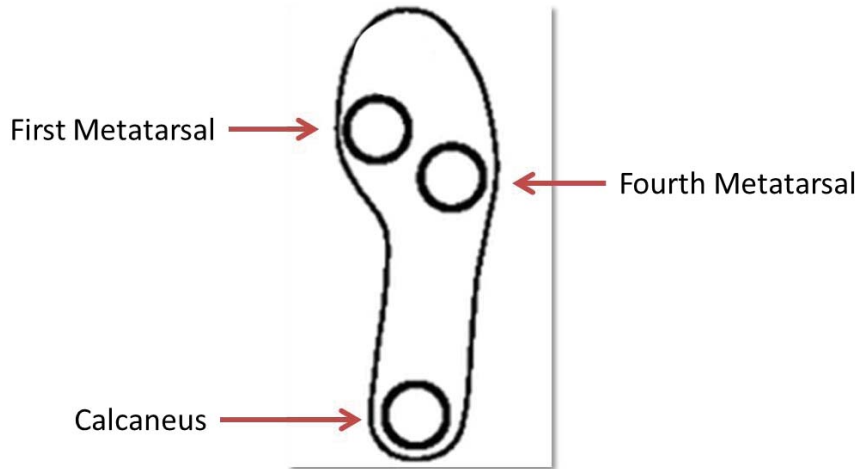


Figure 3.6: Placement of resistive force sensors

### 3.1.3 Electrical Architecture

The assistive device employs the sbRIO-9612 board (National Instruments) as its main processor. It is a reconfigurable embedded data acquisition and control board, which consists of a 400 MHz real-time processor, a 2M-gate reconfigurable field-programmable gate array (FPGA), and some digital and analog I/Os.

Besides the optical incremental encoders, several other types of sensors can also be incorporated into the device to help control and evaluate the device, which include surface-EMG sensors (SX230, Biometrics), resistive force sensors (A401, Tekscan) and accelerometers (CSL04LP3, Crossbow). The resistive force sensors are attached to the insole of the subjects shoe at the first and fourth metatarsal, and the calcaneus positions to measure front, mid and back Ground Reaction Force (GRF), as illustrated in Fig. 3.6. The sEMG, GRF, and acceleration measurements are all analog signals, and they can be directly connected to the analog-to-digital (AD) inputs of the sb-RIO.

The joint actuators are controlled by digital servo drives (Solo-Whistle, ELMO Motion Control) with encoder feedbacks. All the digital servo drives are then connected to a high-speed CAN module (NI 9853, National Instruments), which is

attached to the sb-RIO through CAN bus. CAN communication is implemented at a rate of 1Mbps/s based on CANopen Communication Protocol 2.0A. The electrical hardware, as well as their connections, are illustrated in Fig. 3.7, and the overall electrical architecture is shown in Fig. 3.8.

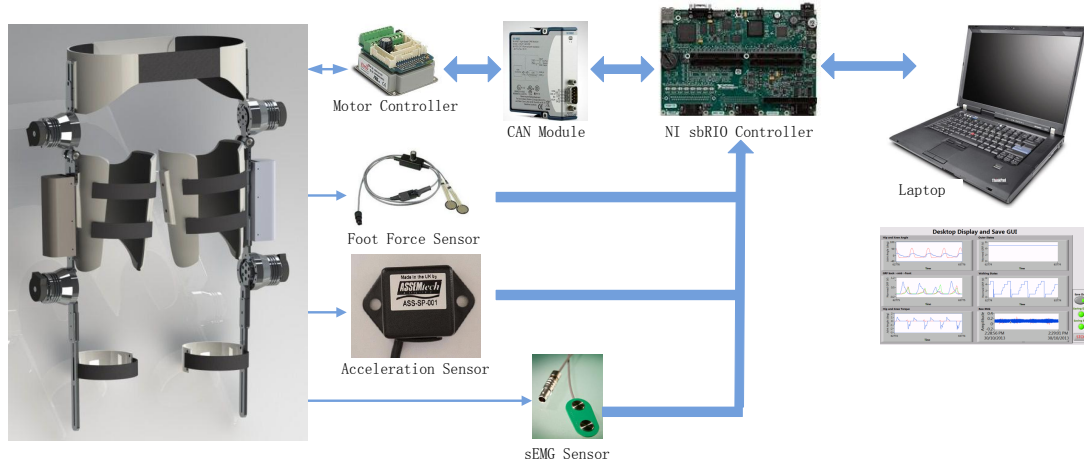


Figure 3.7: The electrical hardware

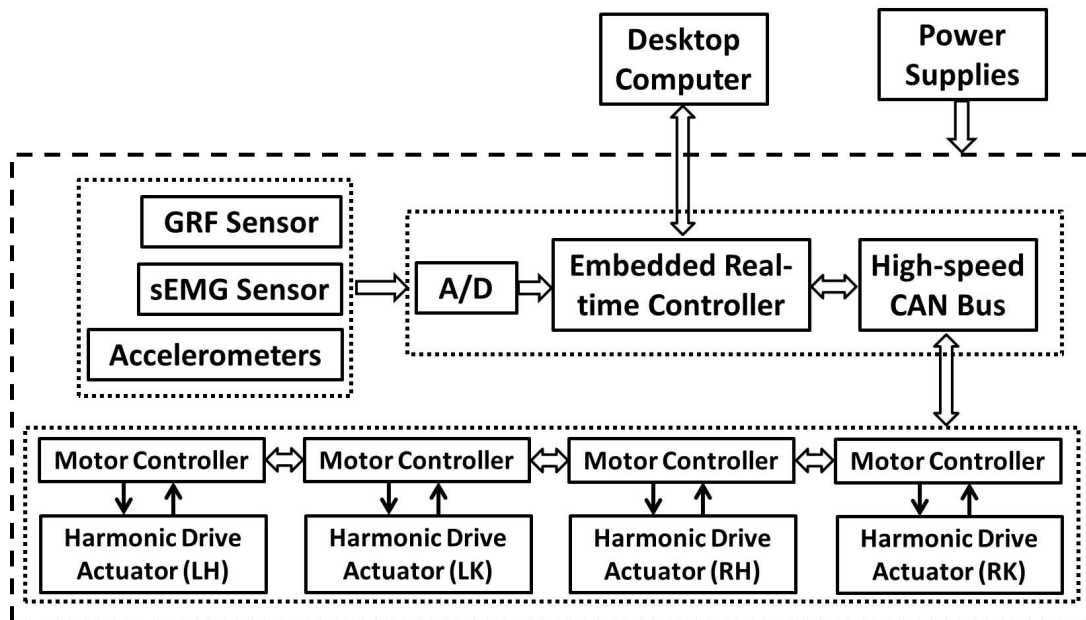


Figure 3.8: The electrical architecture

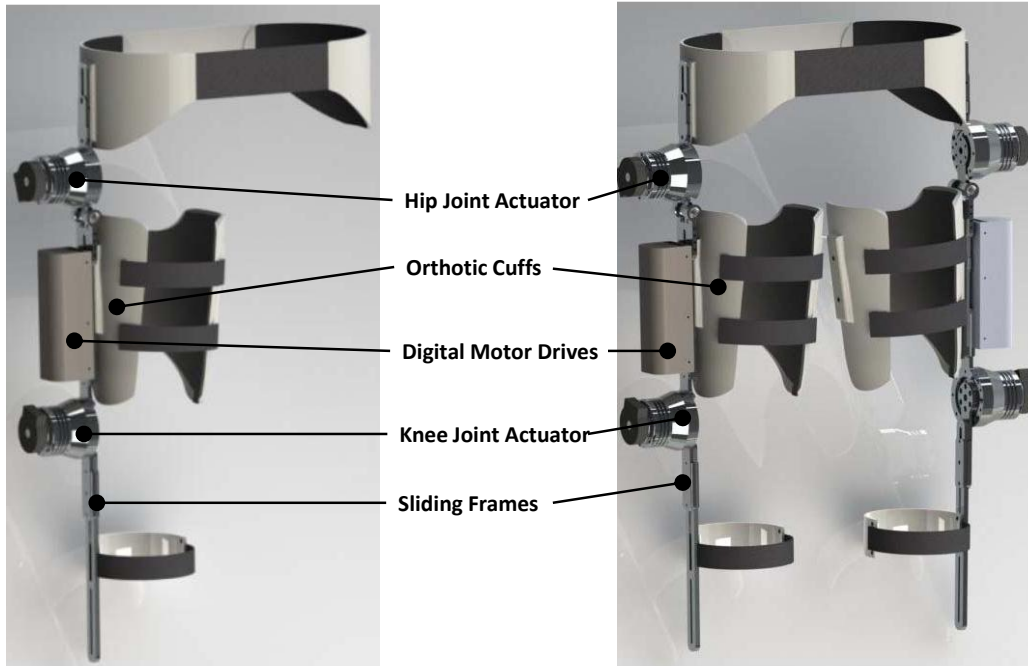


Figure 3.9: The first prototype of lower extremity assistive device: single-leg version and double leg-version

### 3.1.4 Final Experimental Prototypes

Based on the above mechanical design guidelines and the electrical architecture, the first prototype was developed in the lab. The prototype has a single-leg version and a double-leg version, as illustrated in Fig. 3.9. Harmonic drive joint actuator modules are attached to the hip and knee joints to provide active assistance. There are no ankle joints designed for this prototype. Orthotic cuffs are used as the attachment interface, and the sliding frames located at thigh and shank can be adjusted to fit a range of users with different physical sizes. Additionally, this prototype is powered by external power supply source. The power source and embedded controller board are placed at a remote station. Hence, this prototype can be used as a standalone assistive device. The weight of the single-leg version is around 5 kg, and the double-leg version is around 8 kg.

There are some drawbacks with the hardware of the first prototype. Firstly,

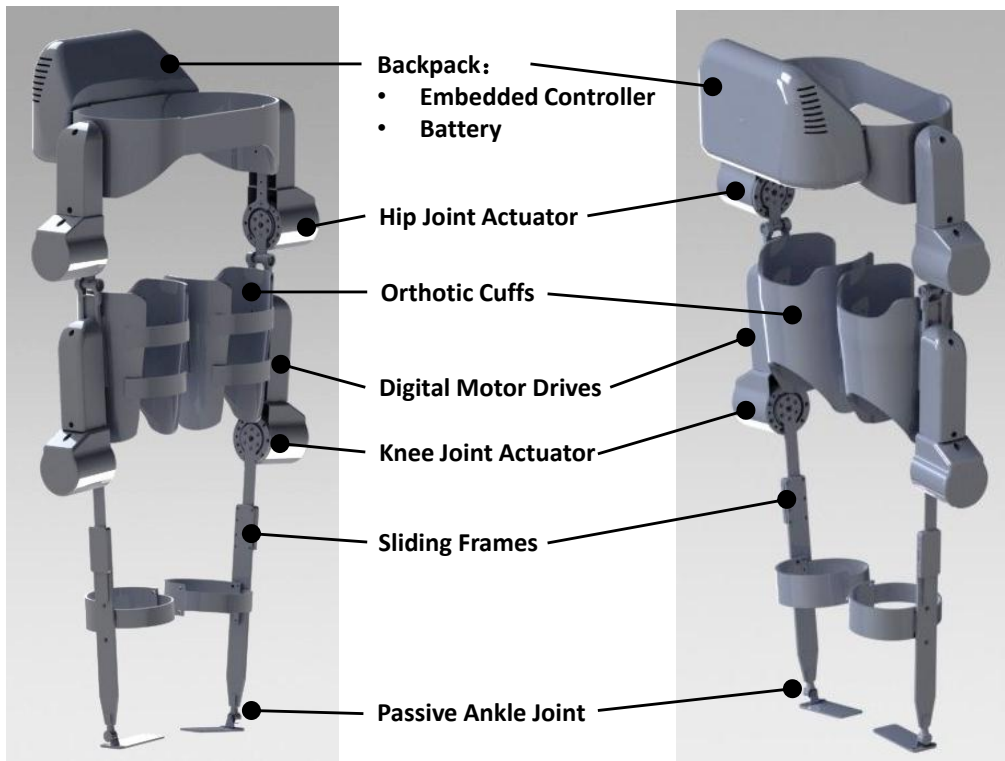


Figure 3.10: The second prototype of lower extremity assistive device

the weight of the entire device is supported by the user’s waist, which could easily discomfort and fatigue the user. Secondly, it is not a standalone device with the controller and battery backpack. Last but not least, the weight and the exterior appearance can still be optimized and improved.

Taking into account of these factors, the improvements were made to the first prototype to develop the second prototype as seen in Fig. 3.10. A passive ankle joint with three degree-of-freedom is designed to ground the weight of the device. A backpack is included around the waist to carry the controller and the battery. Finally, 3D printed covers are used to hide the wires and improve exterior appearance, and the structures are also optimized to reduce the weight. The total weight of the second prototype is around 11 kg. The total costs are less than S\$30,000, which is much cheaper than those similar products available in the market.

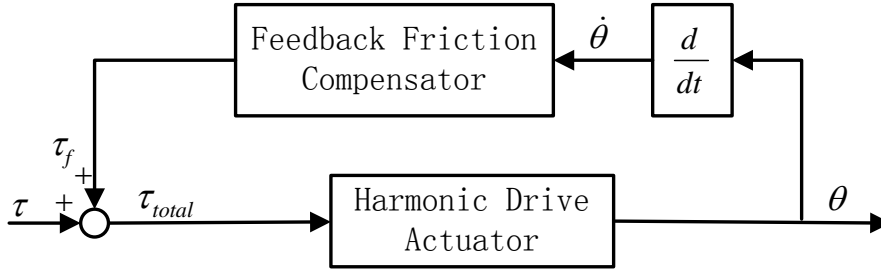


Figure 3.11: A model-based feedback friction compensation scheme for harmonic drive actuator

## 3.2 Friction Compensation for Harmonic Drive Actuator

As described in Section 3.1.2, the customized harmonic drive joint actuator consists of a DC frameless high-torque motor with a high gear-ratio harmonic drive. This joint actuator could provide high output torque, however, its design also inherently introduces substantial internal friction. This would decrease the back-drivability of the actuator under free motion. Moreover, the inherent friction also affects the performance of the high-level controller. Therefore, prior to the development of any high-level control algorithm, it is mandatory to perform the low-level friction compensation for the harmonic drive joint actuator.

There is no output torque sensor employed in the current joint actuator design. Therefore, the most straight forward solution of using torque feedback to compensate friction cannot be applied. The friction compensation technique used in this study is a model-based feedback friction compensation scheme [102]. Specifically, we feed-forward the predicted friction torque to the controller using the friction model obtained from multiple experiments, as shown in Fig. 3.11. The exponential friction model is selected as the friction model. This model provides a more general description of friction force, especially in the low velocity range as it consists of the Stribeck effect. Stribeck effect is the phenomenon whereby the

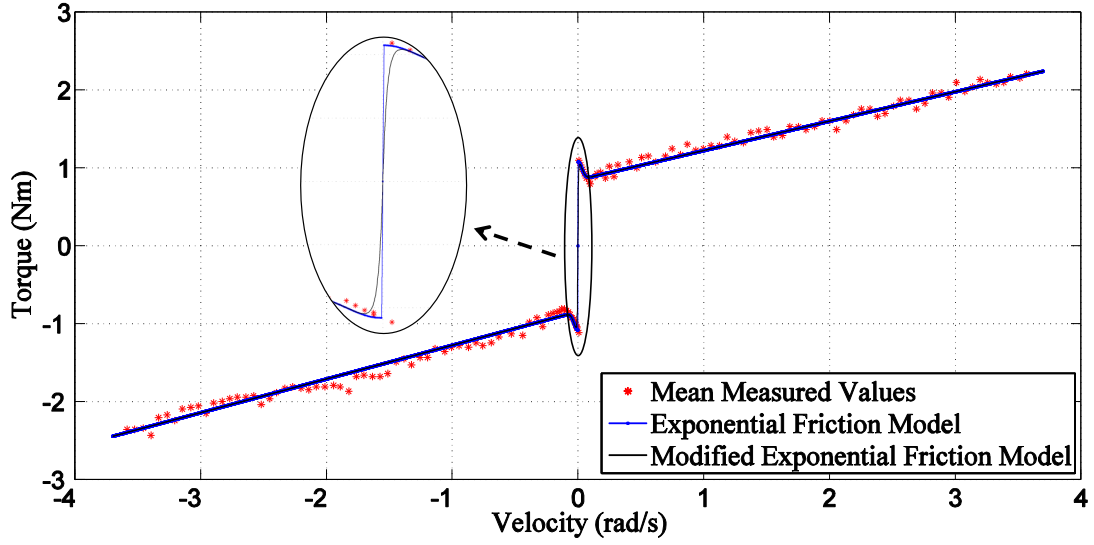


Figure 3.12: Frictional torque in a harmonic drive actuator (left knee joint) as function of its rotational velocity

friction force in low-velocity range increases as a continuous function velocity as the velocity decreases.

The exponential friction model has the following form

$$\tau_f = (\alpha_0 + \alpha_1 \exp -(\dot{\theta}/v_s)^2) \text{sgn}(\dot{\theta}) + \alpha_2 \dot{\theta} \quad (3.1)$$

where  $\tau_f$  is the predicted frictional torque,  $\dot{\theta}$  refers to the rotational velocity of the actuator, and  $\alpha_0$ ,  $\alpha_1$ ,  $\alpha_2$  and  $v_s$  are the four coefficients identified by experiments. In particular,  $\alpha_0$  represents the coefficient of Coulomb friction,  $\alpha_1$  represents the coefficient that describe the difference between the stiction and Coulomb friction,  $\alpha_2$  presents the coefficient of viscous friction, and  $v_s$  refers to the Stribeck velocity which is the velocity range where Stribeck effect is observed.

Fig. 3.12 depicts the friction torque to velocity data collected by experiments conducted on the harmonic drive joint actuator from left knee joint. The mean values of the measured torque are obtained from multiple experiments. They are



used to perform the curve fitting in Curve Fitting Toolbox of Matlab to obtain the unknown model coefficients.

It also can be observed from Fig. 3.12 that the friction-velocity map has a near infinite slope at zero velocity. Such an slope causes high sensitivity to minor deformation of the motor and the noises in the velocity measurement, resulting in chattering problems. This issue can be solved through modification of the friction-velocity map through multiplication of the map by a term  $(1 - \exp(-|\dot{\theta}|k_s))$  to decrease the slope around zero velocity, where  $k_s$  is the slope adjustment factor. However, the decrease in the slope reduces the performance of friction compensation. Therefore, a compromise between friction compensation performance and suppression of chattering is required to determine  $k_s$  properly.  $k_s$  is chosen by trial and error through experiments. Table 3.4 shows the final fitting coefficients of the exponential model for different joint actuators. Once the friction model coefficients are obtained, then they can be implemented in the feedback friction compensation scheme, as shown in Fig. 3.11, and nearly complete friction compensation can be attained.

Table 3.4: Fitting coefficients of exponential friction model for each joint actuator

Parameter	Left Hip	Left Knee	Right Hip	Right Knee
$\alpha_0$ [Nm]	1.4950	0.8440	1.0600	0.9682
$\alpha_1$ [Nm]	0.4392	0.2349	0.4906	0.2869
$\alpha_2$ [Nm rad <sup>-1</sup> s]	0.4731	0.4327	0.5090	0.4777
$v_s$ [rad s <sup>-1</sup> ]	0.0480	0.0427	0.0768	0.0443
$k_s$ [rad <sup>-1</sup> s]	300	300	300	300

### 3.3 Chapter Summary

In this chapter, the design considerations for developing a light-weight, wearable lower extremity assistive device are firstly discussed, namely the degree of freedom, range of motion, power and torque requirements, adjustability and attachment. Then the joint harmonic drive actuator design and electrical architecture are presented. Based on these design considerations, two prototype versions of lower extremity assistive device are successfully developed in the lab. Lastly, the friction compensation scheme for the harmonic drive joint actuator are also studied.



# Chapter 4

## FAT-based Adaptive Gait

## Trajectory Tracking Control

In this chapter, the Function Approximation Techniques (FAT) based adaptive gait trajectory tracking control strategy will be presented. It intends to aid those stroke patients who are in the early stage of rehabilitation to perform passive gait training. Preliminary evaluations through simulation and physical implementation will also be presented. This remainder of this chapter will be structured as follows. Section 4.1 will give a brief introduction. Section 4.2 will derive a simplified dynamics model for controller derivation and simulation purposes. Section 4.3 will present hip and knee reference trajectory generation using Fourier series fitting method. Then in Section 4.4, the FAT-based adaptive control scheme will be developed. This control scheme will be tested and verified by hip and knee trajectory tracking performance through simulations in Section 4.5 and physical implementation on a healthy subject in Section 4.6, respectively. Lastly, Section 4.7 summarizes this chapter.

### 4.1 Introduction

The position-controlled passive gait training is well suited for the stroke patients who are in the early stage of rehabilitation. Most commercialized assistive devices for gait rehabilitation have adopted this kind of position-controlled gait training. Hence, for our developed assistive device, the gait trajectory tracking control strategy using the position-based controller will be firstly developed.

The proportional-derivative (PD) computed torque controller is a widely applicable position controller in robotics. However, its accuracy is dependent on the precision of dynamics model. In this application, the assistive device could be attached to various users, making it difficult to obtain a precise dynamics model with different users. Even though the dynamics model is satisfactorily accurate, some parameters of interest such as the center of link mass and the moment of inertia cannot be precisely measured in reality. Due to this shortcoming, different adaptive control approaches are proposed, among which Slotine and Li's approach [103] has been widely used because it gets rid of acceleration feedback and avoids singularity problem. Nonetheless, it still needs to derive regressor matrix, and the derivation of this matrix is usually tedious and its computation in real applications is quite time-consuming. Huang and Chen [104, 105] proposed another adaptive controller based on function approximation techniques, which is a regressor free and computation-efficient adaptive control approach. This adaptive controller has demonstrated its feasibility in the control of industrial robot manipulators [106]. In this chapter, we would apply this FAT-based adaptive controller to the lower extremity assistive device for passive gait rehabilitation training and demonstrate its feasibility via simulation and physical implementation.

## 4.2 Dynamics Modelling

The developed assistive device is actuating on the hip and knee joint. We assume it is perfectly fixed with human thigh and shank. Hence, it can be considered that the human lower limb and the assistive device is one entire system, and the human active joint torques can act as external torques to this system. Under these assumptions, the system dynamics model can be greatly simplified. This simplified model will only be employed for controller derivation and simulation purposes. The adaptive controller design in Section 4.4 does not depend on this model. Additionally, it is assumed that the user's torso is suspended to allow for passive gait training.

The coordinate frames are defined as shown in Fig. 4.1. With regards to Steiner's Theorem [107], masses can be concentrated at the center of the link, and the equivalent masses are denoted as  $m_1$  and  $m_2$ . The joint angular variables are defined as  $\theta = [\theta_1, \theta_2]^T$ , the actuator torques are denoted as  $\tau = [\tau_1, \tau_2]^T$ , and the human active joint torques are denoted as  $\tau_h = [\tau_{h1}, \tau_{h2}]^T$ . Finally, the length of the links are denoted by  $L_1$  and  $L_2$ , respectively.

The dynamics model of this two link limb-device system in the joint space has the following form

$$D(\theta)\ddot{\theta} + C(\theta, \dot{\theta})\dot{\theta} + G(\theta) = \tau + \tau_h \quad (4.1)$$

where  $D(\theta) \in R^{2 \times 2}$  represents the joint-space inertia matrix,  $C(\theta, \dot{\theta}) \in R^{2 \times 2}$  denotes the Centripetal and Coriolis matrix, and  $G(\theta) \in R^2$  represents the gravitational components.

Through the Euler-Lagrange approach (derivation procedures seen in Appendix), the matrices  $D(\theta)$ ,  $C(\theta, \dot{\theta})$ , and  $G(\theta)$  can be derived as

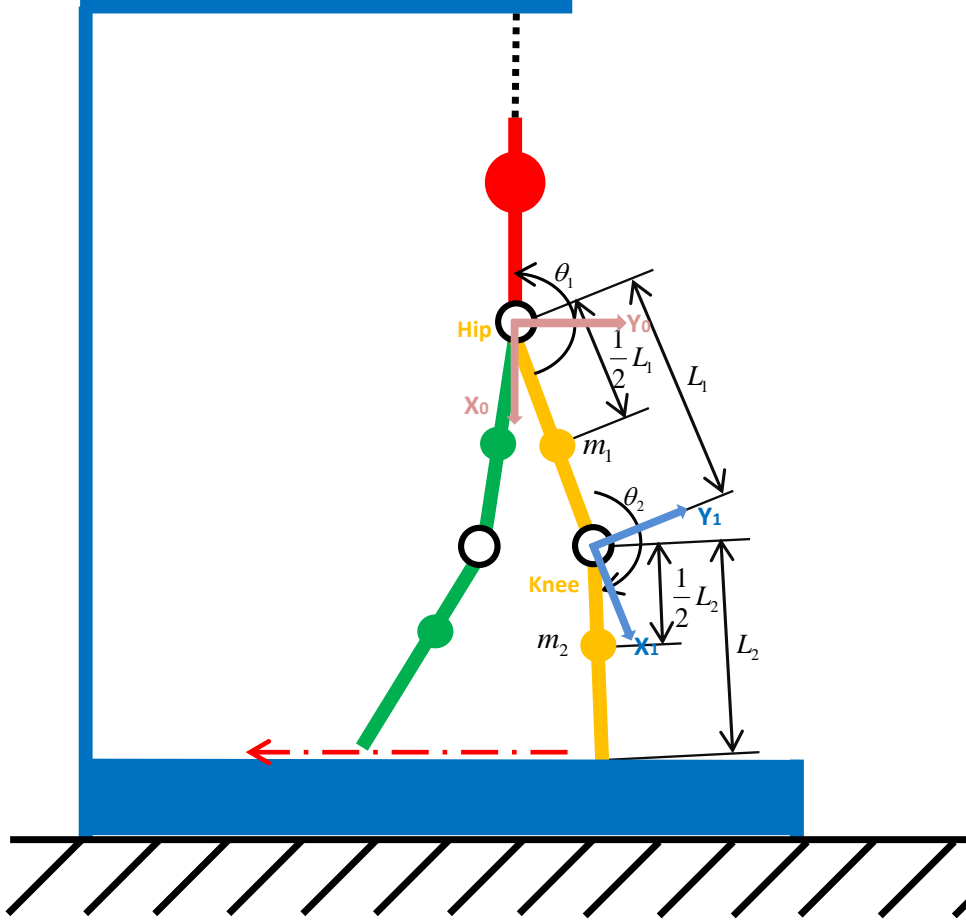


Figure 4.1: A simplified two link model

$$D(\theta) = \begin{bmatrix} \left( \frac{1}{4}m_1 + m_2 \right)L_1^2 + \frac{1}{4}m_2L_2^2 + m_2L_1L_2 \cos \theta_2 & \frac{1}{4}m_2L_2^2 + \frac{1}{2}m_2L_1L_2 \cos \theta_2 \\ \frac{1}{4}m_2L_2^2 + \frac{1}{2}m_2L_1L_2 \cos \theta_2 & \frac{1}{4}m_2L_2^2 \end{bmatrix} \quad (4.2)$$

$$C(\theta, \dot{\theta}) = \begin{bmatrix} -\frac{1}{2}m_2L_1L_2 \sin \theta_2 \dot{\theta}_2 & -\frac{1}{2}L_1L_2 \sin \theta_2 (\dot{\theta}_1 + \dot{\theta}_2) \\ \frac{1}{2}m_2L_1L_2 \sin \theta_2 \dot{\theta}_1 & 0 \end{bmatrix} \quad (4.3)$$

$$G(\theta) = \begin{bmatrix} \left( \frac{1}{2}m_1gL_1 + m_2gL_1 \right) \sin \theta_1 + \frac{1}{2}m_2gL_2 \sin(\theta_1 + \theta_2) \\ \frac{1}{2}m_2gL_2 \sin(\theta_1 + \theta_2) \end{bmatrix} \quad (4.4)$$

### 4.3 Gait Trajectory Generation

Implementing position-based gait trajectory tracking control strategy requires the desired gait trajectories to be specified. Therefore, the reference gait trajectories will be obtained before the development of the controller. In this work, we use the normal hip and knee gait trajectories from healthy subjects that are provided by reference [108]. One cycle of hip or knee gait trajectory can be approximated by fifteen terms of Fourier series as described in Eq. (4.5), where  $a_0$ ,  $a_j$ ,  $b_j$  and  $w$  ( $j = 1 \cdots 7$ ) are curve fitting parameters obtained through Matlab,  $x$  represents the gait cycle, and  $\theta_{hip/knee}$  denotes the gait angle in degrees. Table 4.1 shows the Fourier series parameters for hip and knee points, and Fig. 4.2 shows the fitting results. It is observed that good fitting results with small errors can be obtained through this approach.

Table 4.1: Fourier series fitting results

Parameters	$a_0$	$a_1$	$b_1$	$a_2$	$b_2$	$a_3$	$b_3$	$a_4$
Hip	17.63	20.16	-3.356	-3.09	-1.422	0.02337	1.325	-0.1398
Knee	25.59	-3.313	-18.79	-12.84	6.821	-0.3184	3.738	-0.8908
Parameters	$b_4$	$a_5$	$b_5$	$a_6$	$b_6$	$a_7$	$b_7$	$w$
Hip	-0.1995	0.02123	0.1208	0.09569	0.05315	-0.09582	-0.07109	6.28
Knee	0.3473	-0.5027	0.422	-0.1007	0.09104	0.05284	-0.02913	6.28

$$\theta_{hip/knee}(x) = a_0 + \sum_{j=1}^7 a_j \cos(jxw) + \sum_{j=1}^7 b_j \sin(jxw) \quad (4.5)$$



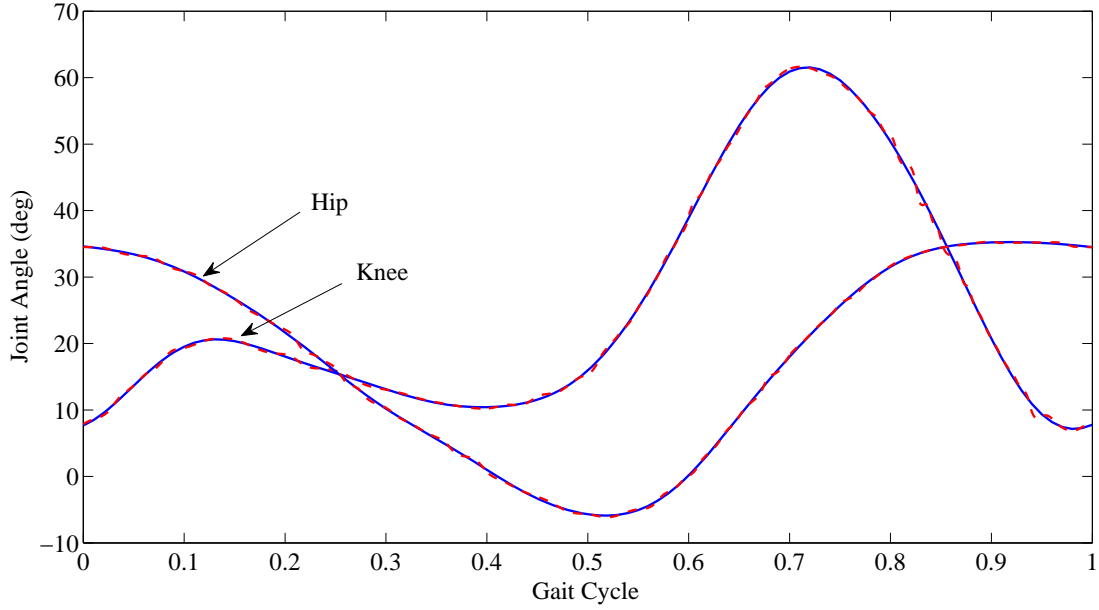


Figure 4.2: Normal gait trajectory fitting results: normal hip and knee trajectories are plotted in red dashed lines, and fitting hip and knee trajectories are plotted in blue solid lines

In order to fit the trajectories to various subjects and alter the gait cycle time, several terms of parameters were incorporated to yield the final desired gait trajectories  $\theta_d$  in Eq. (4.6), whereby  $A$  represents amplitude scaling,  $B$  represents amplitude offset, and  $T$  represents gait cycle time. These parameters can be adjusted by users. The achieved trajectories as well as their first and second order derivatives can be employed as reference trajectories in the following section.

$$\theta_d(t) = A\theta_{hip/knee}\left(\frac{t}{T}\right) + B \quad (4.6)$$

## 4.4 FAT-based Adaptive Controller

This gait trajectory tracking control applies for those stroke patients who are in early stage of rehabilitation or are severely affected by the stroke. Hence, we

can assume they are completely passive, and the human active torques would be zeros. The dynamics model Eq. (4.1) from Section 4.2 can be further simplified to the following Eq. (4.7) for controller derivation.

$$D(\theta)\ddot{\theta} + C(\theta, \dot{\theta})\dot{\theta} + G(\theta) = \tau \quad (4.7)$$

The desired reference gait trajectory obtained from Section 4.3 is represented by  $\theta_d$ , while the tracking error is denoted as  $e = \theta - \theta_d$ . A new error vector is defined as  $s = \dot{e} + \Lambda e$ , where  $\Lambda = \text{diag}(\lambda_1, \lambda_2)$  with  $\lambda_i > 0$  ( $i = 1, 2$ ). By this definition, the convergence of  $e$  can be implied from the convergence of  $s$ . The dynamics model Eq. (4.7) can be rewritten as

$$D\dot{s} + Cs + G + D\ddot{\theta}_d - D\Lambda\dot{e} + C\dot{\theta}_d - C\Lambda e = \tau \quad (4.8)$$

Suppose the model parameters can be known, an intuitive model based controller can be selected as

$$\tau = D\ddot{\theta}_d - D\Lambda\dot{e} + C\dot{\theta}_d - C\Lambda e + G - K_d s \quad (4.9)$$

where  $K_d$  is a diagonal positive definite matrix.

Hence, the closed-loop system becomes

$$D\dot{s} + Cs + K_d s = 0 \quad (4.10)$$

Define a Lyapunov function candidate as  $V = \frac{1}{2}s^T Ds$ , and then  $\dot{V} = -s^T K_d s + \frac{1}{2}s^T (\dot{D} - 2C)s$ . Since  $\dot{D} - 2C$  is skew-symmetric,  $\dot{V} = -s^T K_d s \leq 0$  with  $K_d$  as a diagonal positive definite matrix. It can be proved that  $s$  is uniformly bounded and square integrable, and  $\dot{s}$  is uniformly bounded. Hence,  $s \rightarrow 0$  as  $t \rightarrow \infty$ . Therefore, the tracking error  $e$  converges asymptotically.

## Chapter 4 FAT-based Adaptive Gait Trajectory Tracking Control

---

The model parameters  $D$ ,  $C$  and  $G$  are unknown and also not easy to obtain in real-life applications. A modified controller based on the estimation can be constructed as Eq. (4.11) as long as some proper update laws for the estimates  $\hat{D}$ ,  $\hat{C}$  and  $\hat{G}$  can be designed.

$$\tau = \hat{D}\ddot{\theta}_d - \hat{D}\Lambda\dot{e} + \hat{C}\dot{\theta}_d - \hat{C}\Lambda e + \hat{G} - K_d s \quad (4.11)$$

If we further denote  $v = \dot{\theta}_d - \Lambda e$ , the controller can be rewritten as

$$\tau = \hat{D}\dot{v} + \hat{C}v + \hat{G} - K_d s \quad (4.12)$$

Hence, the closed-loop system can be represented as

$$D\dot{s} + Cs + K_d s = -\tilde{D}\dot{v} - \tilde{C}v - \tilde{G} \quad (4.13)$$

where  $\tilde{D} = D - \hat{D}$ ,  $\tilde{C} = C - \hat{C}$  and  $\tilde{G} = G - \hat{G}$  are parameter estimation errors.

If proper update laws can be designed so that  $\hat{D} \rightarrow D$ ,  $\hat{C} \rightarrow C$  and  $\hat{G} \rightarrow G$ , then  $e \rightarrow 0$  can be concluded from Eq. (4.13). In the FAT-based adaptive control, function approximation techniques are used to represent the estimates  $\hat{D}$ ,  $\hat{C}$  and  $\hat{G}$  with the assumption that sufficient numbers of basis function are employed.

$$\begin{aligned} \hat{D} &= \hat{W}_D^T Z_D \\ \hat{C} &= \hat{W}_C^T Z_C \\ \hat{G} &= \hat{W}_G^T Z_G \end{aligned} \quad (4.14)$$

where  $\hat{W}_D$ ,  $\hat{W}_C$  and  $\hat{W}_G$  denote the estimated weighting matrices, and  $Z_D$ ,  $Z_C$  and  $Z_G$  denote the matrices of basis functions.

The final controller Eq. (4.12) becomes

$$\tau = \hat{W}_D^T Z_D \dot{v} + \hat{W}_C^T Z_C v + \hat{W}_G^T Z_G - K_d s \quad (4.15)$$

and the closed loop system dynamics can be represented as

$$D\dot{s} + Cs + K_d s = -\tilde{W}_D^T Z_D \dot{v} - \tilde{W}_C^T Z_C v - \tilde{W}_G^T Z_G \quad (4.16)$$

where  $\tilde{W}_D = W_D - \hat{W}_D$ ,  $\tilde{W}_C = W_C - \hat{W}_C$  and  $\tilde{W}_G = W_G - \hat{W}_G$ .

Using Lyapunov stability analysis, the update laws can be obtained. The Lyapunov candidate function is selected as

$$\begin{aligned} V(s, \tilde{W}_D, \tilde{W}_C, \tilde{W}_G) = & \frac{1}{2} s^T D s \\ & + \frac{1}{2} \text{Tr}(\tilde{W}_D^T Q_D \tilde{W}_D + \tilde{W}_C^T Q_C \tilde{W}_C + \tilde{W}_G^T Q_G \tilde{W}_G) \end{aligned} \quad (4.17)$$

where  $Q_D$ ,  $Q_C$  and  $Q_G$  denote the positive definite weighting gain matrices.

The time derivative of  $V$  along the trajectory of Eq. (4.16) can be calculated as

$$\begin{aligned} \dot{V} = & s^T (-Cs - K_d s - \tilde{W}_D^T Z_D \dot{v} - \tilde{W}_C^T Z_C v - \tilde{W}_G^T Z_G) \\ & + \frac{1}{2} s^T \dot{D} s + \text{Tr}(\tilde{W}_D^T Q_D \dot{\tilde{W}}_D + \tilde{W}_C^T Q_C \dot{\tilde{W}}_C + \tilde{W}_G^T Q_G \dot{\tilde{W}}_G) \end{aligned} \quad (4.18)$$

Using the fact that the matrix  $\dot{D} - 2C$  is skew-symmetric, we can further have

$$\begin{aligned} \dot{V} = & -s^T K_d s - \text{Tr}[\tilde{W}_D^T (Z_D \dot{v}_s^T + Q_D \dot{\tilde{W}}_D)] \\ & - \text{Tr}[\tilde{W}_C^T (Z_C v_s^T + Q_C \dot{\tilde{W}}_C)] - \text{Tr}[\tilde{W}_G^T (Z_G s^T + Q_G \dot{\tilde{W}}_G)] \end{aligned} \quad (4.19)$$

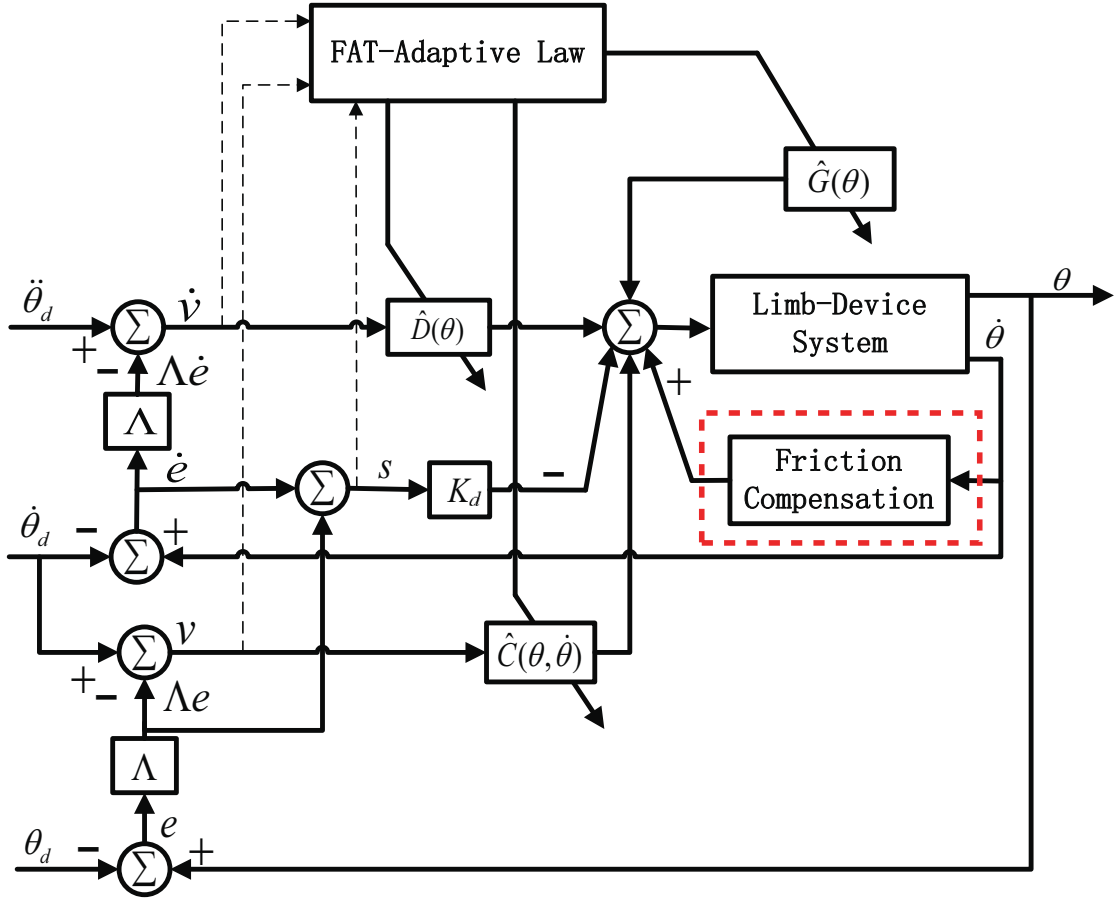


Figure 4.3: FAT-based adaptive control scheme

The adaptive law can be selected as

$$\begin{aligned}
 \dot{W}_D &= -Q_D^{-1} Z_D \dot{v}_s^T \\
 \dot{W}_C &= -Q_C^{-1} Z_C v_s^T \\
 \dot{W}_G &= -Q_G^{-1} Z_G s^T
 \end{aligned} \tag{4.20}$$

where  $\dot{v}_s^T = s \dot{v}^T$ ,  $v_s^T = s v^T$ .

The Eq. (4.19) becomes

$$\dot{V} = -s^T K_d s \tag{4.21}$$

If  $K_d$  is properly chosen as diagonal positive definite matrix, then  $\dot{V} < 0$  and

the stability can be guaranteed.

Two critical conclusions for the FAT-based adaptive controller can be derived:

- Tracking errors  $e$  converge to zeros asymptotically.
- Estimates  $\hat{D}$ ,  $\hat{C}$  and  $\hat{G}$  are bounded. Their convergence depends on the persistent excitation condition of input.

The entire implementation diagram of this FAT-based adaptive control approach is shown in Fig. 4.3. For simulation, there is no need to consider friction compensation. Additionally, no model parameters, acceleration feedback or regressor matrix computation are needed for the controller and adaptive update law, which can greatly simplify its controller design and implementation.

### 4.5 Simulation Results

The FAT-based adaptive control algorithm was tested and verified firstly by simulation in Matlab/Simulink with the simplified model Eq. (4.7). The subject is considered completely passive, and the active torques are simulated with Gaussian white noise ( $mean = 0$  and  $variance = 1$ ). The model parameters were selected as  $m_1 = 10(kg)$ ,  $m_2 = 6(kg)$ , and  $L_1 = L_2 = 0.4(m)$ . The initial conditions were set to  $\theta = [25, 0]^T$  and  $\dot{\theta} = [0, 0]$ . For the desired trajectories in Eq. (4.6),  $A = 1$ ,  $B = 0$ , and  $T = 3(s)$ . The controller described in Eq. (4.11) was employed in conjunction with the gain matrices  $K_d = diag(100, 20)$  and  $\Lambda = diag(30, 20)$ . Eleven terms of Fourier series were selected as the basis functions for approximation, and the initial weighting matrices were assigned to be zero matrices. The weighting gain matrices used in the adaptive update law Eq. (4.20) were selected as  $Q_D^{-1} = 10^{-5}I_{44}$ ,  $Q_C^{-1} = 10^{-5}I_{44}$ , and  $Q_G^{-1} = 10^{-4}I_{22}$ . The actuator saturation

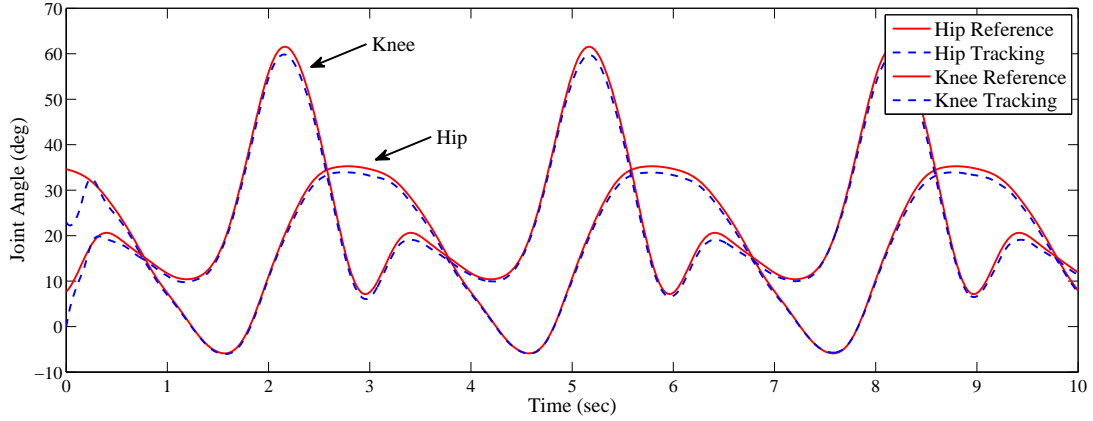


Figure 4.4: [SIM] Tracking performance for hip and knee joint (reference trajectories are plotted in solid lines, and tracking trajectories are plotted in dashed lines)

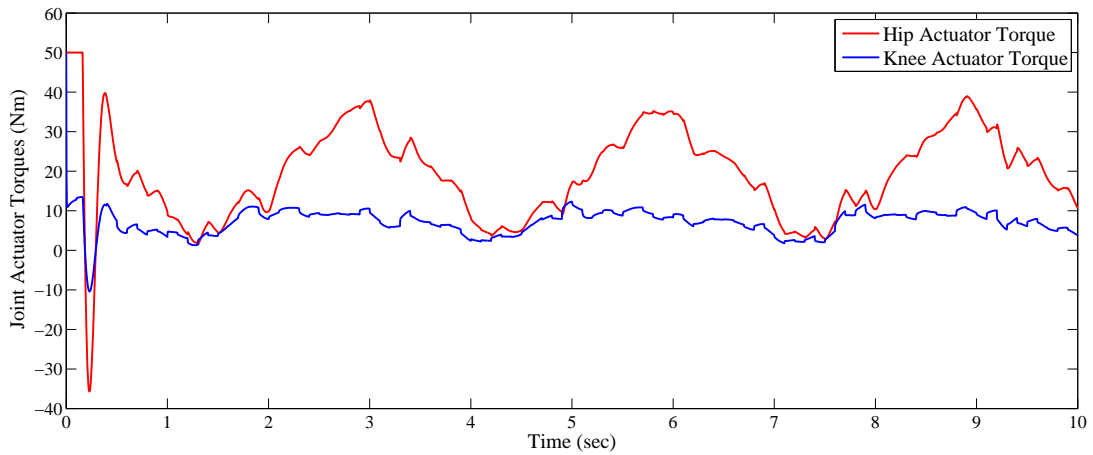


Figure 4.5: [SIM] Output torques of hip and knee actuator

torques were set to be  $50 \text{ Nm}$ , which is less than actuator maximum momentary torque  $55 \text{ Nm}$ . The results of the simulation are shown from Fig. 4.4 to Fig. 4.6.

Fig. 4.4 shows the tracking performance of the hip and knee gait trajectories. It can be observed that the hip and knee joint trajectories can converge accurately and fast to the desired reference trajectories, irrespective of the fact that the initial angle position errors are large. Additionally, there are no observed undesired overshoots or oscillations.

Fig. 4.5 shows the hip and knee joint actuator output torques. In the transient

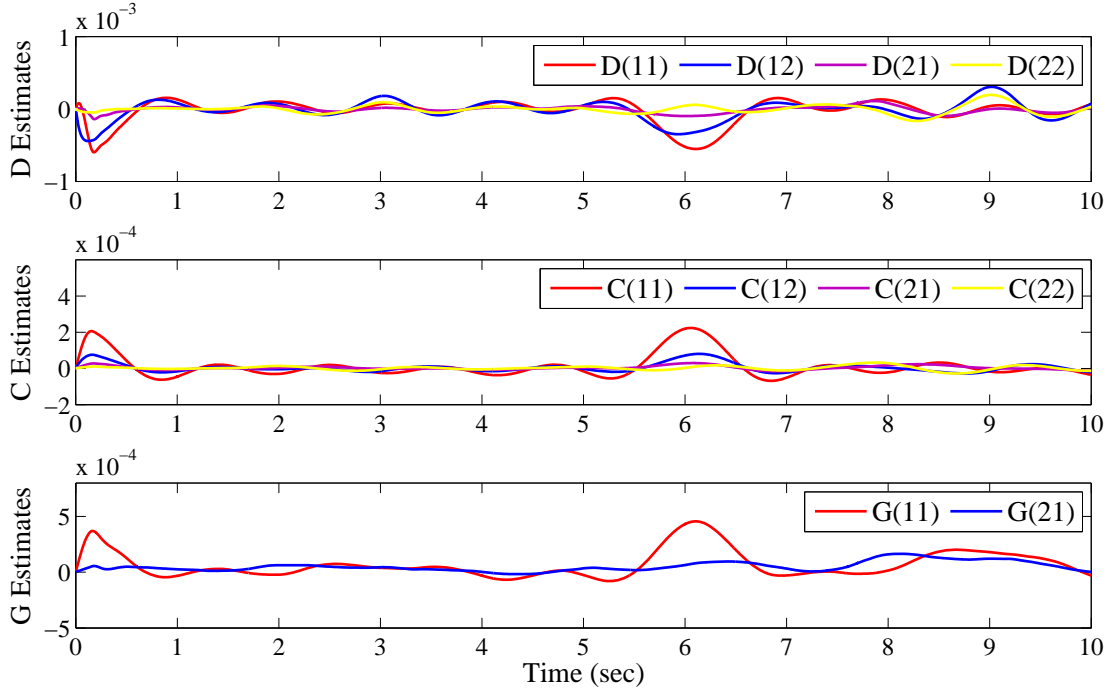


Figure 4.6: SIM FAT adaptive gains for D, C and G matrices

state, the actuator output torques are quite high due to the large initial tracking errors. Hip joint actuator even reaches to the saturation torque  $50 \text{ Nm}$  momentarily. Nonetheless, in steady state, both the hip and knee joint actuator torques fall below the saturation torque. Additionally, it is observed that the hip joint actuator is required to output higher torque.

Lastly, Fig. 4.6 shows the parameter estimation performance using function approximation. They are all bounded as desired. All the above simulation results imply that this FAT-based adaptive control algorithm can be potentially implemented in real-time applications for passive rehabilitation training.

## 4.6 Implementation Results

This control scheme was then implemented in the sbRIO embedded controller through Labview programming. One young healthy subject wore the single-leg



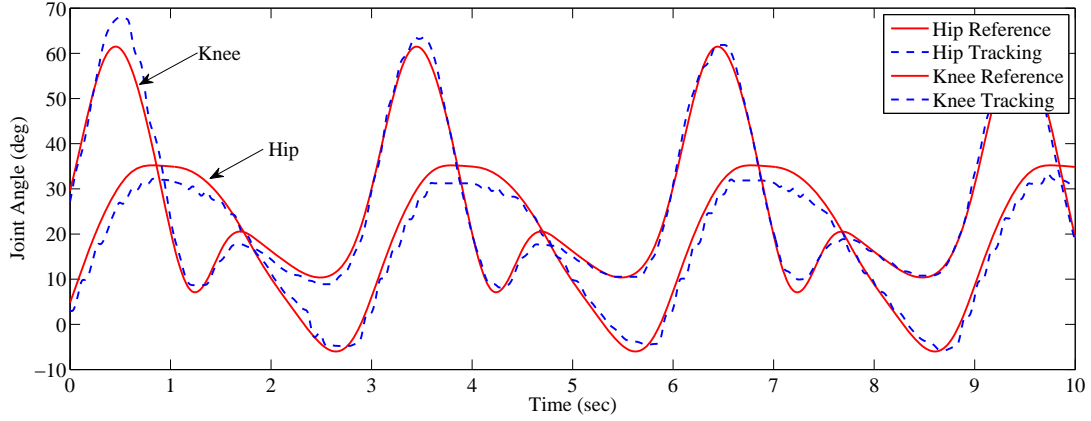


Figure 4.7: **REAL** Tracking performance for hip and knee joint (reference trajectories are plotted in solid lines, and tracking trajectories are plotted in dashed lines)

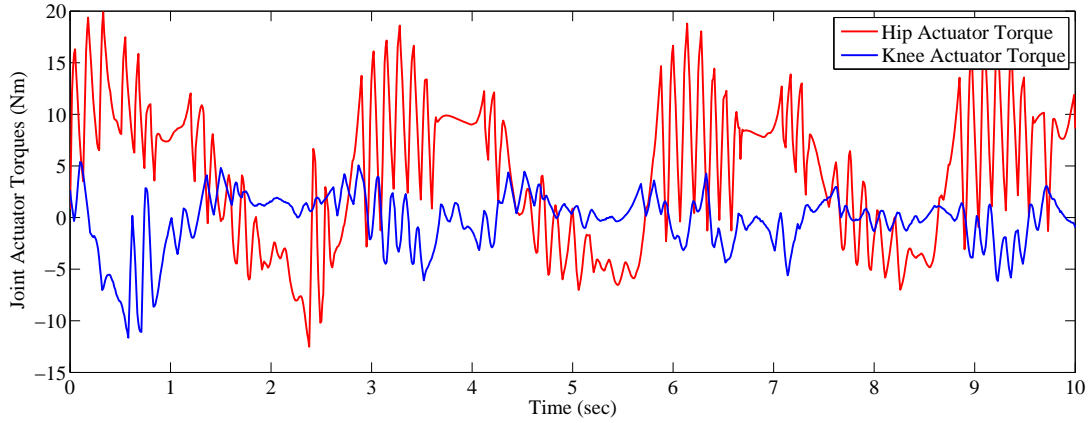


Figure 4.8: **REAL** Output torques of hip and knee actuator

lower extremity assistive device and walked on the treadmill at a speed of  $0.8 \text{ km/h}$  during the experiment. The ‘impaired’ leg attached to the device was required not to exert any hip and knee torques during walking. This was because the subject was taken as a passive wearer, akin to early-stage stroke patients. The reference trajectories described in Eq. (4.6) were selected as  $A = 1$ ,  $B = 0$ , and  $T = 3 \text{ (s)}$ . The control loop rate was set to be  $200 \text{ Hz}$ . The controller envisioned in Eq. (4.15) was applied with the gain matrices of  $K_d = \text{diag}(5, 5)$  and  $\Lambda = \text{diag}(20, 10)$ . Eleven terms of Fourier series with period time  $5 \text{ s}$  was selected as the basis functions for approximation. The initial weighting matrices were

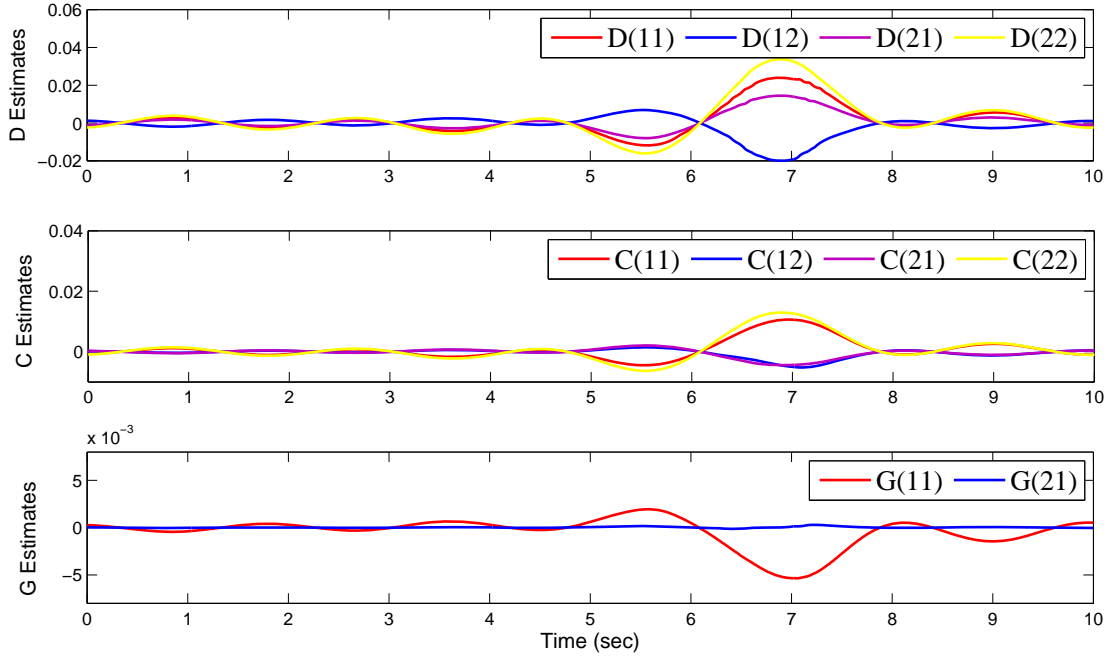


Figure 4.9: REAL FAT adaptive gains for D, C and G matrices

assigned to be zero matrices. The weighting gain matrices in the adaptive update law Eq. (4.20) were selected as  $Q_D^{-1} = 10^{-4}I_{44}$ ,  $Q_C^{-1} = 10^{-4}I_{44}$ , and  $Q_G^{-1} = 10^{-4}I_{22}$ . The actuator saturation torques were set to be 25  $Nm$  to guarantee safety. The implementation results with the assistive device are elaborated from Fig. 4.7 to Fig. 4.9.

Fig. 4.7 shows the tracking performance of hip and knee gait trajectories. It is observed that the hip and knee joint can track the reference gait trajectories precisely with acceptable errors. Essentially, perfect tracking control is not desired for the assistive device, since it might be too rigid and threaten the wearer's safety. Also, there are no overshoots or oscillations observed.

Fig. 4.8 shows the hip and knee joint actuator output torques. Both of the actuator output torques are below the preset saturation torque 25  $Nm$ . In addition, it is observed that the hip actuator needs to provide higher torque.

Lastly, Fig. 4.9 shows the parameter estimation performance for  $D$ ,  $C$  and  $G$

matrices using function approximation. They are all bounded as anticipated. All the above implementation results are consistent with the simulation results, which verify that this FAT-based adaptive control algorithm can be used for passive gait rehabilitation training.

### 4.7 Chapter Summary

In this chapter, a FAT-based adaptive gait trajectory tracking control strategy is developed to control the assistive device for passive gait rehabilitation training. The feasibility of this control algorithm is firstly verified by the tracking performance of hip and knee joint trajectories via simulation. Then this algorithm is implemented along with friction compensation on the assistive device and assessed on one healthy subject. Both simulation and implementation results show that this FAT-based adaptive control algorithm has the potential to be used for passive gait rehabilitation training. The advantage of this controller is that it does not need acceleration feedback and regressor matrix computation.

With the gait trajectory tracking approach, the subjects cannot actively modify their leg's movements. Hence, it is only applicable to the stroke patients who are in early stage of rehabilitation. For those patients who have already obtained some voluntary motor control capabilities, it would limit the possibility of motor learning and may also result in discomfort during usage. To address this shortcoming, a functional task-based impedance control algorithm based on the virtual gait period sequence will be developed in the very next chapter.

# Chapter 5

## Functional Task-based Impedance Control

In this chapter, a function task-based impedance control algorithm based on the virtual gait period sequence will be presented. This controller intends to assist the stroke patients who have regained some voluntary motor control capabilities to carry on rehabilitative gait training. Compared with the previous gait trajectory tracking approach, this controller will introduce compliance to the assistive device using impedance control techniques, and the compliance can be easily customized for each individual both in the whole gait cycle and in each virtual gait period by adjusting the assistance levels. This chapter will be structured as follows: Section 5.1 will present a brief introduction. Section 5.2 will propose the functional task-based impedance controller based on virtual gait period sequence. Section 5.3 will describe the experimental protocols and data analysis. Section 5.4 will present the experimental results on the healthy subjects and some discussions will also be provided. Lastly, Section 5.5 will summarize this chapter.

### 5.1 Introduction

Early robotic assistive devices such as the Lokomat were entirely passively position controlled. The assistive device simply moved the patient's legs to follow a fixed and rigid gait pattern, and the patient could not adjust their movements actively. This made it only applicable in the early rehabilitation stage for acute stroke patients. However, the strong guidance from the assistive device does not provide an ideal training ground for those stroke patients capable of some voluntary motor control. If the patients are allowed to behave completely passive all the time, it will limit the possibility of motor learning for them. To resolve this shortcoming, control strategies to promote active gait training are being developed, among which impedance control is the most commonly used approach.

Various impedance control approaches applied to the existing gait training devices have been reviewed in Section 2.2.2 of Chapter 2. The majority of these approaches still use the classical impedance control, which relies on the reference gait trajectories to produce assistive force. Essentially, they are still point-by-point trajectory tracking just with adjustable compliance. The patient might feel their assistive or resistive torques if they lag behind or lead the predefined trajectory of equilibrium points.

Conventional manually assisted treadmill gait training delivered by physical therapists has been proved effective in improving gait for neurological patients [109, 110]. If we observe the training process, it can be found that the therapists concentrate more on providing necessary assistance to the patient's legs and thus helping them achieve the walking gait functionality instead of simply track a fixed gait pattern. Actually, there are no rigid gait trajectories in the mind of physical therapists, so the gait training provided by them is not point-by-point based. To best mimic the physical therapist's gait training, the assistance should not be generated

based on the entire reference gait trajectories like the classical impedance control. Recent simulation and experimental studies [111, 112] showed that level walking consists of some basic sub-tasks (e.g., body weight support, forward propulsion or foot clearance). For stroke survivors, each of these subtasks can be impaired to some degree without affecting others. Therefore, it would be more meaningful to generate task-specific impedance-based assistance during gait training. In the present study, we will propose to use a functional task-based impedance control based on virtual gait period sequence. In this controller, the assistance will be provided in the virtual gait period level using the Virtual Model Control (VMC) framework [69], and the objectives are to directly achieve the specific functionality for each gait period. Hence, it would behave much more like the therapist's gait training. Preliminary evaluations will be carried on with healthy participants to validate its performance.

## 5.2 Functional Task-based Impedance Controller

We will firstly look into the subdivision of the normal walking gait cycle since the proposed controller is greatly related to the knowledge. It is widely accepted that a basic human gait cycle during level walking can be categorized into two major gait phases: stance phase and swing phase. The stance phase is when the foot is in contact with the ground and the swing phase is when the foot is in the air. Each gait phase can be further generalized into a periodic sequence of events. These events are also known as gait periods. While there is a debate as to how many sections the gait cycle should be divided into, six major periods will be presented in this work. They are Early Stance (ESt), Mid Stance (MSt), Late Stance (LSt), Early Swing (ESw), Mid Swing (MSw) and Late Swing (LSw) for a single limb [92, 113]. Fig. 5.1 illustrates these six gait periods in details.

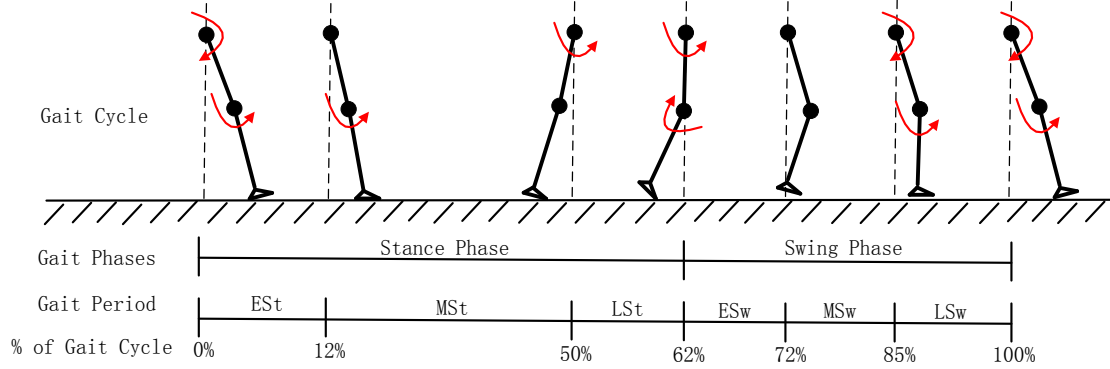


Figure 5.1: Normal walking cycle for a single limb illustrating major gait phases, subdivided gait periods and their starting and ending percentage [92]. The red arrows indicate the intended motion in the coming gait period for hip and knee joint

Table 5.1: Gait periods and functions

Gait Period	Functions
ESt	Loading, weight transfer
MSt	Support of entire body weight, center of mass moving forward
LSt	Unloading and preparing for swing
ESw	Foot clearance
MSw	Limb advances in front of body
LSw	Limb deceleration, preparation for weight transfer

Different gait periods have different functional requirements as summarized in Table 5.1. Based on the functionality in each gait period, the intended motion of the limb in that specific gait period could be determined.

From the above analysis, we understand that different gait periods have different gait functional requirements. Therefore, it is postulated that if we can generate a virtual gait period sequence and then in each virtual gait period, a simple impedance-based assistance controller can be designed to generate the correct assistive joint torque to achieve that specific gait period functionality, overall the normal gait pattern can be possibly achieved in the whole gait cycle. As the

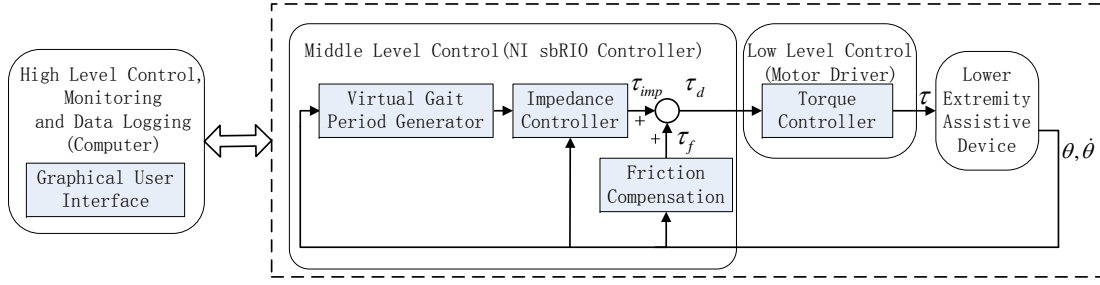


Figure 5.2: Functional task-based impedance control architecture

impedance-based assistance is produced based on gait period task functionality, it is referred to as “functional task-based impedance control” in this work.

Fig. 5.2 shows this functional task-based impedance control architecture on three different levels. The low level control made the output torque track the desired input torque via a PID control algorithm implemented in torque mode of the motor driver. The high level control handled with higher level control, monitoring, and data logging on a PC. The functional task-based impedance control with friction compensation was implemented in the middle level in the embedded sbRIO controller, which was the main focus of this work. The realization of this control are twofold. Firstly, the virtual gait period generator can produce a virtual gait period sequence for a whole gait cycle. The cycle time could be set by the user, and the virtual gait periods from early stance to late swing are generated based on their timing percentages (see Fig. 5.1) in a gait cycle. Next, in each virtual gait period, an impedance-based controller was utilized to generate the assistive joint torque. Specifically, the torque of each joint was modulated with an impedance property which consists of a unidirectional passive spring and damper characteristic with a fixed equilibrium position, as described by the following equation

$$\tau_i = k_i(\theta - \theta_{0i}) + b_i\dot{\theta} \quad (5.1)$$



Table 5.2: Impedance parameters under 100% assistance

Gait Period	$k(Nm/deg)$		$b(Nm/deg\ s^{-1})$		$\theta_0(deg)$	
	Hip	Knee	Hip	Knee	Hip	Knee
ESt	1.0	0.5	0.1	0.05	0.0	-5.0
MSt	0.0	0.5	0.0	0.05	0.0	-5.0
LSt	1.0	0.0	0.1	0.0	30.0	0.0
ESw	1.0	0.5	0.1	0.05	30.0	50.0
MSw	0.0	0.0	0.0	0.0	0.0	0.0
LSw	1.0	0.5	0.1	0.05	0.0	0.0

where the joint torque  $\tau_i$  in the  $i^{th}$  virtual gait period, is related to the input joint angular position  $\theta$  and angular velocity  $\dot{\theta}$  through the stiffness term  $k_i$ , viscosity term  $b_i$ , and equilibrium angle  $\theta_{0i}$ , respectively. Additionally, an assistance percentage factor denoted as  $Assist_i$  can be introduced to multiply the above joint torque  $\tau_i$ , which can be used to adjust the assistance levels in each virtual gait period. The assistance level  $Assist_i$  can be selected from 0% to 100%. Under 100% of assistance level, the impedance parameters (see Table 5.2) are properly tuned and selected to specify the maximum assistance.

The direction of assistive torque at each joint and within each virtual gait period is presented in Table 5.3. If the joint is in extension, the assistive torque is zero when the computed  $\tau_i$  is less than zero. On the other hand, for the joint in flexion, the assistive torque is zero when the computed  $\tau_i$  is greater than zero. The assistive torque for joints in neutral mode is set zero. In this way, the generated torque in each virtual gait period can be guaranteed not hinder the movements in that specific virtual gait period.

After resolving the problem of generating assistance for each independent virtual gait period, we need to consider how to transit the assistance between two adjoining virtual gait periods. Since different fixed equilibrium positions are em-

Table 5.3: Direction of assistive torque of joints for each virtual gait period

No.	Gait Period	Direction of Assistive Torque at Joint	
		Hip	Knee
1	ESt	Extension	Extension
2	MSt	Neutral	Extension
3	LSt	Flexion	Neutral
4	ESw	Flexion	Flexion
5	MSw	Neutral	Neutral
6	LSw	Extension	Extension

ployed for different virtual gait periods, the generated assistive torques will be jerky during the transition. Therefore, some smoothing techniques are required to smooth the generated torque profiles. In this work, a sigmoid function is introduced to smooth this transition effect during each transition to fade away the previous torque while fading in the desired assistive torque at its current state. The sigmoid function is

$$y = \frac{1}{1 + \exp\{-\tilde{A}(t - \tilde{T})\}} \quad (5.2)$$

where  $t$  denotes the time elapsed since the previous transition.  $\tilde{A}$  and  $\tilde{T}$  are the parameters to adjust the steepness and time shift of the function, respectively. Fig. 5.3 shows the output of the sigmoid function, with the parameters  $\tilde{A}$  and  $\tilde{T}$  being set to 50 and 0.1, respectively.

The torque with the sigmoid fading is

$$\tau_{imp} = (1 - y)\tau_{prev} + y\tau_{curr} \quad (5.3)$$

where  $\tau_{imp}$  denotes the smoothed assistive torque,  $\tau_{prev}$  denotes the assistive torque

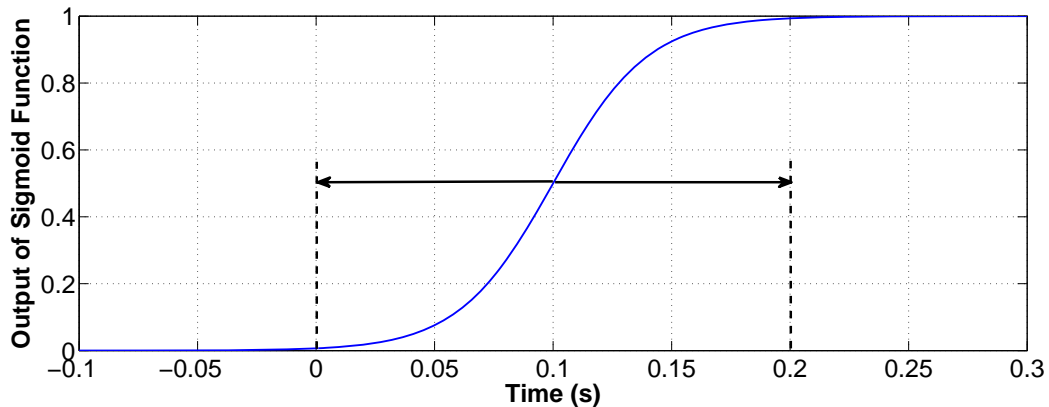


Figure 5.3: Sigmoid function used to smooth the torque profile

from the previous virtual gait period and  $\tau_{curr}$  denotes the assistive torque in the current virtual gait period. The final desired torque  $\tau_d$  is the sum of the smoothed assistive torque  $\tau_{imp}$  and the friction compensation torque  $\tau_f$ , which will be provided to the subject (see Fig. 5.2).

### 5.3 Experimental Study with Healthy Subjects

An experimental study was carried out on healthy subjects to preliminarily evaluate the functional task-based impedance control. The experiments involved three volunteer young male subjects (age range 27 – 29 years, weight  $60 \pm 5$  kg, height  $1.70 \pm 0.05$  m). None of them have previously shown any orthopedic or neurological disorders. All the participants were informed about the purpose of the experiments and consent forms were signed before conducting the experiments.

Fig. 5.4 shows the setup of the experiment. At the beginning of each experiment, the length segments of the assistive device were adjusted to fit the physical characteristics of each individual (e.g., height, size, etc.). The joint angle of the assistive device was initialized to zero when the subject was in a natural upright standing posture before each walking trial began. A general familiarization process was needed for each subject. The subject was instructed to walk on the



Figure 5.4: The experimental setup: the subject was wearing the assistive device and performing treadmill gait training with body weight support

treadmill to familiarize them with the assistive device that was operated in transparent mode<sup>1</sup>. After the familiarization process, each subject would perform the treadmill gait training under the assisted conditions with body weight support. During the gait training, the subjects were required not to exert joint torques to guarantee that the achieved gait pattern could only be attributed to the assistance of the device.

The experimental study consisted of two experiments. The first experiment involved one healthy subject to assess the control performance under different assistance levels both in the whole gait cycle and in certain virtual gait periods. The gait training was performed only on the left leg while the right leg operated

---

<sup>1</sup>Transparent mode means the assistive device is operated with friction compensation only.

in transparent mode. Three walking trials were performed:

- In the 1st walking trial, the assistance levels for the whole gait cycle were slowly adjusted from 20%, 30%, 40%, 50%, 60%, 70% to 80% every few seconds.
- In the 2nd walking trial, the assistance levels for flexion motion (corresponding virtual gait period early swing) were slowly adjusted from 0%, 20%, 40%, 60%, to 80% every few seconds. For other virtual gait periods, the assistance levels keep constant 50%.
- In the 3rd walking trial, the assistance levels for extension motion (corresponding virtual gait period late swing and early stance) were slowly adjusted from 0%, 20%, 40%, 60%, to 80% every few seconds. For other virtual gait periods, the assistance levels keep constant 50%.

For all the walking trials above, the virtual gait period sequence, joint kinematics and assistive torques were recorded. The second experiment was designed to further validate the control performance among three different healthy subjects. The gait training was performed on both legs with body weight support. Assistance levels were adjusted in the whole gait cycle from 20%, 40%, 60%, to 80%. Under each assistance level, the walking duration last for five minutes. The joint kinematics and assistive torques were recorded, and then normalized in terms of percentage of the gait cycles. Mean and standard deviation values were calculated for analysis.

For all the walking trials, the virtual gait cycle time was set to 2 *s*. The control loop and data collection rate for the NI sbRIO real-time controller of the assistive device was set to 250 *Hz*.

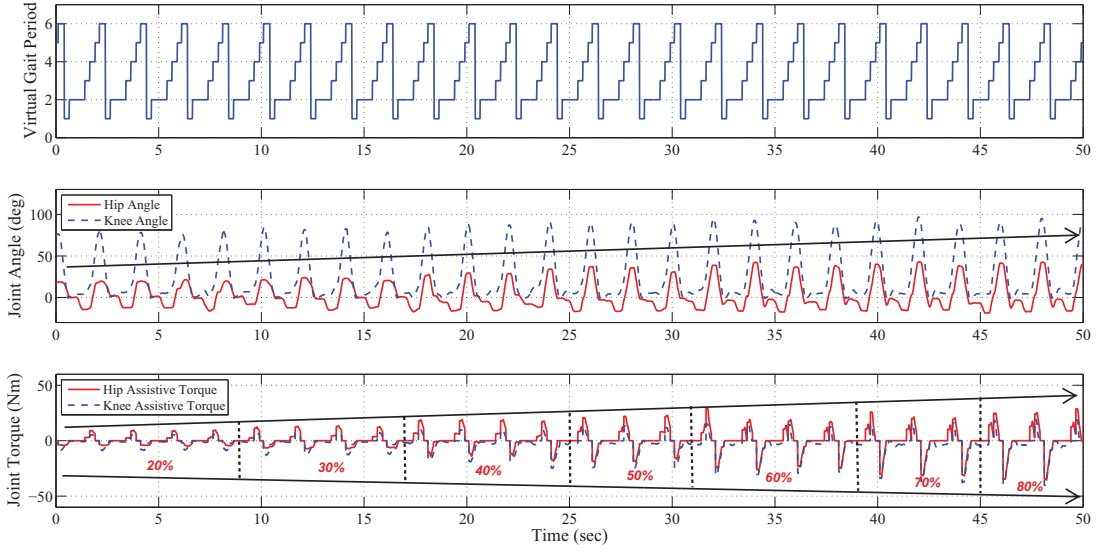


Figure 5.5: REAL Results under different assistance levels for the whole gait cycle

## 5.4 Results and Discussions

In this section, we present the preliminary results of the functional task-based impedance control strategy. The presented data were obtained from the above two experiments, and the virtual gait periods are labelled as follows:  $ES_t = 1$ ,  $MS_t = 2$ ,  $LS_t = 3$ ,  $ES_w = 4$ ,  $MS_w = 5$  and  $LS_w = 6$ .

Fig. 5.5 shows the results of joint angles and torques under different assistance levels for the whole gait cycle. It can be observed that a periodic virtual gait period sequence with cycle time 2 s can be generated. Based on this virtual gait period sequence, continuous and smooth hip and knee flexion and extension torques have been produced, and proper gait patterns similar to normal walking gait have been achieved. Additionally, the assistive torques can be modulated by adjusting the assistive levels. Under low assistance level of 20%, the generated flexion and extension torques are low ( $\leq 10 Nm$ ). Thus, the corresponding joint flexion and extension angles are also small. This shows that the device behaves

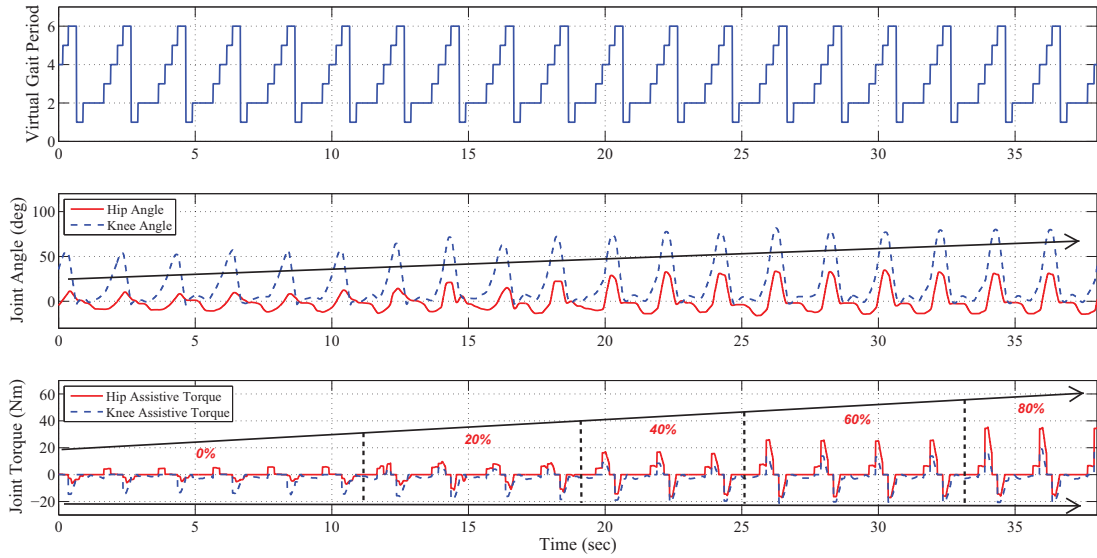


Figure 5.6: REAL Results under different assistance levels for the flexion motion quite compliant. With the assistance level increasing, the generated flexion and extension torques increase accompanied by an increase in the maximal hip flexion and knee flexion angle. When the assistance level reaches 80%, the hip and knee flexion torques increase to approximately 30  $Nm$  and extension torques nearly to 40  $Nm$ . The hip and knee flexion angles also attain their maximum values, approximately 30 degrees and 80 degrees respectively. Afterwards the subject also reported an apparent feeling of increased assistance from the device. From the results, it can be concluded that the assistance levels from the device can be customized in the whole gait cycle.

Fig. 5.6 and Fig. 5.7 present the results of joint angles and torques under different assistance levels for the flexion motion and the extension motion, respectively. The assistive joint torques and the corresponding gait patterns can be properly produced based on the virtual gait period sequence, which is similar to the results from Fig. 5.5. In the second experiment, the assistance for flexion motion was only modulated in early swing. Hence, it can be observed that under 0% assistance,

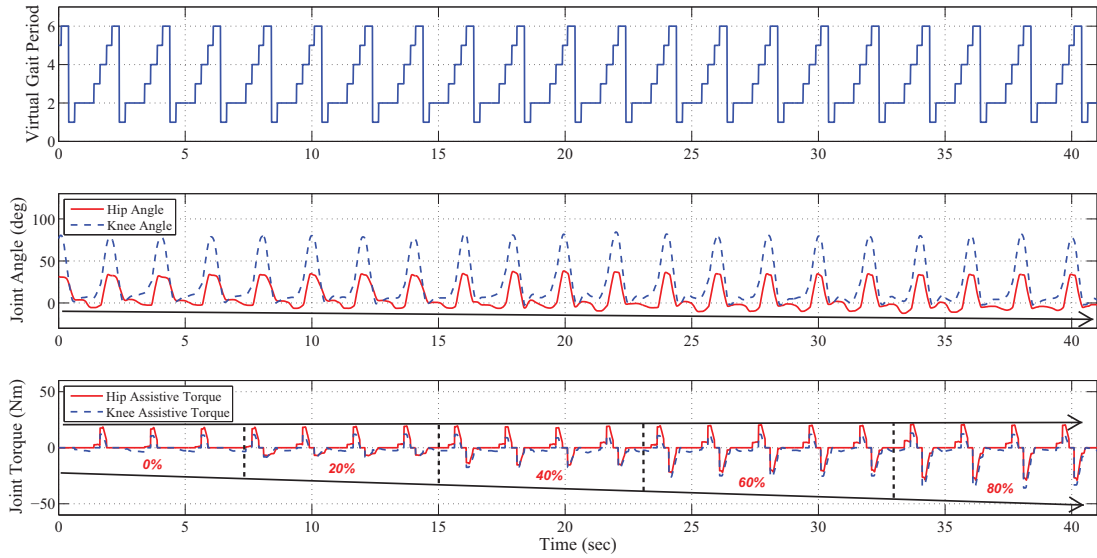


Figure 5.7: REAL Results under different assistance levels for the extension motion

the hip and knee flexion torque in early swing is also zero, and the hip and knee flexion angles are small. There is low hip flexion torque (around  $5\text{ Nm}$ ) observed, this is due to the flexion assistance in late stance. With the increase in assistance, the hip and knee flexion torques increase as well while the hip and knee extension torques almost keep constant  $20\text{ Nm}$ . Under the assistance level 80%, the hip and knee flexion torques in early swing reach  $40\text{ Nm}$  and  $20\text{ Nm}$  respectively. The hip and knee flexion angles reach to their maximum values, approximately 30 degrees and 80 degrees respectively. From the results for the extension motion, similar results can be obtained. The extension motion can be modulated by adjusting the relevant assistance levels while the flexion motion would not be affected. The hip and knee extension torques can be more than  $30\text{ Nm}$  under assistance level 80%. Overall, from these results, it can be concluded that the assistance levels from the device can also be customized in certain gait periods.



## Chapter 5 Functional Task-based Impedance Control

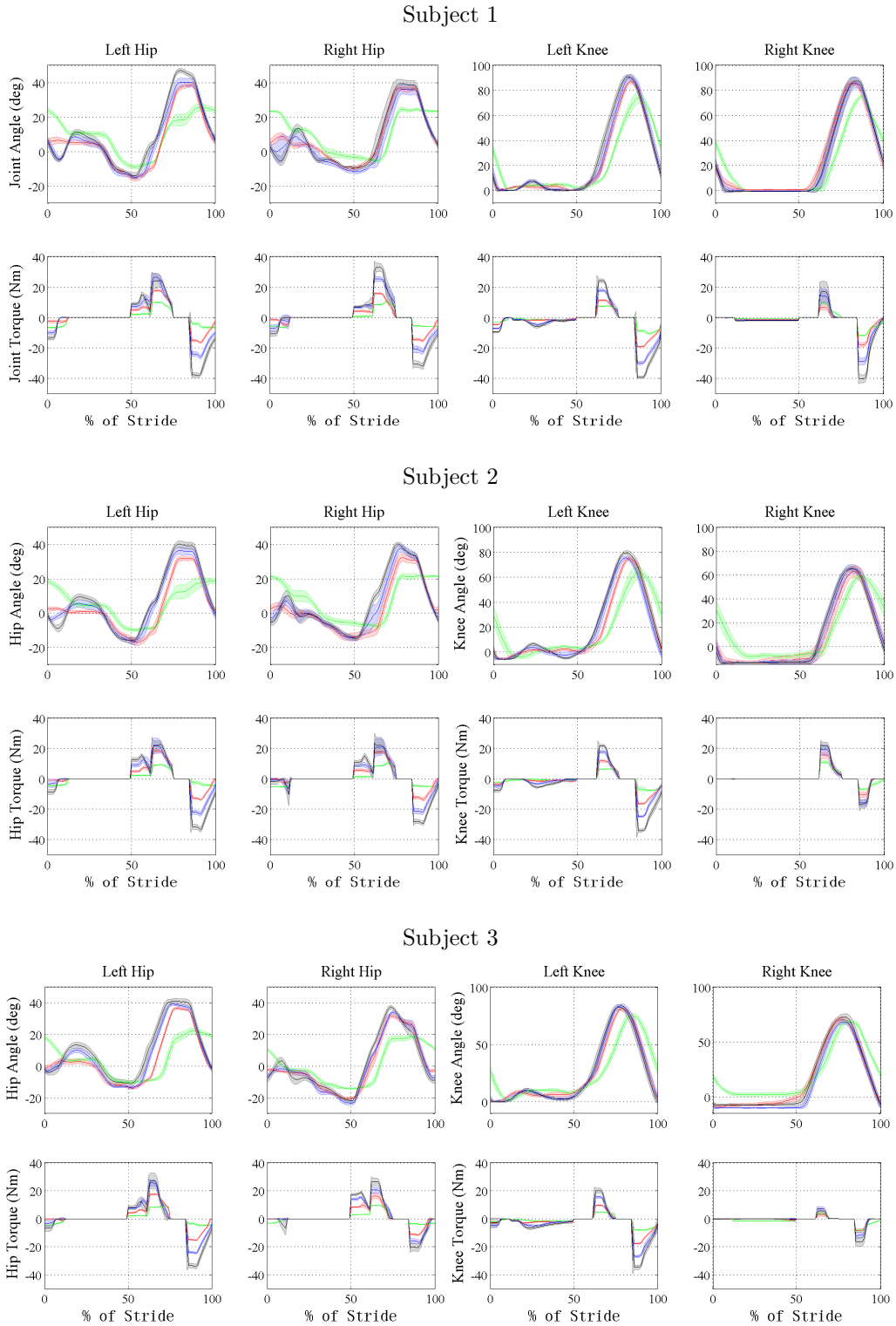


Figure 5.8: REAL Average joint trajectories and assistive joint torques from all gait cycles for three subjects (assistance level labeled as: green-20%, red-40%, blue-60%, black-80%). All plots show  $\pm 1$  standard deviations in lighter colored bands.

Lastly, Fig. 5.8 depicts the mean and the standard deviations within  $\pm 1$  intervals of the joint angles and assistive joint torques under different assistance levels in the whole the gait cycle for all three healthy subjects. The results are consistent among different healthy subjects. It is observed that the assistive joint torques can be easily adjusted by assistance levels. Under lower assistance, the gait trajectories are more compliant. As the assistive torques increase, the angles of hip extension, hip flexion and knee flexion also increase, and the gait patterns would be more rigid and would resemble the normal walking gait. The above results indicate that the proposed approach is capable of customizing the compliance for each individual by tuning the assistance levels.

There are significant benefits for this functional task-based impedance control. Conceptually, gait is made up of different gait periods that all have to be accomplished successfully to progress without failing. However, for stroke survivors, some gait periods can be impaired to some degree while others might be unaffected. Since the proposed controller can adjust the assistance independently in gait period level, the patients can be left free to perform the non-impaired gait periods while the assistive device only provides support in performing the impaired gait periods. This feature makes it quite similar to the physical therapist's gait training and allow the patients to focus on training on the certain gait periods that are impaired. This cannot be achieved using the conventional impedance controllers.

The approach presented in this study can be best compared to the "virtual tunnel" force-field control approach, which has been implemented in the ALEX [39] and the Lokomat [31]. There are two major differences between the above mentioned control and the proposed functional task-based impedance control in this study. First, both the ALEX and the Lokomat use some sort of support that potentially helps the ankle, or joint, move along the trajectory. If the subject

deviates from the user-defined range of desired trajectory, the subject would be pushed towards the path until within the desired trajectory. The impedance and assistance modulation is achieved by adjusting the user-defined range of desired trajectory, which is also called “virtual tunnel”. However, this sort of impedance modulation could only be performed in the whole gait cycle. Within the proposed functional task-based impedance control strategy, the impedance can be modulated both in the whole gait cycle just like the force-field control approach, and also in each gait period individually. Second, both studies use the “virtual tunnel” that lifts the ankle [39], or increases joint angles [31], but can also do the opposite when the subject leads the reference. For our proposed approach, a unidirectional spring and damper model was used. Thus the generated assistance is intended to support the subject in achieving the desired movements in each gait period, and not hinder the movements. In contrast to the force-field assistance, the assistance in gait periods is an end-point-based-control strategy instead of a trajectory-based-control strategy.

It should be acknowledged that this is only a preliminary study mainly evaluating control performance of the proposed functional task-based impedance control algorithm on healthy subjects. A pilot study is still needed to validate its rehabilitation effectiveness on actual stroke patients. Moreover, the assistance levels are currently adjusted manually. Some adaptive control algorithms can be employed to modulate the assistance based on the user’s real-time walking performance.

### 5.5 Chapter Summary

In summary, the proposed functional joint assistive torque controller presented in this chapter can help to achieve normal gait pattern for gait training, and the assistance both in the whole gait cycle and in each virtual gait period can be easily

## **Chapter 5 Functional Task-based Impedance Control**

---

adjusted. This in turn will assist stroke patients who have some voluntary motor control capabilities to continue gait rehabilitation training. The customization of the assistance levels for the experiments reveals the ease in which the control can be used to achieve life-like gait rehabilitation therapy.



# Chapter 6

## Functional Task-based Gait Assistance Control

In the previous two chapters, two control strategies have been developed and implemented mainly for rehabilitative gait training. In this chapter, a novel approach to functional task-based gait assistance control architecture and its preliminary evaluations will be presented. This approach utilizes a Finite State Machine (FSM) to implement a gait period detector to estimate the current gait period of the user among the six major periods. Furthermore, an impedance-based controller is used to produce the functional gait assistance at the hip and the knee joint in each detected gait period. The goal of this control architecture is to provide gait assistance for the impaired persons in order to reduce the walking efforts in their daily living. The performance of this approach is investigated on the single-leg lower extremity assistive device with a group of healthy subjects walking on a treadmill. The remainder of this chapter is structured as follows: Section 6.1 will give a brief introduction. In Section 6.2, it will introduce the functional task-based gait assistance control architecture, which mainly consists of a FSM-based gait period detector and an impedance-based assistance controller.

Then Section 6.3 will describe the experimental protocol and data analysis and the experimental results of the proposed control architecture will be presented in Section 6.4. Lastly, Section 5.5 will summarize this chapter.

### 6.1 Introduction

Over the years, research and development of wearable lower extremity assistive devices has grown in leaps and bounds for impaired individuals seeking gait assistance [114–120]. As covered in the literature review, there are several examples of these devices that include ReWalk (Argo Medical Technologies, Israel) [53], Ekso (Ekso Bionics, USA) [57], Hybrid Assistive Limb also known as HAL (Cyberdyne, Japan) [50], and Vanderbilt exoskeleton (Vanderbilt University, USA) [60]. The majority of these devices like the Rewalk, Ekso and Vanderbilt exoskeleton were developed specifically for the restoration of mobility among paraplegic individuals. The HAL was developed to aid the elderly or weaken patients in walking. It was also capable of increasing the strength of an able-bodied individual [86]. Even though some other robotic lower extremity assistive devices are still emerging, controlling these devices to offer smooth and comfortable assistance to the user is still a challenging problem, especially during walking. Additionally, it is crucial that the control of these devices be user-oriented and intuitive during use, particularly for those impaired persons with some voluntary motor control capabilities.

Control of the existing robotic assistive devices primarily relies on the estimation of the user’s movement intention. Existing devices can distinguish between different activity modes (sitting, standing and walking) through various approaches. For example, based on the product information provided on the ReWalk website, the device utilizes a wrist-mounted keypad to manually select between different types of movements and a tilt-sensor to initialize walking steps. The Ekso can

be controlled by a device operator who pushes buttons on a hand-held controller to switch between different activity modes, and walking steps are triggered by the forearm crutches worn by its user. Early vanderbilt exoskeleton relies on voice command from the user and an operator to manually switch between different movement states [60]. A recent research develops a finite state machine controller based on the user's upper body movement [61]. Once in walking activity mode, these devices would be position-controlled to reproduce fixed and predefined gait patterns, and the user cannot actively modify the walking movements. This has been proven feasible for paraplegic patients since their lower limbs are paralyzed, and the device is required to take over their muscle function completely. However, if the impaired person has some voluntary motor control while walking, this method would induce discomfort on its user. In severe cases, the device might resist the user's gait motion if the user cannot synchronize with the it, which may result in a fall. This problem can be mitigated if the user lets the device take over the motion of his limbs. However, complete reliance on the support from assistive device would lead to muscle atrophy [121] and limit motor learning [15] and gait recovery.

This drawback can be addressed through the development of an autonomous walking gait controller to realize the intended walking pattern of the users, which enforces the robot to comply with their motions to provide assistance, if necessary. There exist robotic devices that have already exploited gait phase detection method to provide timely assistance during the user's gaits. For instance, HAL 3 broadly classifies the walking cycle to support phase and swing phase based on resistive force sensor threshold, and in each phase mode, constant torque is applied to provide assistance to hip and knee joint [81]. More recently, HAL 5 applies a similar resistive force sensor threshold based method to further divide the walking motion into three phases: swing phase, landing phase and support phase [91].



Reference hip and knee patterns from a healthy subject are used to generate the assistive torques for each phase. However, above classification of the gait to two or three phases is still an oversimplification considering that stance and swing phases can still be further divided into several sub gait periods based on the walking gait functionalities [92]. Moreover, the assistance controller based on constant torque or reference gait patterns also cause some other issues. Constant assistance does not consider the gait dynamics, and the user would feel unconformable. Reference pattern tracking based assistance still has synchronization problem, and the user also cannot change the walking speed. Thus, the above gait phase detection based assistance needs to be further improved.

The authors postulate that if the subdivided gait periods could be properly detected, the intended action of the joints can be determined based on the functionality of that specific gait period. As a result, the assistive device can provide the required functional assistance in the appropriate direction at the gait period level and would aid the user during level walking. Functional assistance will be provided in an elegant way to prevent synchronization problems based on the Virtual Model Control (VMC) framework [69] instead of reference gait patterns. Several robust and reliable gait phase detection approaches have been proposed to further divide stance and swing phases to subdivided gait periods [90, 122, 123]. However, these algorithms are mainly applied for gait monitoring, although these studies also claim that they will be useful in improving control of the assistive device. To the authors' best knowledge, no research tries to integrate the subdivided gait period detection algorithms into the robotic assistive device for improving gait assistance control to this date.

This work extends the function task-based impedance control in Chapter 5. In the previous controller, a virtual gait period sequence was used to implement the impedance controller, and it was employed to perform gait training. In the

present work, it will utilize a FSM gait period detector to detect each gait period and then functionally assist the user in each detected gait period during level walking. It could be used as an autonomous controller to provide gait assistance.

The performance of this approach is evaluated on a group of healthy individuals using the developed single-leg version assistive device. The experiments described in this chapter attempt to deal with two key problems regarding the gait assistance for level walking:

1. Does the proposed control architecture effectively provide functional hip and knee assistance at each detected gait period based on the functionality requirements of that specific gait period?
2. Does it help to reduce human physical effort if the functional gait assistance can be provided?

## 6.2 Functional Task-based Gait Assistance Control Architecture

Fig. 6.1 shows the three-level hierarchy control architecture. The low level control made the output torque track the desired input torque via a PID control algorithm implemented in torque mode of the motor driver. The middle level control classified the gait periods using a FSM gait detector and obtained the functional assistive torques based on an impedance-based control algorithm. The friction compensation scheme for harmonic drive actuator and GRF signal processing (low-pass filtered by a 4<sup>th</sup> order Butterworth filter with cutoff frequency 4 Hz and then normalized to 0 – 1) were also realized in this level. All the algorithms in this level were implemented in the NI sbRIO real-time controller. The high level control handled the higher level control, monitoring, and data logging

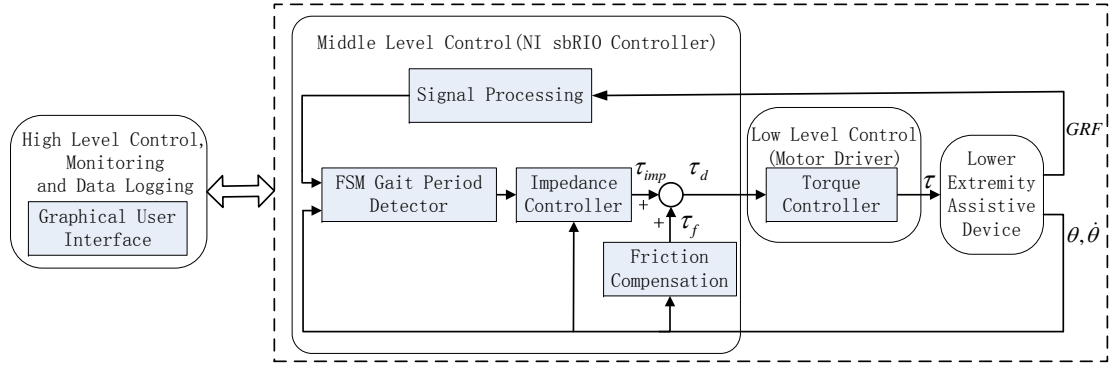


Figure 6.1: Functional task-based gait assistance control architecture

on a PC. The control architecture above was implemented in joint-space. The middle level control generates the desired joint torques  $\tau_d$ , as a sum of functional task-based impedance torques  $\tau_{imp}$  and friction compensation torques  $\tau_f$ . The design of this level is the primary focus of this section.

### 6.2.1 FSM-based Gait Period Detector

In this work, the basic human gait cycle during level walking for a single limb is still divided into six major gait periods, namely Early Stance (ESt), Mid Stance (MSt), Late Stance (LSt), Early Swing (ESw), Mid Swing (MSw) and Late Swing (LSw), as illustrated in Fig. 6.2. Then a FSM is utilized to model the transitions between various gait periods and their functional dependencies where each period forms a discrete state in the FSM, as seen in Fig. 6.3. It is worth noting that the gait period of a healthy individual transits sequentially during normal level walking. This is due to the repetitive nature of gait patterns. It holds true as long as the conditions for the state transition is properly set. Moreover, additional transition conditions between swing and stance states (i.e.,  $t-1$  and  $t-4$ ) are introduced to prevent states from entrapment. This can occur for a gait cycle if the swing or the stance phase of the user terminates prematurely.

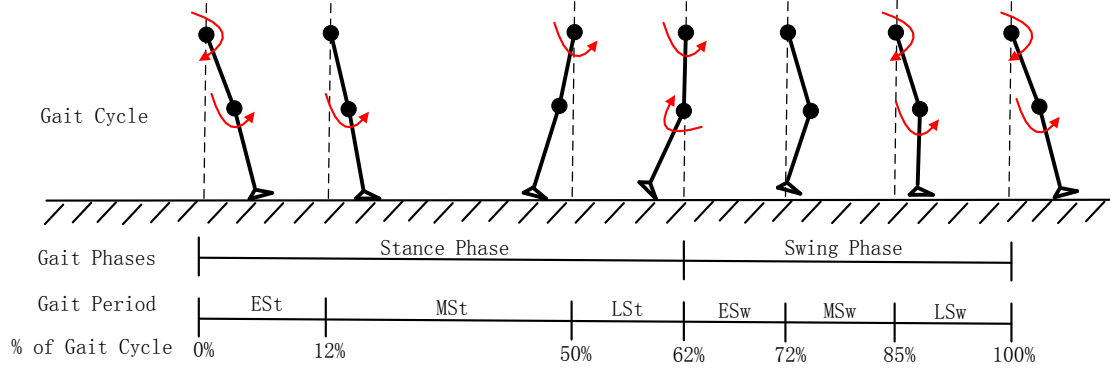


Figure 6.2: Normal walking cycle for a single limb

Appropriate Gaussian Mixture Models (GMMs) are selected to characterize the probability of the subject in each gait period. The GMM classifier considers both the mean and covariance of the sensor data to model a multivariate Gaussian distribution [124] to evaluate its probability in each state. Moreover, its level of complexity can be controlled based on the number of mixture components defined by the designer. A small number of mixture components could be used to achieve fast computational speed, and thus it can be easily implemented in real-time applications. A similar approach was also applied to a powered lower limb prosthesis [125].

A separate GMM is used to describe each gait period  $\lambda_k$ . The probability of being in a certain gait period  $\lambda_k$ , for a given set of D-dimensional sensor measurements  $\vec{x}$ , is [126]

$$p(\vec{x}|\lambda_k) = \sum_{i=1}^N \omega_i^k g_i^k(\vec{x}|\vec{\mu}_i^k, C_i^k) \quad (6.1)$$

where  $N$  is the number of components of the mixture model,  $\omega_i^k$  is the mixture weight of the  $k^{th}$  GMM for  $i^{th}$  component, and  $g_i^k(\vec{x}|\vec{\mu}_i^k, C_i^k)$ , is a multivariate Gaussian probability density function for the  $k^{th}$  GMM. Each component density is a D-variate Gaussian function of the form

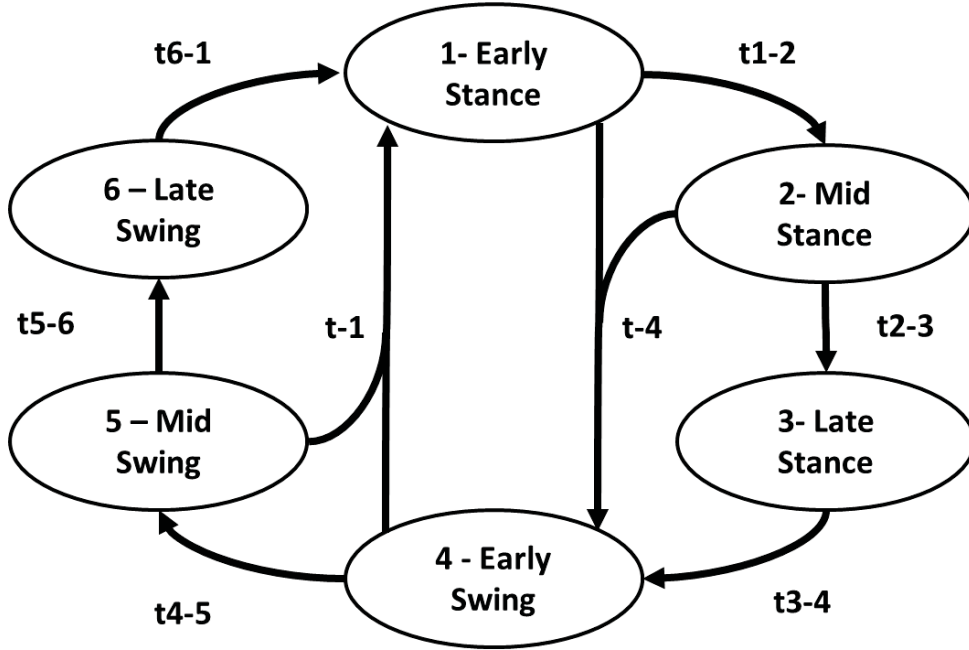


Figure 6.3: Diagram of FSM-based gait detector for level walking

$$g_i^k(\vec{x} | \vec{\mu}_i^k, C_i^k) = \frac{1}{\sqrt{(2\pi)^D |C_i^k|}} \exp\left\{-\frac{1}{2}(\vec{x} - \vec{\mu}_i^k)'(C_i^k)^{-1}(\vec{x} - \vec{\mu}_i^k)\right\} \quad (6.2)$$

where  $\vec{\mu}_i^k$  and  $C_i^k$  are the  $D \times 1$  mean vector and  $D \times D$  full covariance matrix, respectively. The mixture weights satisfy the constraint of  $\sum_{i=1}^N \omega_i^k = 1$  and  $\omega_i^k \geq 0$ .

Each GMM is parameterized by the mean vectors, covariance matrices and mixture weights from all component densities, given as

$$\lambda_k = \{\omega_i^k, \vec{\mu}_i^k, C_i^k\}, \quad i = 1, \dots, N \quad (6.3)$$

Given the training data and GMM configuration, Expectation Maximization (EM) algorithm [127] is used to find the Maximum Likelihood (ML) estimates of the parameters for each GMM. Table 6.1 shows the transition conditions for

Table 6.1: Finite state transitions for level walking

Transitions	Conditions
t1-2	$p(\vec{x} \lambda_2) > p(\vec{x} \lambda_1)$
t2-3	$p(\vec{x} \lambda_3) > p(\vec{x} \lambda_2)$
t3-4	$p(\vec{x} \lambda_4) > p(\vec{x} \lambda_3)$
t4-5	$p(\vec{x} \lambda_5) > p(\vec{x} \lambda_4)$
t5-6	$p(\vec{x} \lambda_6) > p(\vec{x} \lambda_5)$
t6-1	$p(\vec{x} \lambda_1) > p(\vec{x} \lambda_6)$
t-1	$GRF_{total} > GRF_{thres}$
t-4	$GRF_{total} < GRF_{thres}$

each gait period. The transition occurs when the probability for a given input of sensor measurements,  $\vec{x}$ , in the next gait period is higher than its probability in the current gait period. Input sensor measurements include hip angle, knee angle, front GRF, mid GRF and back GRF from the limb worn the device. The additional transition conditions  $t-1$  and  $t-4$  are based on the total GRF which is the sum of the three GRFs and a total-GRF threshold.

### 6.2.2 Impedance-based Assistance

After the gait period is determined, an assistive torque is applied in a manner to help the subject achieve the intended joint motion in that specific gait period. In this work, an impedance-based method [68] is used to generate the functional assistive torque. The torque of each joint is modulated with an impedance property which consists of a passive spring and a damper characteristic with a fixed equilibrium position. A different set of impedance property is used at different periods of a gait cycle.

Assistive torques are provided in the desired direction to help achieve the intended motion at each gait period. This allows the device to assist the impaired

Table 6.2: Direction of assistive torque of joints for each gait period

No.	Gait Period	Direction of Assistive Torque at Joint	
		Hip	Knee
1	ESt	Extension	Extension
2	MSt	Neutral	Extension
3	LSt	Flexion	Neutral
4	ESw	Flexion	Flexion
5	MSw	Neutral	Neutral
6	LSw	Extension	Extension

functional tasks to preserve the freedom of motion for unimpaired tasks to the subjects.

Table 6.2 presents the direction of assistive torque at each joint and within each gait period, as demonstrated in [92]. In each gait period, a simple unidirectional impedance model for a joint is given by

$$\tau_i = k_i(\theta - \theta_{0i}) + b_i\dot{\theta} \quad (6.4)$$

where the joint torques  $\tau_i$  in the  $i^{th}$  gait period, are related to the input joint angular position  $\theta$  and angular velocity  $\dot{\theta}$  through the stiffness term  $k_i$ , damping term  $b_i$ , and equilibrium angle  $\theta_{0i}$ , respectively. If the direction of assistance is in extension, the assistive joint torque is zero when the computed  $\tau_i$  is less than zero. On the other hand, for joint in flexion, the assistive torque is zero when the computed  $\tau_i$  is greater than zero. The assistive torque for joints in neutral mode is set zero. The studies [125, 128, 129] apply a similar impedance-based approach to a powered transferal prosthesis to accomplish tasks such as sitting, standing, walking, stair ascent and descent.

The implementation trials show that the switching between the states results in

a rapid switching between their corresponding assistive torques. This causes unnatural and jerky movements as the new assistance torques take effect. Therefore, the same sigmoid function used in Section 5.2 is used to smooth this transition effect during each transition to fade away the previous torque while fading in the desired assistive torque at its current state. The sigmoid function is

$$y = \frac{1}{1 + \exp\{-\tilde{A}(t - \tilde{T})\}} \quad (6.5)$$

where  $t$  is the time elapsed since the previous transition, and  $\tilde{A}$  and  $\tilde{T}$  are parameters to adjust the steepness and time shift of the function, respectively.  $\tilde{A}$  and  $\tilde{T}$  is still set to 50 and 0.1, respectively.

The output torque with the sigmoid fading is

$$\tau_{imp} = (1 - y)\tau_{prev} + y\tau_{curr} \quad (6.6)$$

where  $\tau_{prev}$  is the assistive torque from the previous gait period and  $\tau_{curr}$  is the assistive torque in the current gait period. This smoothed torque  $\tau_{imp}$  is the final assistive torque provided to the subject.

## 6.3 Experimental Protocols and Data Analysis

### 6.3.1 Experimental Protocols

The training data collection and training process to parameterize GMM classifier for each subject have been elaborated in the earlier work by Shen [20]. In this thesis, only the experimental parts are the primary focus. It should be noted that the training is performed under a constant speed of 1 *km/h*. After parameterizations are complete, the GMM-based FSM gait period detector can be implemented



on the assistive device for online gait period detection. The impedance parameters for each gait period can be customized to provide different levels of assistance to individuals. However, the same set of calibrated impedance parameters are used to simplify the evaluation in this work (see Table 6.3).

Table 6.3: Calibrated impedance parameters

Gait Period	$k(Nm/deg)$		$b(Nm/deg\ s^{-1})$		$\theta_0(deg)$	
	Hip	Knee	Hip	Knee	Hip	Knee
ESt	0.4	0.2	0.04	0.02	0.0	-5.0
MSt	0.0	0.4	0.0	0.04	0.0	-5.0
LSt	0.4	0.0	0.04	0.0	30.0	0.0
ESw	0.4	0.4	0.04	0.04	30.0	50.0
MSw	0.0	0.0	0.0	0.0	0.0	0.0
LSw	0.4	0.2	0.04	0.02	0.0	0.0

Five healthy young subjects (four male and one female, age range 24-29 years, weight  $60 \pm 9\ kg$ , height  $1.70 \pm 0.048\ m$ ) volunteered to participate in the experiments. None of them have previously shown any orthopedic or neurological disorders. All the participants were informed about the purpose of the experiments and signed consent forms before conducting the experiments.

The length segments of the assistive device were adjusted to fit the physical characteristics of each individual (e.g., height, size, etc.). The joint angle of the assistive device was initialized to zero when the subject is in a natural upright standing posture before each walking trial begun. Each subject was familiarized with the the assistive device by wearing and walking on the treadmill before the experiment. After the familiarization process, each subject performed level walking trials on the treadmill.

Two experiments are designed and performed. The first experiment evaluates the performance of the gait period detector and assistance controller under three

different treadmill speeds  $1.0 \text{ km/h}$ ,  $1.5 \text{ km/h}$  and  $2.0 \text{ km/h}$ . Each time, one healthy subject worn the device participates in this experiment and performs level walking trials with assistance on the treadmill. Under each walking speed, the walking trial lasts five minutes. The second experiment is designed to further validate whether the proposed controller can provide functional gait assistance to achieve normal walking gait and thus reduce physical efforts for different subjects. A group of five participants are involved in this experiment and walk on the treadmill at a constant speed of  $1.0 \text{ km/h}$  in each of the following configurations:

1. Free walking
2. Unassisted
3. Assisted

A walking speed of  $1.0 \text{ km/h}$  is chosen as it is comparable to the walking speed of impaired persons post stroke [130] and the GMM classifier is also trained under this speed. The free walking trial serves as a control group, where the subject walks without wearing the assistive device. In the unassisted trial, the subject wears the assistive device in the transparent mode with only friction compensation for harmonic drive actuator (see Section 3.2). Under the assisted trial, the subject wears the assistive device with both friction compensation and functional gait assistance.

Each walking trial lasts 15 minutes. Heart rate sensors (MN-01, Pulse Plus) are used to measure the heart rate of each participant (i.e., the measurement of physical exertion) in a 30 seconds intervals. Each subject rests for 30 minutes before the start of each trial to ensure sufficient time for the heart rate to return to baseline. The heartbeat of each individual (every 30 seconds for 15 minutes) is measured before the commencement of the first trial (seated and calm) to determine the resting heart rate.

The control loop and data collection rate for the NI sbRIO real-time controller of the assistive device is set to  $250Hz$  for all the trials, and all the algorithms are able to be completed within  $4\text{ ms}$ .

### 6.3.2 Data Analysis

Joint kinematics, assistive torques from assisted trial and heart rates in resting, free walking, unassisted and assisted trials for each subject are recorded. For the joint kinematics and assistive torques, the heel strike events (triggered by back GRF) are used to segment the data to separate steps. This helps realize the variations among all the gait cycles for an individual. Furthermore, the duration time between two consecutive heel strike events is utilized to normalize these values in terms of the percentage of gait cycles. The mean and standard deviation of these gait cycles are obtained for the analysis. For heart rates, the boxplots from the four different trials are used for statistical analysis.

## 6.4 Results and Discussions

In this section, we present the preliminary results of the above control strategy. In general, the effectiveness of the proposed control architecture is assessed by determining whether it can effectively provide the corresponding functional task based assistance in the intended motion and overall reduce human physical efforts. Then the limitations of this study will also be discussed.

### 6.4.1 Experimental Results

Fig. 6.4 shows three samples of 20 seconds representative data which are recorded from the three different treadmill speeds  $1.0\text{ km/h}$ ,  $1.5\text{ km/h}$  and  $2.0\text{ km/h}$  in the first experiment. Fig. 6.4.A.(a) shows the gait periods that are detected by the

FSM gait period detector under the speed  $1.0 \text{ km/h}$ . It is observed that the FSM gait period detector can effectively detect each gait period. Moreover, it depicts the sequential transition behaviour of gait periods in increasing order. However, some variations exist for the transition timings of different gait periods in particular from mid stance to late stance and then to early swing. Fig. 6.4.A.(b) and Fig. 6.4.A.(c) represent the joint angles and GRFs respectively. They indicate that data are periodic with minor cycle-to-cycle variations. In addition, the hip trajectory is not very smooth, especially during periods with the addition of assistive torque. This is mainly attributed to compliance of the attachment between the subject and the device. In other words, the subject is mostly pushing the device during these periods in the absence of assistive torques. This situation is reversed when the assistive torques are present. Fig. 6.4.A.(d) shows the assistive torques provided by the device to the hip and knee joint. The assistive torques are continuous and smooth. It is evident in this figure that the device can generate appropriate flexion and extension torques at the hip based on the gait period detector. Peak flexion and extension assistive torques of the hip average about  $10 \text{ Nm}$  and  $8 \text{ Nm}$  respectively. These correspond to 19.4% and 15.8% of the respective peak hip flexion and extension torque of the subject during normal level walking based on the subject's weight and CGA data. It is also possible to observe the assistive extension torque for the knee joint in stance phase since knee needs to be fully extended for weight bearing in this phase. No knee flexion torque is observed in early swing since combination of hip flexion moment and shank inertia is able to flex knee joint sufficiently to clear foot. The generated assistive torques for hip and knee joint are consistent with the results from human normal walking [92]. As for the effects of variant transition timings between gait periods on assistive torques, we can see that they only affect the assistive torque peak values and do not change the overall patterns. In other words, they only

affect assistance levels. From the subject's perspective, the subject still feels assistance. This robustness is mainly attributed to the designed impedance-based controller and torque smoothing function.

Fig. 6.4.B and Fig. 6.4.C show similar results in joint angles and joint assistive torques under the treadmill speed  $1.5 \text{ km/h}$  and  $2.0 \text{ km/h}$  as long as the FSM gait period detector succeed to detect all gait periods. However, it is possible to notice that the FSM gait period detector fails to detect certain key gait period when walking speed increases. Misdetections mainly occur in late stance and mid swing (See Fig. 6.4.B.(b) and Fig. 6.4.C.(b)). When late stance is missing, the gait period detector assumes it to be still in mid stance. It is observed that hip flexion torque disappears and knee extension torque increases, but the device does not hinder the intended motions of the subject. In the other case, mid swing is missing and the gait period detector assumes it to be still in early swing. Hip extension torque is only slightly changed which does not affect the hip movement. However, knee flexion torque increases significantly and its effect extends to late swing in which knee should be prepared to extend. This is not expected since the subject may experience some difficulty in extending the knee joint in actual late swing period. For the above two trials, the misdetections happen primarily because the GMM classifier is trained under a constant speed of  $1 \text{ km/h}$  (See Section 6.3.1). In fact, this is one disadvantage of GMM classifier. The performance of GMM classifier depends on its training process, and usually this process is quite tedious. To overcome this weakness, the FSM gait period detector can be based on other classifiers such as fuzzy logic [90, 123] to further improve its robustness.

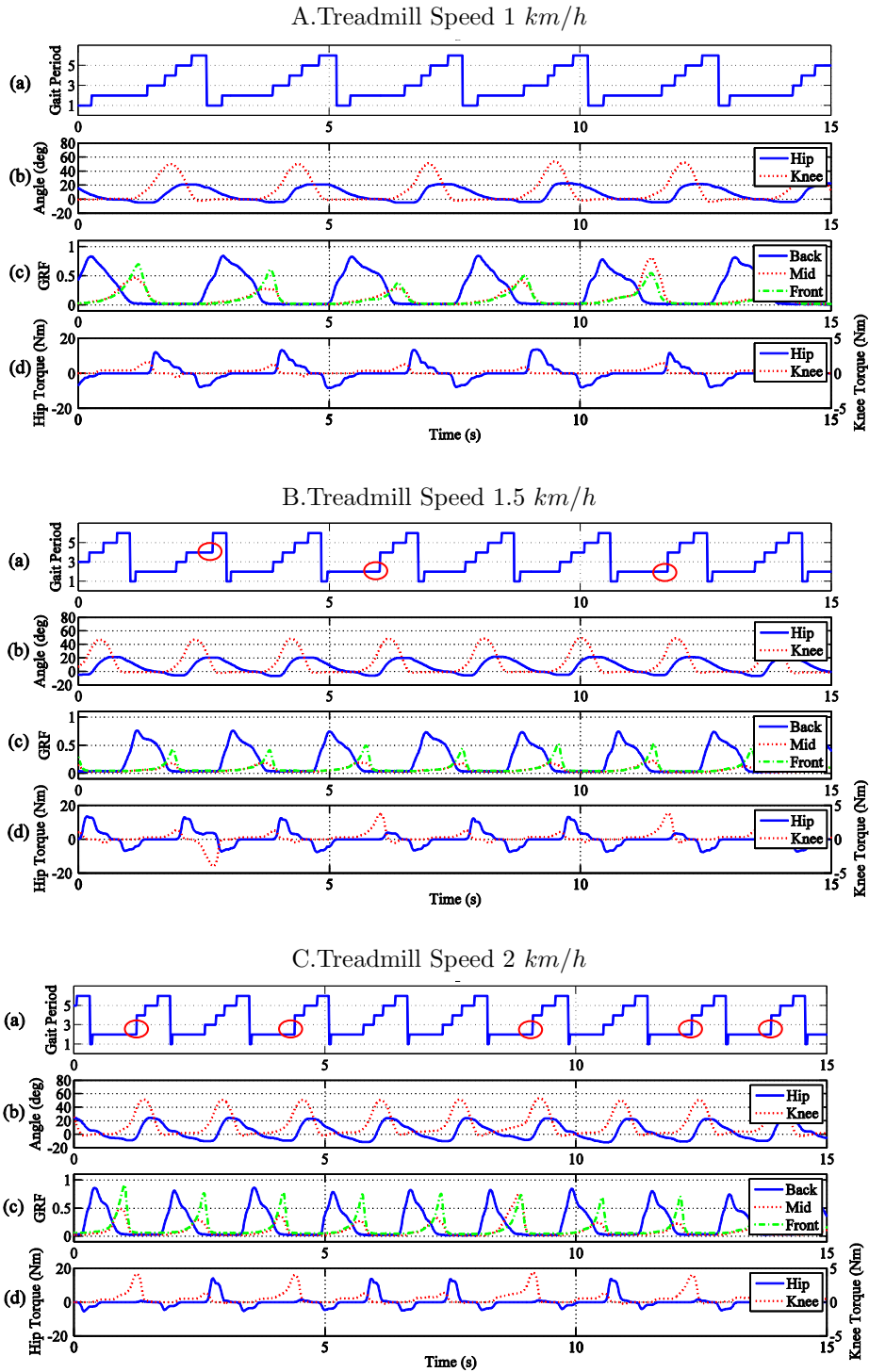


Figure 6.4: REAL Three samples of 20 seconds gait assistance results from one subject under different treadmill speeds of 1 km/h, 1.5 km/h and 2 km/h

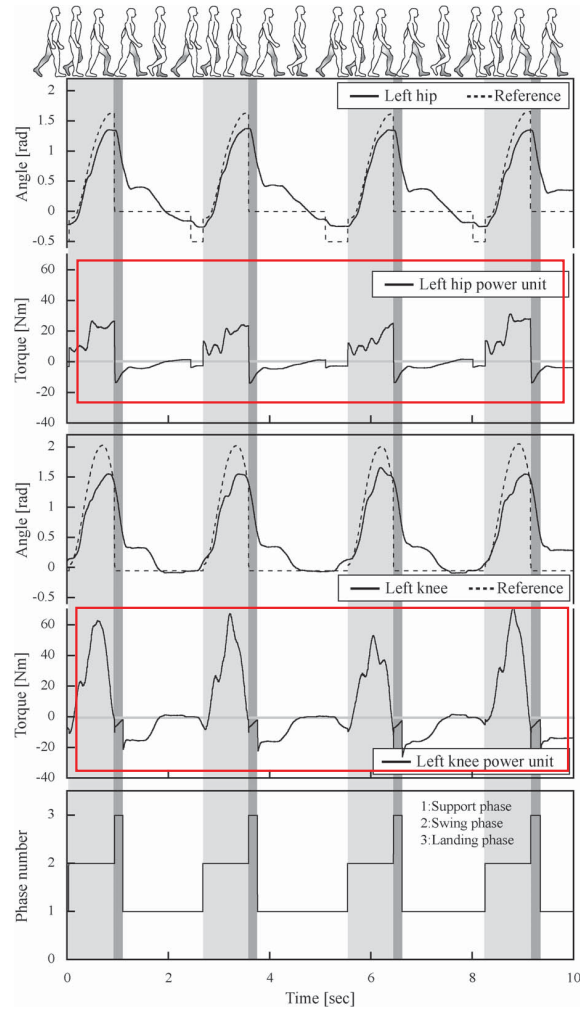


Figure 6.5: Experimental results from HAL 5 for comparison [91]

The above results indicate that the functional gait assistance can be effectively provided in the intended gait motion as long as the FSM gait period detector can detect all six gait periods even with some variations in transition timings. Compared to the most recent results (shown in Fig. 6.5) from HAL 5 [91], the proposed approach has significantly improved the smoothness of the gait assistance, especially transiting from swing phase to stance phase. Additionally, the assistance is not generated based on predefined walking pattern as HAL 5 so leaves users free to use their preferred one. Both of these would help improve the comfortability of the subject.

Fig. 6.6 shows the mean and the standard deviations within  $\pm 1$  intervals of the joint trajectories and assistive joint torques among all the gait cycles for all five healthy subjects. It shows that the joint trajectories for all subjects are consistent, overall as is the case in normal walking gait pattern [131]. The hip angle profile is characterized by a general extension side angle around 20 degrees and flexion side angle 0 to 10 degrees. The flexion knee angle reaches around 50 degrees. For Subject 2 and 5, the knee joint attains larger negative angles. This is mainly due to the joint angle initialization and the compliance between the subject and the device. For joint torques, the assistance provided at the joints is synchronous with the gait cycle of each subject. The assistive hip flexion torque that corresponds to late stance and early swing period, and assistive hip extension torque at late swing and early stance period are observed for all the participants. Assistive knee extension torque is observed at the late stance period, and low assistive knee flexion torque at early swing for Subject 5. The above results indicate that the device is capable of providing functional task based gait assistance in the intended gait motion for different subjects.

Next, the effectiveness of the functional task gait assistance in reducing human physical efforts is analyzed. Heart rates are accurate estimates of energy consumption during steady-state sub-maximal work in normal and disabled adults [132]. It has been used as a physiological parameter to determine physical effort during robotic gait training [133, 134].

Fig. 6.7 shows the heart rate values of all participants during 15 minutes of different trial configurations. The boxplots in this figure correspond to the last 10 minutes of these trials. The first 5 minutes in these plots are discarded to eliminate the contingent transient effects. The heart rate results obtained from Subject 3 are inconclusive across the three walking trials as they are all statistically similar. For other subjects, the heart rate results show a significant difference.



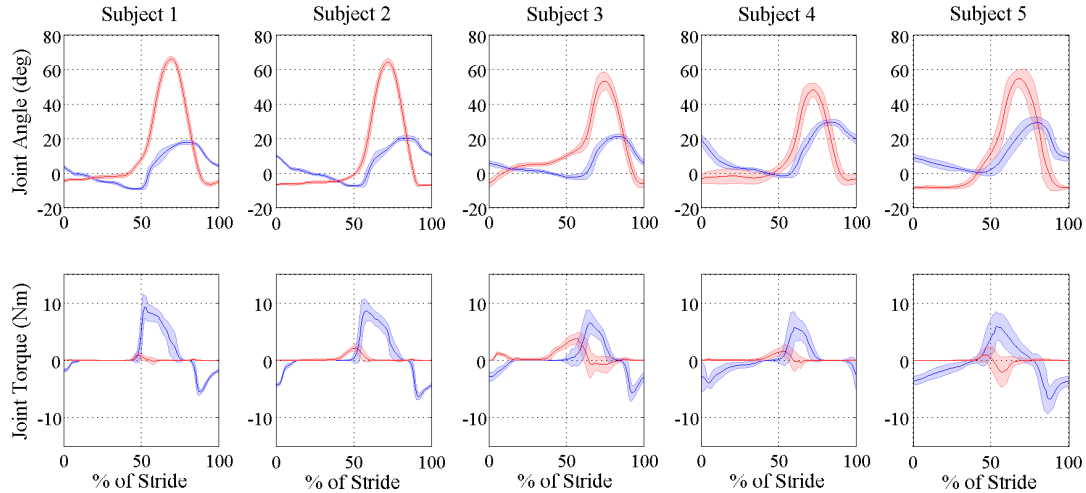


Figure 6.6: REAL Average joint trajectories and assistive torques among all gait cycles for five healthy subjects. The top plots show the hip (blue) and knee (red) angles, and the bottom plots show the hip (blue) and knee (red) assistive torques. All plots show  $\pm 1$  standard deviations in lighter colored bands

In particular, heart rates under unassisted trial are significantly higher ( $p < 0.05$ ) than those under the free walking trial. This indicates the need for more physical efforts when the device is used. This is not unexpected, since the device adds additional weight to the leg. In fact, the net metabolic rate during walking increases with leg-load magnitude and more distal leg-load location [135]. The heart rate under assisted trial is lower ( $p < 0.05$ ) than the heart rates under the unassisted trial. This indicates that the subjects benefit from the proposed functional gait assistance controller during level walking.

When comparing the heart rates under assisted trial and the free walking trial, heart rate of Subject 1 under assisted trial is lower ( $p < 0.05$ ) than the heart rate under free walking trial. This differs from other subjects whose heart rates under both trials are statistically similar. The result from Subject 1 indicates that the assistance provided by the device is able to offset the detrimental effects of walking with it. For others, the assistance provided by the proposed controller is shown to be able to assist in the walking task. However, the assistance is insufficient

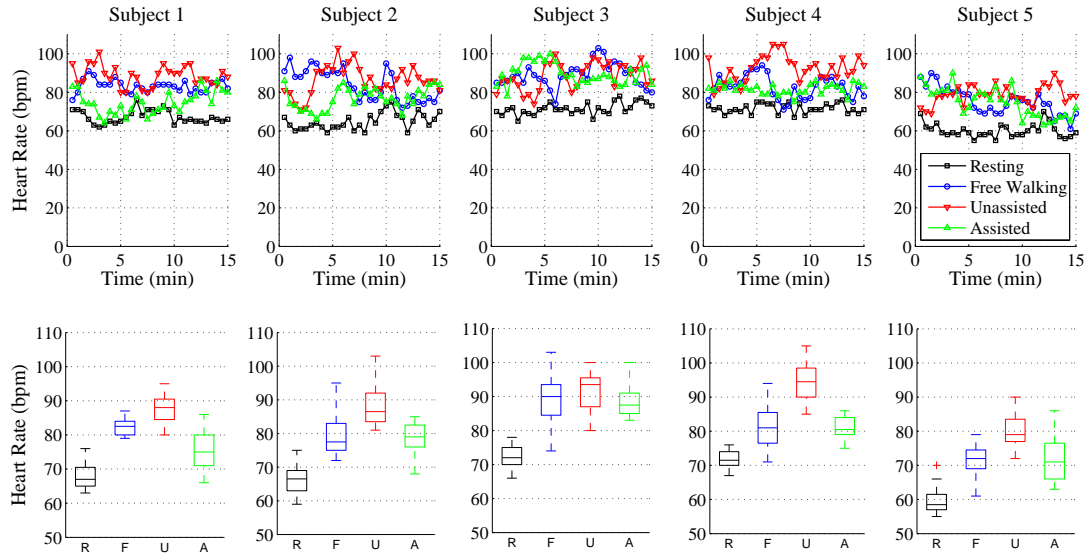


Figure 6.7: **REAL** Boxplots of heart rate values from five healthy subjects. The healthy subject’s heart rate was measured under four conditions: resting (R), free walking (F), unassisted (U) and assisted (A)

to completely compensate for the negative effects induced by the weight addition of the device to the subject’s leg on walking. Although the energy exertion and physical efforts are similar to free walking, subjects with weakened muscles or gait disorders may still benefit from the functional task gait assistance to walk normally.

Additionally, all the participants admit apparent feeling of assistance to their limb during their walks in the assisted trial. This supports the claim that the main advantage of this method is to allow the user to actively control the device while being smoothly assisted. Therefore, it shows the potential for use in daily gait assistance of home-based lower extremity assistive device.

### 6.4.2 Limitations of the Study

There are some limitations associated with this study. Firstly, present subject’s joint angles are measured by the actuator encoders. It is apparent that

the measurements cannot be very accurate due to considerable compliance between the attachment and the subject. This explains the presence of variations in the joint profiles compared to well-known free-walking condition [131]. Moreover, kinematics from free walking for comparisons cannot be obtained due to the same limitation. Advanced gait analysis system using video analysis software can be used in the future to measure accurate kinematic and kinetic data. Secondly, the constant speed of 1 *km/h* that is used for all subjects throughout the second experiments is well below the average normal walking speed of around 5.0 *km/h* [136]. Free walking with speeds less than the individual preferred walking speed lead to higher energy consumption [137]. Therefore, experiments under varying walking speeds are necessary to further study human physical effort. In addition, it is possible to adjust the assistance level under each gait period by tuning the impedance property in that specific gait period. However, the same sets of impedance parameters are used in all trials. Furthermore, the gait pattern for impaired persons differs from that of unimpaired subjects. More studies are mandatory to determine the effect of gait of the impaired persons on the performance of the gait period detector and the assistance controller. Overall, the control architecture and its preliminary evaluation presented in this study can serve as a framework for the development of home-based lower extremity assistive device.

### 6.5 Chapter Summary

This chapter presents a novel functional task-based gait assistance control architecture along with its preliminary evaluation on the developed single-leg lower extremity assistive device for level walking on a treadmill. The proposed control architecture is intuitive. Using a FSM-based gait period detector, it is able to

## Chapter 6 Functional Task-based Gait Assistance Control

---

detect the six major gait periods. After which it provides functional task-based hip and knee assistance at each detected gait period, which is found to be consistent with the functionality requirements of that specific gait period. An essential feature of the present approach is that the assistive device can be fully controlled by its user. Experimental results with healthy participants confirm that it is a feasible and improved approach for providing smoother gait assistance to the subjects and aiding in achieving normal gait patterns. Additionally, it could also help in decreasing human physical efforts required as long as the device can be more lightweight. It is our expectation that the proposed control architecture could be used in daily gait assistance among impaired and stroke affected individuals in the future.



# Chapter 7

## Conclusion and Future Work

This thesis elaborated on a low-cost, lightweight and wearable lower extremity assistive device developed for gait training and gait assistance at home for stroke patients. In particular, this thesis concentrated on trying three different control strategies aimed at different stages of gait rehabilitation on the assistive device. Preliminary studies were conducted to evaluate these strategies on healthy subjects. It was expected that the control methodologies elaborated in this thesis could be applied to actual stroke patients for gait rehabilitation training and gait assistance in the future.

For stroke patients who are in the early rehabilitation stage, position-based gait trajectory tracking control is still pertinent to gait training. This thesis applied a FAT-based adaptive gait trajectory tracking control algorithm. It was found that proper hip and knee joint tracking trajectory performance could be achieved both in simulation and physical implementation on a healthy subject. Compared with the conventional PD computed torque controller, this algorithm used does not require any knowledge of the system model. In comparison with other adaptive controllers, it does not require acceleration feedback and regressor matrix derivation and computation. These advantages make this adaptive controller easy to

implement in real world applications and it also saves computation time.

The above control algorithm makes those stroke patients who have some voluntary motor control capabilities feel rigid and uncomfortable. In an effort to improve their active involvement and promote motor learning during gait training, a functional task-based impedance control algorithm based on virtual gait period sequence was developed. For this controller, functional task-specific assistive torques for hip and knee joints could be generated according to a preset virtual gait period sequence. Through experimentation on healthy subjects, it was found that the assistive joint torques could be properly produced and a normal gait pattern could be achieved. The assistance levels could be easily adjusted for the entire gait cycle or for a specific sub-virtual gait period. Thus it could be customized for each individual. The importance of this controller is that different levels of compliance can be achieved between the users and the device. This means that it can be applied for patients with different levels stroke severities.

Lastly, this thesis introduced an autonomous controller to provide functional task assistance based on a FSM-based gait period detector. The control architecture used is intuitive. Firstly, it detects the six major gait periods using a FSM-based gait period detector. Next, it provides adequate functional hip and knee assistance at each detected gait period, which was found to be consistent with the functionality requirements of that specific gait period. A crucial aspect of the approach used is its potential to increase the motivation of the patient as it could be entirely controlled by its user. The results from healthy subject experiments revealed that it could effectively provide smooth assistance to the subject and help to achieve normal gait patterns. Moreover, it may also help to reduce human physical efforts as long as the device can be more lightweight. The significance of this controller is that it could be potentially applied in daily gait assistance for impaired persons in the future.

## Chapter 7 Conclusion and Future Work

---

It is important to acknowledge that this study only carried out preliminary evaluations on a few healthy subjects. No actual stroke patient experiments were performed. This is mainly because the current research project did not apply for funds to perform patient experiments. While the proposed control strategies were shown to be effective on healthy subjects, further studies need to be carried out to validate the effectiveness of the proposed methods on actual stroke patients. Pilot trials on actual stroke subjects need to be performed in the future. Additionally, experimental and evaluation protocols for stroke patients also need to be carefully designed. Another limitation for the proposed controllers is that the assistance levels had to be manually adjusted. Future research should attempt to develop some algorithms, which could adaptively modulate the assistance levels based on the user's real-time requirements.





# Publications by the Author

## Journal Publications

1. **J. Li**, B. Shen, C. M. Chew, C. L. Teo and A. N. Poo, “Novel Functional Task-based Gait Assistance Control of Lower Extremity Assistive Device for Level Walking,” in *Industrial Electronics, IEEE Transactions on*, doi: 10.1109/TIE.2015.2477347

## Conference Proceedings

1. **J. Li**, B. Shen, and C. M. Chew, “Functional Hip and Knee Joint Assistive Torque Controller for Gait Training,” in *14th International Conference on Electronics, Information and Communication (ICEIC 2015)*, January 2015.
2. **J. Li**, B. Shen, and C. M. Chew, “FAT based Adaptive Control for a Lower Extremity Rehabilitation Device: Simulation Results,” in *Advanced Intelligent Mechatronics (AIM), 2013 IEEE/ASME International Conference on*, July 2013, pp.828-832.
3. **J. Li**, B. Shen, F. Bai, C. M. Chew, and C. L. Teo, “First implementation results on FAT based adaptive control for a lower extremity rehabilitation device,” in *Mechatronics and Automation (ICMA), 2013 IEEE International Conference on*, August 2013, pp.945-950.
4. B. Shen, **J. Li**, and C. M. Chew, “Functional task based assistance during

walking for a lower extremity assistive device,” in Robotics and Automation (ICRA), 2014 IEEE International Conference on, June 2014, pp.246-251.

5. B. Shen, **J. Li**; F. Bai and C. M. Chew, “Motion intent recognition for control of a lower extremity assistive device (LEAD),” in Mechatronics and Automation (ICMA), 2013 IEEE International Conference on, August 2013, pp.926-931.
6. B. Shen, **J. Li**, F. Bai, and C. M. Chew, “Development and control of a lower extremity assistive device (LEAD) for gait rehabilitation,” in Rehabilitation Robotics (ICORR), 2013 IEEE International Conference on, June 2013, pp.1-6.
7. F. Bai, C. M. Chew, **J. Li**, B. Shen and T. M. Lubecki, “Muscle force estimation method with surface EMG for a lower extremities rehabilitation device,” in Rehabilitation Robotics (ICORR), 2013 IEEE International Conference on, June 2013, pp.1-6.

# Bibliography

- [1] D. Lloyd-Jones, R. J. Adams, T. M. Brown *et al.*, “Heart disease and stroke statistics - 2010 update: A report from the American Heart Association,” *Circulation*, vol. 121, no. 7, pp. e46–e215, 2010. [Online]. Available: <http://circ.ahajournals.org/content/121/7/e46.short>
- [2] M. Visintin, H. Barbeau, N. Korner-Bitensky, and N. E. Mayo, “A new approach to retrain gait in stroke patients through body weight support and treadmill stimulation,” *Stroke*, vol. 29, pp. 1122–1128, 1998.
- [3] Y. Laufer, R. Dickstein, Y. Chefez, and E. Marcovitz, “The effect of treadmill training on the ambulation of stroke survivors in the early stages of rehabilitation: a randomized study,” *J. Rehabil. Res. Dev.*, vol. 38, pp. 69–78, 2001.
- [4] I. T. Da Cunha, P. A. Lim, H. Qureshy *et al.*, “Gait outcomes after acute stroke rehabilitation with supported treadmill ambulation training: a randomized controlled pilot study,” *Arch. Phys. Med. Rehabil.*, vol. 83, pp. 1258–1265, 2002.
- [5] G. Colombo, M. Joerg, R. Schreier, and V. Dietz, “Treadmill training of paraplegic patients using a robotic orthosis.” *Journal of Rehabilitation Research & Development*, vol. 37, no. 6, 2000.
- [6] R. G. West, “Powered gait orthosis and method of utilizing SAME,” Feb. 10 2004, US Patent 6689075.
- [7] S. Freivogel, J. Mehrholz, T. Husak-Sotomayor, and D. Schmalohr, “Gait

- training with the newly developed 'LokoHelp'-system is feasible for non-ambulatory patients after stroke, spinal cord and brain injury. a feasibility study," *Brain Injury*, vol. 22, no. 7-8, pp. 625–632, 2008.
- [8] D. Reinkensmeyer, J. Wynne, and S. Harkema, "A robotic tool for studying locomotor adaptation and rehabilitation," in *Engineering in Medicine and Biology, 2002. 24th Annual Conference and the Annual Fall Meeting of the Biomedical Engineering Society EMBS/BMES Conference, 2002. Proceedings of the Second Joint*, vol. 3, Oct 2002, pp. 2353–2354.
- [9] D. J. Reinkensmeyer, D. Aoyagi, J. L. Emken *et al.*, "Tools for understanding and optimizing robotic gait training." *Journal of rehabilitation research and development*, vol. 43, no. 5, pp. 657–670, 2006.
- [10] S. Banala, S. Agrawal, and J. Scholz, "Active Leg Exoskeleton (ALEX) for gait rehabilitation of motor-impaired patients," in *Rehabilitation Robotics, 2007. ICORR 2007. IEEE 10th International Conference on*, 2007, pp. 401–407.
- [11] J. F. Veneman, R. Kruidhof, E. E. Hekman *et al.*, "Design and evaluation of the LOPES exoskeleton robot for interactive gait rehabilitation," *Neural Systems and Rehabilitation Engineering, IEEE Transactions on*, vol. 15, no. 3, pp. 379–386, 2007.
- [12] R. Adams, S. Gandevia, and N. Skuse, "The distribution of muscle weakness in upper motoneuron lesions affecting the lower limb," *Brain*, vol. 113, no. 5, pp. 1459–1476, 1990.
- [13] R. W. Bohannon and A. W. Andrews, "Relationships between impairments in strength of limb muscle actions following stroke," *Perceptual and motor skills*, vol. 87, no. 3f, pp. 1327–1330, 1998.
- [14] H. Stolze, S. Klebe, C. Baecker, C. Zechlin, L. Friege, S. Pohle, and G. Deuschl, "Prevalence of gait disorders in hospitalized neurological pa-

- tients,” *Movement disorders*, vol. 20, no. 1, pp. 89–94, 2005.
- [15] L. L. Cai, A. J. Fong, C. K. Otsoshi, Y. Liang *et al.*, “Implications of assist-as-needed robotic step training after a complete spinal cord injury on intrinsic strategies of motor learning,” *The Journal of Neuroscience*, vol. 26, pp. 10 564–10 568, 2006.
- [16] M. Lotze, C. Braun, N. Birbaumer, S. Anders, and L. G. Cohen, “Motor learning elicited by voluntary drive,” *Brain*, vol. 126, no. 4, pp. 866–872, 2003.
- [17] A. Kaelin-Lang, L. Sawaki, and L. G. Cohen, “Role of voluntary drive in encoding an elementary motor memory,” *Journal of neurophysiology*, 2004.
- [18] G. Colombo, M. Wirz, V. Dietz *et al.*, “Driven gait orthosis for improvement of locomotor training in paraplegic patients,” *Spinal Cord*, vol. 39, no. 5, pp. 252–255, 2001.
- [19] R. Riener, L. Lunenburger, S. Jezernik, M. Anderschitz *et al.*, “Patient-cooperative strategies for robot-aided treadmill training: first experimental results,” *Neural Systems and Rehabilitation Engineering, IEEE Transactions on*, vol. 13, no. 3, pp. 380–394, 2005.
- [20] B. Shen, “Design and control methodology of a lower limb assistive device LEAD,” PhD Thesis, National University of Singapore, 2014.
- [21] M. M. Williamson, “Robot arm control exploiting natural dynamics,” Ph.D. dissertation, Massachusetts Institute of Technology, 1999.
- [22] A. M. Dollar and H. Herr, “Lower extremity exoskeletons and active orthoses: challenges and state-of-the-art,” *Robotics, IEEE Transactions on*, vol. 24, no. 1, pp. 144–158, 2008.
- [23] I. Díaz, J. J. Gil, and E. Sánchez, “Lower-limb robotic rehabilitation: literature review and challenges,” *Journal of Robotics*, vol. 2011, 2011.
- [24] S. Viteckova, P. Kutilek, and M. Jirina, “Wearable lower limb robotics: A

- review,” *Biocybernetics and Biomedical Engineering*, vol. 33, no. 2, pp. 96–105, 2013.
- [25] M. A. M. Dzahir and S.-i. Yamamoto, “Recent trends in lower-limb robotic rehabilitation orthosis: Control scheme and strategy for pneumatic muscle actuated gait trainers,” *Robotics*, vol. 3, no. 2, pp. 120–148, 2014.
- [26] W. Meng, Q. Liu, Z. Zhou, Q. Ai, B. Sheng, and S. S. Xie, “Recent development of mechanisms and control strategies for robot-assisted lower limb rehabilitation,” *Mechatronics*, 2015.
- [27] G. Colombo, M. Wirz, and V. Dietz, “Driven gait orthosis for improvement of locomotor training in paraplegic patients,” *Spinal Cord*, vol. 39, no. 5, pp. 252–255, 2001.
- [28] M. Wirz, D. H. Zemon, R. Rupp *et al.*, “Effectiveness of automated locomotor training in patients with chronic incomplete spinal cord injury: a multicenter trial,” *Archives of Physical Medicine and Rehabilitation*, vol. 86, no. 4, pp. 672–680, 2005.
- [29] T. G. Hornby, D. H. Zemon, and D. Campbell, “Robotic-assisted, body-weight-supported treadmill training in individuals following motor incomplete spinal cord injury,” *Physical Therapy*, vol. 85, no. 1, pp. 52–66, 2005.
- [30] J. Hidler, D. Nichols, M. Pelliccio *et al.*, “Multicenter randomized clinical trial evaluating the effectiveness of the lokomat in subacute stroke,” *Neurorehabilitation and Neural Repair*, vol. 23, no. 1, pp. 5–13, 2009.
- [31] A. Duschau-Wicke, J. von Zitzewitz, A. Caprez, L. Lunenburger, and R. Riener, “Path control: a method for patient-cooperative robot-aided gait rehabilitation,” *Neural Systems and Rehabilitation Engineering, IEEE Transactions on*, vol. 18, no. 1, pp. 38–48, 2010.
- [32] R. G. West, “Powered gait orthosis and method of utilizing SAME,” May 9 2006, US Patent 7041069.

- [33] S. Fisher, L. Lucas, and T. Adam Thrasher, “Robot-assisted gait training for patients with hemiparesis due to stroke,” *Topics in stroke rehabilitation*, vol. 18, no. 3, pp. 269–276, 2011.
- [34] S. Freivogel, D. Schmalohr, and J. Mehrholz, “Improved walking ability and reduced therapeutic stress with an electromechanical gait device,” *Journal of Rehabilitation Medicine*, vol. 41, no. 9, pp. 734–739, 2009.
- [35] J. F. Veneman, R. Ekkelenkamp, R. Kruidhof *et al.*, “A series elastic- and bowden-cable-based actuation system for use as torque actuator in exoskeleton-type robots,” *The international journal of robotics research*, vol. 25, no. 3, pp. 261–281, 2006.
- [36] B. Koopman, E. van Asseldonk, and H. Van der Kooij, “Selective control of gait subtasks in robotic gait training: foot clearance support in stroke survivors with a powered exoskeleton,” *J Neuroeng Rehabil*, vol. 10, no. 3, 2013.
- [37] S. K. Banala, S. H. Kim, S. K. Agrawal, and J. P. Scholz, “Robot assisted gait training with Active Leg Exoskeleton (ALEX),” *Neural Systems and Rehabilitation Engineering, IEEE Transactions on*, vol. 17, no. 1, pp. 2–8, 2009.
- [38] S. Banala, S. H. Kim, S. Agrawal, and J. Scholz, “Robot assisted gait training with Active Leg Exoskeleton (ALEX),” in *Biomedical Robotics and Biomechatronics, 2008. BioRob 2008. 2nd IEEE RAS EMBS International Conference on*, 2008, pp. 653–658.
- [39] S. Banala, S. Agrawal, S. H. Kim, and J. Scholz, “Novel gait adaptation and neuromotor training results using an Active Leg Exoskeleton,” *Mechatronics, IEEE/ASME Transactions on*, vol. 15, no. 2, pp. 216–225, 2010.
- [40] T. Lenzi, M. C. Carrozza, and S. K. Agrawal, “Powered hip exoskeletons can reduce the user’s hip and ankle muscle activations during walking,” *Neu-*



- ral Systems and Rehabilitation Engineering, IEEE Transactions on*, vol. 21, no. 6, pp. 938–948, 2013.
- [41] J. L. Emken, J. H. Wynne, S. J. Harkema, and D. J. Reinkensmeyer, “Robotic device for manipulating human stepping,” *IEEE Transactions on robotics*, vol. 22, no. 1, 2006.
- [42] J. L. Emken, S. J. Harkema, J. A. Beres-Jones *et al.*, “Feasibility of manual teach-and-replay and continuous impedance shaping for robotic locomotor training following spinal cord injury,” *Biomedical Engineering, IEEE Transactions on*, vol. 55, no. 1, pp. 322–334, 2008.
- [43] D. J. Reinkensmeyer, D. Aoyagi, J. L. Emken *et al.*, “Tools for understanding and optimizing robotic gait training.” *Journal of rehabilitation research and development*, vol. 43, no. 5, pp. 657–670, 2006.
- [44] D. Aoyagi, W. E. Ichinose, S. J. Harkema, *et al.*, “A robot and control algorithm that can synchronously assist in naturalistic motion during body-weight-supported gait training following neurologic injury,” *Neural Systems and Rehabilitation Engineering, IEEE Transactions on*, vol. 15, no. 3, pp. 387–400, 2007.
- [45] D. Aoyagi, W. E. Ichinose, S. J. Harkema, D. J. Reinkensmeyer, and J. E. Bobrow, “A robot and control algorithm that can synchronously assist in naturalistic motion during body-weight-supported gait training following neurologic injury,” *Neural Systems and Rehabilitation Engineering, IEEE Transactions on*, vol. 15, no. 3, pp. 387–400, 2007.
- [46] M. Pietrusinski, I. Cajigas, Y. Mizikacioglu *et al.*, “Gait rehabilitation therapy using robot generated force fields applied at the pelvis,” in *Haptics Symposium, 2010 IEEE*. IEEE, 2010, pp. 401–407.
- [47] M. Pietrusinski, I. Cajigas, M. Goldsmith *et al.*, “Robotically generated force fields for stroke patient pelvic obliquity gait rehabilitation,” in *Robotics and*

- Automation (ICRA), 2010 IEEE International Conference on*, May 2010, pp. 569–575.
- [48] M. Pietrusinski, O. Unluhisarcikli, C. Mavroidis *et al.*, “Design of human-machine interface and altering of pelvic obliquity with RGR trainer,” in *Rehabilitation Robotics (ICORR), 2011 IEEE International Conference on*. IEEE, 2011, pp. 1–6.
- [49] M. Pietrusinski, I. Cajigas, G. Severini, P. Bonato, and C. Mavroidis, “Robotic gait rehabilitation trainer,” *Mechatronics, IEEE/ASME Transactions on*, vol. 19, no. 2, pp. 490–499, April 2014.
- [50] HAL. [Online]. Available: <http://www.cyberdyne.jp/english/>
- [51] S. Maeshima, A. Osawa, D. Nishio, Y. Hirano, K. Takeda, H. Kigawa, and Y. Sankai, “Efficacy of a hybrid assistive limb in post-stroke hemiplegic patients: a preliminary report,” *BMC neurology*, vol. 11, no. 1, p. 116, 2011.
- [52] H. Kawamoto, K. Kamibayashi, Y. Nakata *et al.*, “Pilot study of locomotion improvement using hybrid assistive limb in chronic stroke patients,” *BMC neurology*, vol. 13, no. 1, p. 141, 2013.
- [53] ReWalk. [Online]. Available: <http://rewalk.com/>
- [54] A. Goffer, “Gait-locomotor apparatus,” US patent number 7 153 242, 2006.
- [55] G. Zeilig, H. Weingarden, M. Zwecker, I. Dudkiewicz, A. Bloch, and A. Esquenazi, “Safety and tolerance of the ReWalk exoskeleton suit for ambulation by people with complete spinal cord injury: A pilot study,” *The journal of spinal cord medicine*, vol. 35, no. 2, pp. 96–101, 2012.
- [56] M. Talaty, A. Esquenazi, and J. E. Briceno, “Differentiating ability in users of the ReWalk TM powered exoskeleton: An analysis of walking kinematics,” in *Rehabilitation Robotics (ICORR), 2013 IEEE International Conference on*. IEEE, 2013, pp. 1–5.

- [57] Ekso. [Online]. Available: <http://www.eksobionics.com/>
- [58] K. A. Strausser and H. Kazerooni, "The development and testing of a human machine interface for a mobile medical exoskeleton," in *Intelligent Robots and Systems (IROS), 2011 IEEE/RSJ International Conference on*. IEEE, 2011, pp. 4911–4916.
- [59] Indego. [Online]. Available: <http://www.indego.com/indego/en/home>
- [60] R. Farris, H. Quintero, and M. Goldfarb, "Preliminary evaluation of a powered lower limb orthosis to aid walking in paraplegic individuals," *Neural Systems and Rehabilitation Engineering, IEEE Transactions on*, vol. 19, no. 6, pp. 652–659, Dec 2011.
- [61] H. A. Quintero, R. J. Farris, and M. Goldfarb, "A method for the autonomous control of lower limb exoskeletons for persons with paraplegia," *Journal of medical devices*, vol. 6, no. 4, p. 041003, 2012.
- [62] R. J. Farris, H. A. Quintero, and M. Goldfarb, "Performance evaluation of a lower limb exoskeleton for stair ascent and descent with paraplegia," in *Engineering in Medicine and Biology Society (EMBC), 2012 Annual International Conference of the IEEE*. IEEE, 2012, pp. 1908–1911.
- [63] R. Farris, H. Quintero, S. Murray *et al.*, "A preliminary assessment of legged mobility provided by a lower limb exoskeleton for persons with paraplegia," *Neural Systems and Rehabilitation Engineering, IEEE Transactions on*, vol. 22, no. 3, pp. 482–490, May 2014.
- [64] R. Farris, H. Quintero, T. Withrow, and M. Goldfarb, "Design and simulation of a joint-coupled orthosis for regulating fes-aided gait," in *Robotics and Automation(ICRA), 2009 IEEE International Conference on*, May 2009, pp. 1916–1922.
- [65] H. Quintero, R. Farris, W. Durfee, and M. Goldfarb, "Feasibility of a hybrid-fes system for gait restoration in paraplegics," in *Engineering in Medicine*

- 
- and Biology Society (EMBC), 2010 Annual International Conference of the IEEE*, Aug 2010, pp. 483–486.
- [66] H. Vallery, R. Ekkelenkamp, M. Buss, and H. van der Kooij, “Complementary limb motion estimation based on interjoint coordination: Experimental evaluation,” in *Rehabilitation Robotics, 2007. ICORR 2007. IEEE 10th International Conference on*. IEEE, 2007, pp. 798–803.
- [67] H. Vallery, E. H. van Asseldonk, M. Buss, and H. van der Kooij, “Reference trajectory generation for rehabilitation robots: complementary limb motion estimation,” *Neural Systems and Rehabilitation Engineering, IEEE Transactions on*, vol. 17, no. 1, pp. 23–30, 2009.
- [68] N. Hogan, “Impedance control: an approach to manipulation,” in *American Control Conference, 1984*, 1984, pp. 304–313.
- [69] J. E. Pratt, “Virtual model control of a biped walking robot,” Ph.D. dissertation, Massachusetts Institute of Technology, 1995.
- [70] S. Jezernik, G. Colombo, and M. Morari, “Automatic gait-pattern adaptation algorithms for rehabilitation with a 4-dof robotic orthosis,” *Robotics and Automation, IEEE Transactions on*, vol. 20, no. 3, pp. 574–582, 2004.
- [71] S. Jezernik and M. Morari, “Controlling the human-robot interaction for robotic rehabilitation of locomotion,” in *Advanced Motion Control, 2002. 7th International Workshop on*. IEEE, 2002, pp. 133–135.
- [72] S. Jezernik, G. Colombo, and M. Morari, “Joint-angle trajectory adaptation for the robot orthosis Lokomat,” in *in Proc. Workshop on European Scientific and Industrial Collaboration*, 2001, pp. 451–456.
- [73] S. Jezernik, K. Jezernik, and M. Morari, “Impedance-control-based gait pattern adaptation for robotic rehabilitation device,” in *Mechatronic Systems, 2002. 2nd IFAC Conference*, 2002, pp. 417–421.
- [74] S. Hussain, S. Q. Xie, and P. K. Jamwal, “Adaptive impedance control of

- a robotic orthosis for gait rehabilitation,” *Cybernetics, IEEE Transactions on*, vol. 43, no. 3, pp. 1025–1034, 2013.
- [75] L. Zimmerli, A. Duschau-Wicke, R. Riener, A. Mayr, and L. Lunenburger, “Virtual reality and gait rehabilitation augmented feedback for the Lokomat,” in *Virtual Rehabilitation International Conference, 2009*. IEEE, 2009, pp. 150–153.
- [76] K. Brüttsch, T. Schuler, A. Koenig *et al.*, “Research influence of virtual reality soccer game on walking performance in robotic assisted gait training for children,” *J. Neuroeng. Rehabil*, vol. 15, no. 7, pp. 1–9, 2010.
- [77] A. Mirelman, P. Bonato, and J. E. Deutsch, “Effects of training with a robot-virtual reality system compared with a robot alone on the gait of individuals after stroke,” *Stroke*, vol. 40, no. 1, pp. 169–174, 2009.
- [78] Y. Sankai, “HAL: Hybrid assistive limb based on cybernics,” in *Robotics Research*. Springer, 2011, pp. 25–34.
- [79] K. Kasaoka and Y. Sankai, “Predictive control estimating operator’s intention for stepping-up motion by exo-skeleton type power assist system hal,” in *Intelligent Robots and Systems, 2001. Proceedings. 2001 IEEE/RSJ International Conference on*, vol. 3. IEEE, 2001, pp. 1578–1583.
- [80] H. Kawamoto, S. Lee, S. Kanbe, and Y. Sankai, “Power assist method for hal-3 using emg-based feedback controller,” in *Systems, Man and Cybernetics, 2003. IEEE International Conference on*, vol. 2, Oct 2003, pp. 1648–1653 vol.2.
- [81] H. Kawamoto and Y. Sankai, “Power assist method based on phase sequence and muscle force condition for HAL,” *Advanced Robotics*, vol. 19, pp. 717–734, 2005.
- [82] D. P. Ferris, J. M. Czerniecki, and B. Hannaford, “An ankle-foot orthosis powered by artificial pneumatic muscles,” *Journal of applied biomechanics*,

- vol. 21, no. 2, p. 189, 2005.
- [83] D. P. Ferris, K. E. Gordon, G. S. Sawicki, and A. Peethambaran, “An improved powered ankle-foot orthosis using proportional myoelectric control,” *Gait & posture*, vol. 23, no. 4, pp. 425–428, 2006.
- [84] S. M. Cain, K. E. Gordon, and D. P. Ferris, “An improved powered ankle-foot orthosis using proportional myoelectric control,” *Journal of NeuroEngineering and Rehabilitation*, vol. 4, no. 48, 2007.
- [85] D. Ferris and C. Lewis, “Robotic lower limb exoskeletons using proportional myoelectric control,” in *Engineering in Medicine and Biology Society (EMBC), 2009 Annual International Conference of the IEEE*, Sept 2009, pp. 2119–2124.
- [86] E. Guizzo and H. Goldstein, “The rise of the body bots [robotic exoskeletons],” *Spectrum, IEEE*, vol. 42, no. 10, pp. 50–56, 2005.
- [87] I. P. Pappas, T. Keller, S. Mangold, M. R. Popovic, V. Dietz, and M. Morari, “A reliable gyroscope-based gait-phase detection sensor embedded in a shoe insole,” *Sensors Journal, IEEE*, vol. 4, no. 2, pp. 268–274, 2004.
- [88] K. Kong and M. Tomizuka, “Smooth and continuous human gait phase detection based on foot pressure patterns,” in *in Robotics and Automation (ICRA), 2008 IEEE International Conference on*, May 2008, pp. 3678–3683.
- [89] N. Mijailović, M. Gavrilović, and S. Rafajlović, “Gait phases recognition from accelerations and ground reaction forces: Application of neural networks,” *Telfor Journal*, vol. 1, no. 1, pp. 34–36, 2009.
- [90] C. Senanayake and S. M. N. A. Senanayake, “Computational intelligent gait-phase detection system to identify pathological gait,” *Information Technology in Biomedicine, IEEE Transactions on*, vol. 14, no. 5, pp. 1173–1179, Sept 2010.
- [91] K. Suzuki, G. Mito, H. Kawamoto, Y. Hasegawa, and Y. Sankai, “Intention-

- based walking support for paraplegia patients with robot suit HAL,” *Advanced Robotics*, vol. 21, no. 12, pp. 1441–1469, 2007.
- [92] J. Rose and J. G. Gamble, *Human Walking*, 3rd ed. Lippincott Williams & Wilkins, 2006.
- [93] R. Riener, M. Rabuffetti, and C. Frigo, “Stair ascent and descent at different inclinations,” *Gait & posture*, vol. 15, no. 1, pp. 32–44, 2002.
- [94] W. E. Woodson, B. Tillman, and P. Tillman, *Human factors design handbook: information and guidelines for the design of systems, facilities, equipment, and products for human use*, 2nd ed. McGraw-Hill Education, 1992.
- [95] S. C. Walpole, D. Prieto-Merino, P. Edwards, J. Cleland, G. Stevens, and I. Roberts, “The weight of nations: an estimation of adult human biomass,” *BMC Public health*, vol. 12, no. 1, p. 439, 2012.
- [96] T. K. Chuan, M. Hartono, and N. Kumar, “Anthropometry of the singaporean and indonesian populations,” *International Journal of Industrial Ergonomics*, vol. 40, no. 6, pp. 757 – 766, 2010. [Online]. Available: <http://www.sciencedirect.com/science/article/pii/S0169814110000491>
- [97] [Online]. Available: <http://www.orthomerica.com/product/1607587-newport-3>
- [98] [Online]. Available: <http://www.orthoticsprostheticsne.com/home/orthotics>
- [99] A. B. Zoss, H. Kazerooni, and A. Chu, “Biomechanical design of the berkeley lower extremity exoskeleton (BLEEX),” *Mechatronics, IEEE/ASME Transactions on*, vol. 11, no. 2, pp. 128–138, 2006.
- [100] S. Karlin, “Raiding iron man’s closet [geek life],” *IEEE Spectrum*, vol. 48, no. 8, p. 25, 2011.
- [101] K. Yamamoto, K. Hyodo, M. Ishii, and T. Matsuo, “Development of power assisting suit for assisting nurse labor.” *JSME International Journal Series*

- C Mechanical Systems, Machine Elements and Manufacturing*, vol. 45, no. 3, pp. 703–711, 2002.
- [102] J. Hauschild, G. Hepler, and J. McPhee, “Friction compensation of harmonic drive actuators,” in *Proceedings of 6th International Conference on Dynamics and Control of Systems and Structures in Space*, 2004, pp. 683–692.
- [103] J.-J. E. Slotine and W. Li, “On the adaptive control of robot manipulators,” *The International Journal of Robotics Research*, vol. 6, no. 3, pp. 49–59, 1987.
- [104] M. C. Chien and A. C. Huang, “Adaptive impedance control of robot manipulators based on function approximation technique,” *Robotica*, vol. 22, pp. 395–403, 2004. [Online]. Available: <http://dx.doi.org/10.1017/S0263574704000190>
- [105] A. C. Huang, S. C. Wu, and W. F. Ting, “A FAT-based adaptive controller for robot manipulators without regressor matrix: theory and experiments,” *Robotica*, vol. 24, pp. 205–210, 2006. [Online]. Available: <http://dx.doi.org/10.1017/S0263574705002031>
- [106] A. Huang and M. Chien, *Adaptive Control of Robot Manipulators: A Unified Regressor-free Approach*. World Scientific Publishing Company Incorporated, 2010.
- [107] T. R. Kane and D. A. Levinson, *Dynamics: Theory and Applications*. McGraw Hill, 1985.
- [108] K. P. Granata, M. F. Abel, and D. L. Damiano, “Joint angular velocity in spastic gait and the influence of muscle-tendon lengthening,” *The Journal of Bone and Joint Surgery*, vol. 82, no. 2, pp. 174–186, 2000.
- [109] T. Herman, N. Giladi, L. Gruendlinger, and J. M. Hausdorff, “Six weeks of intensive treadmill training improves gait and quality of life in patients



- with parkinsons disease: a pilot study,” *Archives of physical medicine and rehabilitation*, vol. 88, no. 9, pp. 1154–1158, 2007.
- [110] I. T. da Cunha, P. A. Lim, H. Qureshy, H. Henson, T. Monga, and E. J. Prottas, “Gait outcomes after acute stroke rehabilitation with supported treadmill ambulation training: a randomized controlled pilot study,” *Archives of physical medicine and rehabilitation*, vol. 83, no. 9, pp. 1258–1265, 2002.
- [111] R. R. Neptune, D. J. Clark, and S. A. Kautz, “Modular control of human walking: a simulation study,” *Journal of biomechanics*, vol. 42, no. 9, pp. 1282–1287, 2009.
- [112] C. P. McGowan, R. R. Neptune, D. J. Clark, and S. A. Kautz, “Modular control of human walking: adaptations to altered mechanical demands,” *Journal of biomechanics*, vol. 43, no. 3, pp. 412–419, 2010.
- [113] M. W. Whittle, “Chapter 2-normal gait,” in *Gait Analysis*, 4th ed. Edinburgh: Butterworth-Heinemann, 2007, pp. 47 – 100.
- [114] Y. Ohta, H. Yano, R. Suzuki, M. Yoshida, N. Kawashima, and K. Nakazawa, “A two-degree-of-freedom motor-powered gait orthosis for spinal cord injury patients,” *Proceedings of the Institution of Mechanical Engineers, Part H: Journal of Engineering in Medicine*, vol. 221, no. 6, pp. 629–639, 2007.
- [115] H. K. Kwa, J. H. Noorden, M. Missel, T. Craig, J. E. Pratt, and P. D. Neuhaus, “Development of the IHMC mobility assist exoskeleton,” in *Robotics and Automation, 2009. ICRA’09. IEEE International Conference on*, 2009, pp. 2556–2562.
- [116] P. D. Neuhaus, J. H. Noorden, T. J. Craig, T. Torres, J. Kirschbaum, and J. E. Pratt, “Design and evaluation of Mina: A robotic orthosis for paraplegics,” in *Rehabilitation Robotics (ICORR), 2011 IEEE International Conference on*, 2011, pp. 1–8.
- [117] A. Tsukahara, Y. Hasegawa, and Y. Sankai, “Standing-up motion support

- for paraplegic patient with robot suit HAL,” in *Rehabilitation Robotics, 2009. ICORR 2009. IEEE International Conference on*, 2009, pp. 211–217.
- [118] K. Kong and D. Jeon, “Design and control of an exoskeleton for the elderly and patients,” *Mechatronics, IEEE/ASME Transactions on*, vol. 11, no. 4, pp. 428–432, Aug 2006.
- [119] U. Onen, F. Botsali, M. Kalyoncu, M. Tinkir, N. Yilmaz, and Y. Sahin, “Design and actuator selection of a lower extremity exoskeleton,” *Mechatronics, IEEE/ASME Transactions on*, vol. 19, no. 2, pp. 623–632, April 2014.
- [120] R. Lu, Z. Li, C.-Y. Su, and A. Xue, “Development and learning control of a human limb with a rehabilitation exoskeleton,” *Industrial Electronics, IEEE Transactions on*, vol. 61, no. 7, pp. 3776–3785, July 2014.
- [121] A. S. Ryan, C. L. Dobrovolny, G. V. Smith, K. H. Silver, and R. F. Macko, “Hemiparetic muscle atrophy and increased intramuscular fat in stroke patients,” *Archives of physical medicine and rehabilitation*, vol. 83, no. 12, pp. 1703–1707, 2002.
- [122] I. Pappas, M. Popovic, T. Keller, V. Dietz, and M. Morari, “A reliable gait phase detection system,” *Neural Systems and Rehabilitation Engineering, IEEE Transactions on*, vol. 9, no. 2, pp. 113–125, June 2001.
- [123] K. Kong and M. Tomizuka, “A gait monitoring system based on air pressure sensors embedded in a shoe,” *Mechatronics, IEEE/ASME Transactions on*, vol. 14, no. 3, pp. 358–370, June 2009.
- [124] S. Kotz, N. Balakrishnan, and N. L. Johnson, *Continuous multivariate distributions, models and applications*. John Wiley & Sons, 2004, vol. 1.
- [125] H. Varol, F. Sup, and M. Goldfarb, “Multiclass real-time intent recognition of a powered lower limb prosthesis,” *Biomedical Engineering, IEEE Transactions on*, vol. 57, no. 3, pp. 542–551, March 2010.
- [126] D. A. Reynolds, “Gaussian mixture models,” *Encyclopedia of Biometric*

- Recognition*, Springer, February 2008.
- [127] T. K. Moon, “The expectation-maximization algorithm,” *Signal Processing Magazine, IEEE*, vol. 13, no. 6, pp. 47–60, 1996.
- [128] F. Sup, H. Varol, J. Mitchell, T. Withrow, and M. Goldfarb, “Preliminary evaluations of a self-contained anthropomorphic transfemoral prosthesis,” *Mechatronics, IEEE/ASME Transactions on*, vol. 14, no. 6, pp. 667–676, Dec 2009.
- [129] B. Lawson, H. Varol, A. Huff, E. Erdemir, and M. Goldfarb, “Control of stair ascent and descent with a powered transfemoral prosthesis,” *Neural Systems and Rehabilitation Engineering, IEEE Transactions on*, vol. 21, no. 3, pp. 466–473, May 2013.
- [130] S. A. Hesse, M. T. Jahnke, C. M. Bertelt, C. Schreiner, D. Lücke, and K.-H. Mauritz, “Gait outcome in ambulatory hemiparetic patients after a 4-week comprehensive rehabilitation program and prognostic factors.” *Stroke*, vol. 25, no. 10, pp. 1999–2004, 1994.
- [131] K. P. Granata, M. F. Abel, and D. L. Damiano, “Joint angular velocity in spastic gait and the influence of muscle-tendon lengthening\*,” *The Journal of Bone & Joint Surgery*, vol. 82, no. 2, pp. 174–86, 2000.
- [132] P. Astrand and K. Rodahl, *Textbook of work physiology: physiological bases of exercise*, 2nd ed. McGraw and Hill, 1977.
- [133] R. Riener, A. Koenig, M. Bolliger, M. Wieser, A. Duschau-Wicke, and H. Vallery, “Bio-cooperative robotics: controlling mechanical, physiological and mental patient states,” in *Rehabilitation Robotics (ICORR), 2009 IEEE International Conference on*, June 2009, pp. 407–412.
- [134] A. Koenig, X. Omlin, J. Bergmann *et al.*, “Controlling patient participation during robot-assisted gait training,” *J Neuroeng Rehabil*, vol. 8, no. 14.10, p. 1186, 2011.

- [135] R. C. Browning, J. R. Modica, R. Kram, and A. Goswami, “The effects of adding mass to the legs on the energetics and biomechanics of walking,” *Medicine and Science in Sports and Exercise*, vol. 39, no. 3, p. 515, 2007.
- [136] R. C. Browning, E. A. Baker, J. A. Herron, and R. Kram, “Effects of obesity and sex on the energetic cost and preferred speed of walking,” *Journal of Applied Physiology*, vol. 100, no. 2, pp. 390–398, 2006. [Online]. Available: <http://jap.physiology.org/content/100/2/390>
- [137] H. J. Ralston, “Energy-speed relation and optimal speed during level walking,” *Internationale Zeitschrift für Angewandte Physiologie Einschliesslich Arbeitsphysiologie*, vol. 17, no. 4, pp. 277–283, 1958.

## BIBLIOGRAPHY

---

# Appendix

## Dynamics Model Derivation using Euler-Lagrange Approach

The dynamics model of this two link limb-device system in the joint space has the following form

$$D(\theta)\ddot{\theta} + C(\theta, \dot{\theta})\dot{\theta} + G(\theta) = \tau + \tau_h$$

where  $D(\theta) \in R^{2 \times 2}$  represents the joint-space inertia matrix,  $C(\theta, \dot{\theta}) \in R^{2 \times 2}$  denotes the Centripetal and Coriolis matrix, and  $G(\theta) \in R^2$  represents the gravitational components.  $D(\theta)$ ,  $C(\theta, \dot{\theta})$  and  $G(\theta)$  matrices are required to be found.

From Fig. 4.1 in Section 4.2, the positions of the two mass link can be described by the following equations

$$\begin{cases} x_1 = \frac{1}{2}L_1 \cos \theta_1 \\ y_1 = \frac{1}{2}L_1 \sin \theta_1 \end{cases}$$
$$\begin{cases} x_2 = L_1 \cos \theta_1 + \frac{1}{2}L_2 \cos(\theta_1 + \theta_2) \\ y_2 = L_1 \sin \theta_1 + \frac{1}{2}L_2 \sin(\theta_1 + \theta_2) \end{cases}$$

Then the linear velocities in X and Y axis can be obtained as

$$\begin{cases} \dot{x}_1 = -\frac{1}{2}L_1 \sin(\theta_1)\dot{\theta}_1 \\ \dot{y}_1 = \frac{1}{2}L_1 \cos(\theta_1)\dot{\theta}_1 \end{cases}$$
$$\begin{cases} \dot{x}_2 = -L_1 \sin(\theta_1)\dot{\theta}_1 - \frac{1}{2}L_2 \sin(\theta_1 + \theta_2)(\dot{\theta}_1 + \dot{\theta}_2) \\ \dot{y}_2 = L_1 \cos(\theta_1)\dot{\theta}_1 + \frac{1}{2}L_2 \cos(\theta_1 + \theta_2)(\dot{\theta}_1 + \dot{\theta}_2) \end{cases}$$

Thus the resultant velocities are

$$v_1 = \dot{x}_1^2 + \dot{y}_1^2 = \frac{1}{4}L_1^2\dot{\theta}_1^2$$

$$v_2 = \dot{x}_2^2 + \dot{y}_2^2 = (L_1^2 + \frac{1}{4}L_2^2 + L_1L_2 \cos \theta_2)\dot{\theta}_1^2 + \frac{1}{4}L_2^2\dot{\theta}_2^2 + (\frac{1}{2}L_2^2 + L_1L_2 \cos \theta_2)\dot{\theta}_1\dot{\theta}_2$$

Since the mass has been lumped in the middle of the link, then the kinetic energy is

$$\begin{aligned} K &= \frac{1}{2}m_1v_1^2 + \frac{1}{2}m_2v_2^2 \\ &= (\frac{1}{8}m_1L_1^2 + \frac{1}{2}m_2L_1^2 + \frac{1}{8}m_2L_2^2 + \frac{1}{2}m_2L_1L_2 \cos \theta_2)\dot{\theta}_1^2 + \\ &\quad (\frac{1}{4}m_2L_2^2 + \frac{1}{2}m_2L_1L_2 \cos \theta_2)\dot{\theta}_1\dot{\theta}_2 + \frac{1}{8}m_2L_2^2\dot{\theta}_2^2 \\ &= \frac{1}{2}\dot{\theta}^T \begin{bmatrix} (\frac{1}{4}m_1 + m_2)L_1^2 + \frac{1}{4}m_2L_2^2 + m_2L_1L_2 \cos \theta_2 & \frac{1}{4}m_2L_2^2 + \frac{1}{2}m_2L_1L_2 \cos \theta_2 \\ \frac{1}{4}m_2L_2^2 + \frac{1}{2}m_2L_1L_2 \cos \theta_2 & \frac{1}{4}m_2L_2^2 \end{bmatrix} \dot{\theta} \end{aligned}$$

From above equation,  $D(\theta)$  matrix can be obtained as follows

$$D(\theta) = \begin{bmatrix} (\frac{1}{4}m_1 + m_2)L_1^2 + \frac{1}{4}m_2L_2^2 + m_2L_1L_2 \cos \theta_2 & \frac{1}{4}m_2L_2^2 + \frac{1}{2}m_2L_1L_2 \cos \theta_2 \\ \frac{1}{4}m_2L_2^2 + \frac{1}{2}m_2L_1L_2 \cos \theta_2 & \frac{1}{4}m_2L_2^2 \end{bmatrix}$$

The  $D(\theta)$  matrix can be used to derive  $C(\theta, \dot{\theta})$  matrix, as shown in the following

$$\left\{ \begin{array}{l} C_{111} = \frac{1}{2} \frac{\partial d_{11}}{\partial \theta_1} = 0 \\ C_{112} = \frac{\partial d_{21}}{\partial \theta_1} - \frac{1}{2} \frac{\partial d_{11}}{\partial \theta_2} = \frac{1}{2} m_2 L_1 L_2 \sin \theta_2 \\ C_{121} = C_{211} = \frac{1}{2} \frac{\partial d_{11}}{\partial \theta_2} = -\frac{1}{2} m_2 L_1 L_2 \sin \theta_2 \\ C_{122} = C_{212} = \frac{1}{2} \frac{\partial d_{22}}{\partial \theta_1} = 0 \\ C_{221} = \frac{\partial d_{12}}{\partial \theta_2} - \frac{1}{2} \frac{\partial d_{22}}{\partial \theta_1} = -\frac{1}{2} m_2 L_1 L_2 \sin \theta_2 \\ C_{222} = \frac{1}{2} \frac{\partial d_{22}}{\partial \theta_2} = 0 \end{array} \right.$$

$$\begin{cases} C_{11} = C_{111}\dot{\theta}_1 + C_{211}\dot{\theta}_2 = -\frac{1}{2}m_2L_1L_2 \sin \theta_2\dot{\theta}_2 \\ C_{21} = C_{112}\dot{\theta}_1 + C_{212}\dot{\theta}_2 = \frac{1}{2}m_2L_1L_2 \sin \theta_2\dot{\theta}_1 \\ C_{12} = C_{121}\dot{\theta}_1 + C_{221}\dot{\theta}_2 = -\frac{1}{2}L_1L_2 \sin \theta_2(\dot{\theta}_1 + \dot{\theta}_2) \\ C_{22} = C_{122}\dot{\theta}_1 + C_{222}\dot{\theta}_2 = 0 \end{cases}$$

$$C(\theta, \dot{\theta}) = \begin{bmatrix} -\frac{1}{2}m_2L_1L_2 \sin \theta_2\dot{\theta}_2 & -\frac{1}{2}L_1L_2 \sin \theta_2(\dot{\theta}_1 + \dot{\theta}_2) \\ \frac{1}{2}m_2L_1L_2 \sin \theta_2\dot{\theta}_1 & 0 \end{bmatrix}$$

The potential energy is

$$P = -\frac{1}{2}m_1gL_1 \cos \theta_1 - m_2g \left[ L_1 \cos \theta_1 + \frac{1}{2}L_2 \cos(\theta_1 + \theta_2) \right]$$

From the above equation,  $G(\theta)$  matrix can be obtained as follows

$$G(\theta) = \frac{\partial P}{\partial \theta} = \begin{bmatrix} \frac{\partial P}{\partial \theta_1} \\ \frac{\partial P}{\partial \theta_2} \end{bmatrix}$$

$$G(\theta) = \begin{bmatrix} (\frac{1}{2}m_1gL_1 + m_2gL_1) \sin \theta_1 + \frac{1}{2}m_2gL_2 \sin(\theta_1 + \theta_2) \\ \frac{1}{2}m_2gL_2 \sin(\theta_1 + \theta_2) \end{bmatrix}$$